Design of a Mine Roof Strata Analysis Device

Andrew James Reksten Russell

Thesis submitted to the faculty of the Virginia Polytechnic Institute and State University in partial fulfillment of the requirements for the degree of

Master of Science

of

Mining and Minerals Engineering

Erik C. Westman, Chair

Mario G. Karfakis

Kramer D. Luxbacher

February 11, 2015

Blacksburg, Virginia

Keywords: Mine Roof Analysis, Scratch Test, Ground Control

Design of a Mine Roof Strata Analysis Device

Andrew James Reksten Russell

ABSTRACT

Because the roof lithology in an underground coal mine is typically variable and poorly known, the safety and efficiency of these mines is reduced. To address this shortcoming, a device for analyzing rock properties by way of scratching a mine roof borehole was designed and tested in multiple different media with the goal of determining *in situ* mine roof properties with a nondestructive technique. Tools were developed for measuring extraction force and position of the scratching mechanism and those values were compared versus time for multiple tests to look for changes in applied force over changing positions. Because of signal stability and inconsistencies in scratch depths the data were found to contain too much variation to determine any rock properties or changing rock conditions from the simulated roof material in the concrete block. However, further scratch tests in a sandstone block indicated that increasing the diameter of the wire scratchers (and therefore increasing their stiffness and accompanying normal force) from 0.045 inches to 0.055 inches increased the average pull force from 6.24 to 9.96 lbs. Similar to that test, a scratch test was performed in a PVC pipe where it was found that increasing the scratcher diameter from 0.045 inches to 0.051 inches increased the pull force from a 2.81 lb average to a 36.46 lb average, with considerably better gouging of the host material.

ACKNOWLEDGEMENTS

I would like to thank my advisor, Dr. Erik C. Westman, for the incredible opportunity to be a graduate student in this program and for his perpetual support for me and my work. This project was funded by the National Institute for Occupational Safety and Health (NIOSH) under Contract 200-2011-40313 for "New Technologies for Identifying and Understanding Ground Stability Hazards". I would like to thank NIOSH for the funding to conduct this research

I thank Dr. Mario Karfakis for his consistent insight into my research and for helping me develop my ideas and for access to his lab resources. I thank Dr. Kray Luxbacher for taking time out of her schedule to be on my committee. I also would like to show gratitude to the entire Mining and Minerals Engineering faculty and staff for their help and guidance.

I thank Ben Fahrman and Brent Slaker for their constant guidance and support. I would like to thank Yuncong Teng and Ben Owsley for their assistance in the field. I would like to thank Joseph Amante for his assistance with the lab equipment and Mike Kiser for his general help. I would like to thank the other members of the ground control research group for their input: Kyle Brashear, Billy Thomas, Xu Ma, Enji Sun and Will Conrad. I also thank every other graduate student in our program for their help and support. Thanks to Amritpal Gill and Jacques Delport for their help and resources for the electronic components of my research.

Thank you Jim Waddell for constructing the devices used in my project as well as Robert Bratton for generously assisting with my research and nurturing my interest in mining and mining technology. Thank you to J. H. Fletcher & Co. for allowing me to use their facility, resources and employees to conduct my testing

And lastly, a huge thanks to my loving friends and family for everything they do for me and for believing in me. Thank you to Scott Sr. and Jacqualine Russell for your love, support and sacrifice on my behalf. Thank you to my parents, Scott Jr. and Donna Russell for their support and investment in my success.

Table of Contents

List of Figures

List of Tables

Chapter 1: Introduction

Mining has served the societies and economies of the world for hundreds of years by providing jobs, resources and technology that have far reaching benefits. It is unlikely that mining will ever not have a place in the world considering the growing rate with which humans require valuable minerals and coal. Mining will continue to pose risks from use of vehicles, electricity, powered haulage, as well as the hazards of fires, explosions, and gound falls. Considering the nature of excavating rock masses and subjecting the rock material to physical and chemical changes, the risk of ground related incidents is likely to exist as long as underground structures are excavated.

According to the National Institute for Occupational Safety and Health "Mining Topic: Ground Control Overview", almost 40% of fatalities that occurred underground coal mining between 1999 and 2008 and were the result of stability failure in the face, roof or rib (2012). According to the same source, the fall of rocks between roof supports injures between 400 and 500 miners per year ("Mining Topic: Ground Control Overview", 2012). It has been argued that ground control will be more technically challenging as a result of the need to develop mines in deeper areas or areas with more difficult conditions in order to combat dwindling resources.

The study of ground behavior in mining has brought to light a number of topics that require further investigation. Some of these topics, such as large scale modeling, pillar bump analysis, support optimization and subsidence are given considerable attention and research. There seems, however, to be a lack of investigation in the ability to obtain strength characteristics of mine roof strata at the face and along the panel. Possible prohibitive factors for further investigation in this field may be the hurdles of intrinsically safe equipment certification

as well as a distrust in the ability to make good measurements in such a heterogeneous material. This study covers the design and use of a tool that explores the task of analyzing and categorizing mine roof.

The gathering of information about a rock mass requires the investigator to impart some type of energy into the rock and then analyze the response of the rock. Several tests exist that do this in a lab setting, such as Schmidt hammers which use rebound characteristics of a metal rod on rock masses to determine rock traits. There also exist primary and shear wave tests that use the transmission of waves through a rock mass to gather information about its properties. Most notably, destructive test methods such as the Uniaxial Compression and point load tests or the Brazilian test relay valuable information about rock behavior. Recently, several highly instrumented and controlled testing methods have been developed that provide details about the strength of rock masses in the lab setting without the use of destructive testing methods.

It is hopeful that one of these non-destructive, rock-surface implemented tests could prove to be a means to gather strata properties in a mine setting. The current method of taking a core sample at a mine and coupling it with laboratory analysis is simply too expensive to be able to be considered a suitable roof strength analysis method. Primarily, rock core analysis lacks enough resolution across a property to make widespread entry or panel scale judgments on ground conditions because so few cores are logged on account of their cost. Core analysis also lacks the ability to indicate the changes to the immediate roof strata that would be induced by excavating a room and subjecting the strata to gravity loading. In light of these issues of resolution and cost prohibitive factors, a cheaper, easier and more widespread testing method is needed.

One of the current methods of analyzing the competence of mine roof mid-shift entails a ground inspector running the tip of a tape measure (the off-the-shelf variety that can be found at any hardware store) up the length of the legally required test holes. Test holes in this case refers to the required empty drilled holes that extend 1 foot past the deepest bolt depth in the roof [30 C.F.R. §75.204 (f)(2)]. As the tape measure tip is run along the length of the hole, the bent metal tip of the tape is expected to nest itself in any discontinuities that the roof material may have. Additionally, the inability to extend the tape fully up the hole indicates an obstruction in the roof hole such as shifted roof layers. This test is described in the interactive training lesson for roof bolters (MSHA - Interactive Training - JTA Spiders – Roof Bolter Operator). This tape measure test serves two functions, it indicates the presence of any such discontinuities and bed separations as well as providing an indication of the distance up the hole that the discontinuities exist. While being a good inexpensive test method, this fails to properly extract all the useful information that may be contained in one of these test holes.

Another method of analyzing the composition of the roof is less desirable but more informative. Ground control experts can learn about the roof by looking in areas where a large scale collapse has already occurred. If they can inspect the roof cavity where the rock fell from, they can often see fracture networks that are difficult to interpret by looking only at the skin of the mine roof. Furthermore, this can be a good way to look at the stratigraphy of the immediate roof and see if there are any obvious weaknesses in the roof layers. Depending on the conditions of the roof fall, conclusions about the anchorage characteristics can be drawn. For instance, if the grouting or anchor shell of the bolt is visible in the fallen roof material then it is likely that there was some kind of slippage or loss of anchorage integrity. It also allows the damage inspector to look more closely at the qualities of the strata that the anchorage mechanism is attached to and if

that rock mass has the strength characteristics that it was assumed to have when the bolt was first installed.

In general, the practice of in-cycle roof analysis is often left up to the experience of the bolters. They are the individuals that have the most information about how the drills behave in the roof strata and if there are any conclusions that can be drawn from the drill behavior about possible roof composition and competence. Stewart, et al. outline a roof control program in their 2006 paper that explains a coal mine's use of "Lith-Graphs", which are qualitative forms filled out by bolters as each test hole is drilled. These forms have spaces where information about bit wear, water presence and possible voids are recorded and then provided to the geologists and engineers (Stewart, et al., 2006). Foremen and geologists are encouraged to introduce supplementary support in areas where the roof is troublesome on the basis of information found in these "Lith-Graphs" as well as from discussion with the bolters and observations of roof conditions (Stewart, et al., 2006). The inclusion of information from a quantitative roof strength evaluation test, i.e. the one outlined in this paper, would certainly help compliment and justify some of the roof control decisions that ground control experts, foremen and mine workers will be making about the presence and degree of installed auxiliary support.

The goal of this project is that attention can be given to the apparent lack of panel-scale or entry-scale quantitative ground analysis tools. Prior literature is explored to see what kind of tests exist that could be readapted to bridge this knowledge rift, or at the very least, inspire additional investigation into that technique. The literature review should serve as a good reference for anybody that hopes to find new ways to measure rock properties that go beyond the traditional destruction methods such as, but not limited to Uniaxial Compressive Strength (UCS),

Point Load, and the Brazilian Tensile Test. The creation of a device that evaluates the selected quantitative analysis method(s) for feasibility in a mining setting is also expected.

This device is to be used by people with little to no assistance from powered machinery except for simple transportation of the unit and should therefore be portable. The device should be useful in areas that are out of the mining cycle i.e. not modifying or adding to existing equipment. Ease of use, portability and accuracy will encourage mines to use such a device instead of avoiding it when the information gained from it is not worth the loss in productivity. Above all else, this device should not diminish the stability of the current mine ground or interfere with ventilation in any way and should put the operator at little risk of injury. Ideally, this device will inspire others to continue research in the area of underground strata characterization and hopefully provide enough technical information to advance the ability of other researchers to develop their own devices or expand upon this one.

The principle aspect of the design is to control the motion of a device that interacts with the walls of the borehole. The control of the motion allows each hole to be analyzed relative to itself on account of the similar motion characteristics. Through the interactions with the borehole wall, changes in forces applied to the device are expected in the presence of differing rock types. By looking closely at these force changes and where their changes occur in the borehole, an understanding of the strength and position of constituent rock layers can be gained. The device created for this project addresses the position and removal force of a scratching mechanism in a borehole and monitors those parameters in an effort to extract changes in rock type and properties.

Chapter 2: Literature Review

Geologic Background

Coal seams are notable for their deposition mechanisms and for the way that these mechanisms ultimately define the nature of the adjacent strata. The coal deposits of the eastern United States are the byproduct of swamps left undisturbed for many thousands of years such that biomass accumulated and eventually began coalification (Molinda, 2003). Molinda elaborates on the presence of these swamps and how their eventual coal thickness, middling properties and roof content is subject to the dynamic behavior of ancient river deltas (2003). This is due to the buildup of sediment within the delta network and how it forces a redirection of the distributaries of the river as it drains into a larger body. What was once a swamp gets covered by redirected river water and becomes a new depositional area for sands, silts, clays and other fine rocks which form the roofs, riders and floors of future coal mines (Molinda, 2003). The variety of mining conditions (both favorable and unfavorable) that these processes later induce prove to be the core of the subject of ground control. This variability in ground conditions highlights the concept that any good information on the geology of a coal seam and adjacent strata will be of great help to engineers charged with mitigating their hazards.

A proper characterization of strata is widely believed to be one of the most crucial elements of an effective ground control strategy. Iannacchione and Zelenko speak on the importance of strata characterization in their 1995 work on coal mine pillar bumps by outlining the relationship between thick sandstone layers above and below the coal seam and the corresponding likelihood of violent pillar activity. It is probable that the presence of these massive layers would be detected through traditional methods of geostatistics namely analysis of

logged cores. This is a very useful system but its shortfalls are outlined by Mark, McWilliams, Pappas and Rusnak in that there can be a great deal of Unconfined Compressive Strength (UCS) variability within analyzed individual rock layers, the difference of the same layer between logged cores at different locations can be even more striking (2004). This variation in UCS among the same formation serves to outline the need for more resolute ground control analysis techniques.

Coal Mine Roof Characteristics

Generally, a robust sandstone layer in the roof is considered a favorable geologic feature as it can provide a good anchorage region for a bolt. This is especially true in shallower mines where having that massive sandstone layer wouldn't subject the coal pillars to catastrophic burst failure from the excessively high geostatic stresses seen in deeper mines. However, there are accompanying negatives with having sandstone as a roof. Molinda and Mark describe in their 2010 work on ground failures in weak rock that an interface between sandstone and an underlying shale layer can be riddled with discontinuities and can lead to a frail and unfavorable roof. Although the strength properties of this interface may be difficult to quantify, the location of the sandstone-shale transition is crucial knowledge whoever decides the bolt anchorage depth. The benefits of knowing where sandstone layers are in the roof are obvious and a device that could locate them would better inform choices about roof control design.

Mark and Molinda continue to describe negatives of sandstone by establishing that sandstone layers can serve as a vector for groundwater contained within an aquifer (2010). This sandstone can introduce water into the adjacent shales which are often sensitive to moisture and lead to a crumbly, problematic roof layer (Molinda and Mark, 2010). It was later suggested in that same work that the presence of a test hole may help to bleed the sandstone layer of the water and help slow the time-dependent, moisture-induced degradation of the underlying shaly rock. Again, the knowledge of the relative position and composition of these layers is important to correctly mitigating their complications.

The ability to detect the presence of stackrock, thinly interbedded layers of shale and other friable rock layers, is key to catering a ground control plan to local mine areas. Methods of controlling these features are outlined in the 2008 Molinda, Mark, Pappas and Klemetti paper on

ground control issues in the Illinois basin. Generally, it is suggested that overlaying sandstone or limestone beds are to be sought in the roof strata around these stacked layers to serve as a strong anchorage horizon for the bolt (Molinda, Mark, Pappas, and Klemetti, 2008) (Molinda, Mark, 2010). In fact, Molinda, Mark, Pappas and Klemetti go on to suggest that in the presence of a thick limestone layer, a solid one foot minimum of resin anchorage should be rooted in the overlying limestone to give good suspension support to the weaker underlying layers (2008). With changing thicknesses of limestone and stackrock formations, it is clear that the capacity to make more detailed surveys on the position and dimension of these layers is advantageous. The benefit that would come from having a tool to travel up a test hole and make analyses about the roof composition is undeniable, especially considering the great number of test holes that can be accessed.

The presence of rider seams in coal mines is another noteworthy geologic hazard. According to Molinda in the 2003 Geologic Hazards and Roof Stability in Coal Mines, rider seams are thin coal beds (6-48 inches) that overlay a thick, mineable seam. There is often a small formation of shale between the main coal seam and the rider seam, this interlying shale layer has a low formation strength of 28-40 for the CMRR index (Molinda, 2003). Rider seam thickness and position in the roof can be difficult to categorize and there can be a number of them in the immediate roof layer, further complicating any strategic plan for mapping them. If several adjacent bolts anchor within a rider seam, failure can occur because this seam loses structural integrity easier than other, more solid layers (Molinda, 2003). The wide array of dimensions for rider seams requires a systematic, consistent approach for monitoring. The most effective method for detecting and categorizing rider seams is regular test holes that cross the rider layers and allow the ground control expert to make conclusions about their location (Molinda, 2003).

The presence of clay in the roof matter is another of the principal hazards that changes ground integrity. Clays typically form in veins that intersect the seam and can have a dramatic impact on the solidarity of the roof, so much so, that they were the cause of 90% of ground falls at some mines in Pennsylvania and Illinois (Molinda, 2003). As is typically the case with these roofs, the suspension of the weak clay and shale from a sturdy limestone or sandstone beam of suitable thickness is essential to keeping the entry open (Molinda, 2003). There is a great need to collect and systematically process the thicknesses of the roof material in these areas, as having conclusive strata thicknesses and positions are necessary for the proper anchoring of the bolts and implementation of sufficient supplementary support (Mark, Molinda, and Burke, 2004).

Due to the wide variety of roof conditions outlined in this ground control review, the need to determine their presence in a mine setting is deemed pressing. The fact that the modes of sedimentary rock deposition tend to manifest themselves in horizontal formations, is important because a vertical test hole would likely cross several different rock types between the collar and its deepest point. This provides a valuable opportunity to use a single analysis technique in a single hole that would establish interaction with several different rock layers and expose possible risks to miners that are not immediately visible to them. There are several different analysis techniques to explore that can indicate strength characteristics of these roof rocks.

Rock Analysis Methods

The use of roof drilling parameters to back analyze the characteristics of rock is a promising technology that has the support from industry experts and academic researchers alike. This technology, while providing relevant information on roof strata composition, is beyond the nature of this study because it is purely within the operation cycle and bypasses the desired portability and free implementation of the roof strata analysis device to be constructed in this project. Using a roof bolter to drill new holes for collecting strata strength data would be ineffective at analyzing the roof strength characteristics of mine areas that may not have had any new roof bolts installed in a few years and a roof drill is unlikely to venture again. A portable roof analysis device would function well in a place where it would be economically unfeasible to bring a well-instrumented rock drill into the area to drill a handful of exploratory holes that would determine roof strength parameters.

The process of categorizing roof conditions from drilling data has been attempted on several different occasions. The bulk of attempts have capitalized on Teale's original calculations of drilling parameters and how they relate to the intrinsic specific energy (ε_{10}) of the rock (1964). The equation for specific energy obtained from drilling parameters can be seen below:

$$\varepsilon_{10}(psi) = \left(\frac{F}{A}\right) + \left(\frac{2*\pi}{A}\right)\left(\frac{NT}{u}\right) \qquad \text{Equation (2.1)}$$

Where T (in.*lb) is the torque applied to the drill string, u is the penetration rate (in/sec), N is the rotational velocity (rev/sec), F is the penetration thrust (lbs), and A is the area of the hole (in.^{2}) (Teale 1964). This equation is the sum of the constituent elements of a drill's cutting mechanism, a rotational scraping and a thrust gouging. Taking these two elements into account, the amount

of energy require to remove rock material can be calculated, this same principle will be later discussed to describe energy used to excavate rock via scratch mechanisms. In recent years, several additional authors have used this information to try and incorporate it into the analysis of strata properties. Most recently, the application of systematic evaluation of drilling parameters (and therefore strata properties) as well as a suitable background on the evolution of research in the field can be found in the 2013 work by Bahrampour, et al..

Adapting the technique of using drilling parameters to analyze rock would be useful if it could be made portable and effective. This method was explored in 1996 by Reddish and Yasar wherein an ammeter was run in line with a hand drill that was attached to a drill mount to determine the electrical current applied to a motor for torque and rpm values. Useful parameters about drilled rock samples, namely intrinsic specific energy and therefore UCS, were obtained by standardizing the bit properties and the torque/rpm applied to the bit and by using a mount to keep a standard penetration pattern (Reddish and Yasar, 1996). This rock analysis process could be made relevant to ground control experts because they would be able to take hand size samples from the roof strata and extract the strength characteristics of the material.

A further application of this test method would be to note the location of collected underground rocks and take them to a lab on the surface to have them analyzed and categorized, thus giving a location specific database of strength properties of certain roof layers. This systemic approach would also bypass the issues of rendering this hand drill safe for methane air mixtures as the drilling and analysis would take place outside of the mine environment. This test would be biased towards the shallowest roof layers (the skin layer) as it is the one most likely to be falling at any given time. Nonetheless, this idea still may prove useful for providing inputs to determine ground control techniques for controlling the behavior of the skin and immediate roof.

One non-destructive rock analysis technique that shows great promise is the study of indentation tests. In this case, non-destructive means the entire sample is not destroyed during the testing process as is seen with some current testing methods like the Brazilian and point-load tests. Indentation tests feature a hard metal tip of known geometry that gets pressed into a rock while the displacement and applied load are recorded. This testing procedure was covered extensively in Szwedzicki's 1998 work on indentation and it's relation to rock hardness. The mechanics of the indentation test rely heavily on an accurate means to monitor the load applied to the conical tip and the amount that it has displaced. A diagram of the platen-rock interface can be seen in Figure 2.1.

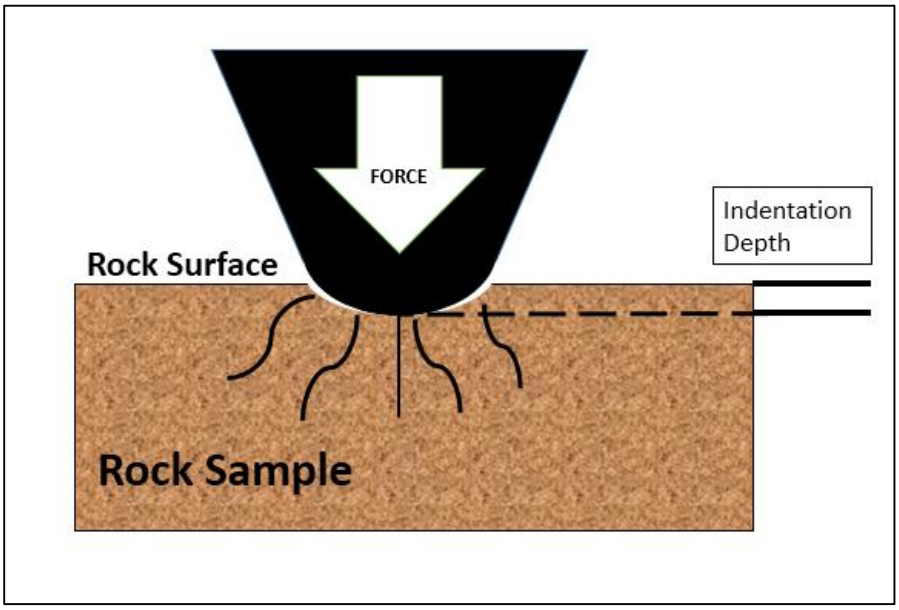

Figure 2.1: Rock Indentation Diagram Showing Crushing and Indentation

In Szwedzicki's paper, an IHI (Indentation Hardness Index) was calculated by the following formula:

$$IHI = \frac{L}{D} \qquad \text{Equation (2.2)}$$

where L is the applied force in (in kN), and D is the tip penetration depth (in mm) (1998). These values are recorded throughout the experiment and when plotted on the same graph, stop at the point of first chipping in the sample. If no chipping occurred, then the reference becomes penetration depth at a 20 kN load or the associated load at the predetermined depth of 1 mm, using whichever condition that is reached first (Szwedzicki, 1998). The Indentation Hardness Index was correlated with uniaxial compressive strength (IHI) to yield an obvious trend, the trend can be expressed by the equation:

$$UCS = 3.1 * IHI^{1.09} \qquad \text{Equation (2.3)}$$

where UCS is in MPa (Szwedzicki, 1998). The simplicity of this test is one of its advantages, requiring few inputs and no extreme testing procedures or tools. Additionally the variability in its results are comparable to other rock strength test such as the UCS test and the Brazilian Tensile Test (Szwedzicki, 1998). It also reinforces the notion that UCS indices can be obtained from simple tests looking at forces and displacement within the rock.

The final rock strength analysis method to be analyzed in this paper is the scratch test methodology developed by G. Schei and E. Fjær SINTEF Petroleum Research based on work conducted by University of Minnesota professor Dr. Emmanuel Detournay. This sedimentary rock testing technique is predicated on continuously logging information about certain cutting parameters of a scratch bit that is equipped with precise kinematic and force controls and is dragged along the length of a core sample that is saddled in a housing (G. Schei et al., 2000). This type of testing, commonly referred to as “scratch testing”, shows great promise for providing inexpensive, quick and useful information about strength characteristics of sedimentary rock without the need to destroy the sample in the process (G. Schei et al., 2000).

The test works by compiling force and cutting depth values and assessing how they correspond to rock strength properties such as compressive strength and elastic modulus.

Primarily, the test controls the depth of cut and the velocity at which the cutting head moves along the core sample (on the order of several mm/s) while monitoring the force applied to a cutting head (G. Schei et al., 2000). The depth of cut and velocity of the cutter are controlled electronically by a computer that sends user inputs about preferred depth and velocity to stepper motors that adjust these parameters. Schei et al. explain that the reason that cutting depth is controlled is that for shallow depths of cut, between 0.5 and 2 mm, the rock behaves in a ductile fashion along the leading edge of the cutting surface (2000). When the cutting depth is increased past this range, macro-scale rock failure behavior takes over and the rock begins to fail with larger, more sporadic failures in the form of chipping (Suarez-Rivera et al., 2002). It is in the ductile region that the scratch test is performed.

The value of horizontal force used in the scratch test is essential for computing the value that actually correlates with uniaxial compressive strength, intrinsic specific energy (ε_{10}). This unit is the same as what was mentioned in R. Teale's research and equals the amount of energy needed to remove a given rock volume, in this case by scratching it (Suarez-Rivera et al., 2002). The formula for this value as obtained from Suarez-Rivera's 2002 paper is seen below:

$$\varepsilon_{10}(psi) = \frac{F_h}{w*d} \qquad \text{Equation (2.4)}$$

where F_h is the horizontal force average from the tested zone, the w is the cutter width and d is the depth of cut (width of cut times depth of cut equals extracted rock area). Note that the units for Equation 2.4 are equal to that of pressure, which is the unit for intrinsic specific energy (Energy per unit volume) where one of the length dimensions from the energy and volume term

cancel to form force per area. The horizontal force is measured from the testing device as the force imparted on the cutter parallel to the rock face. Schei et al. reported an R^2 between UCS and ε_{10} of 0.9092 for dry sandstones and an R^2 for UCS and ε_{10} of 0.8779 for dry carbonates in their 2000 work on scratch testing. The 2002 research by Suarez-Rivera et al. reported an R^2 between UCS and ε_{10} of 0.864. This indicates the relationship between intrinsic specific energy and uniaxial compressive strength.

Overview of Current Rock Analysis Devices

This scratching technology was brought to patent status by inventors Bertrand Peltier, Emmanuel Detournay (mentioned earlier in scratch test research), and Anthony Booer. In this patent, US 5,323,648 A, a tool for being lowered into a gas well borehole with scratching capability was described, featuring transducers for measuring forces and scratch depth. The scratchers suggested in the patent are made from Polycrystalline Diamond, and are imparted into the rock by an unspecified force generating element (US Patent No. 5, 323,648 A, 1994). No information regarding the successful development or implementation of this device in a field setting was found.

The Formation Evaluation Tool patent was later referenced for the development of a laboratory core log analysis device for which the patent was awarded to Terratek inc. out of Salt Lake City, Utah. This device, patented under the title "Apparatus for Continuous Measurement of Heterogeneity of Geomaterials", was invented by a team of individuals of which Roberto Suarez-Rivera (author of a technical paper on scratching referenced earlier in this paper) was a member. This device functions by traversing a scratching head under precise kinematic conditions and closely monitoring the resulting force and depth of cut being applied to the scratcher (US 8,234,912 B2, 2012). This device entered development and is used by Schlumberger to do scratch evaluations on cores that they logged for the development of oil and gas wells.

An additional scratching device has already been patented for evaluating borehole wells *in situ*. The patent is held by Chee Phuat Tan of Kuala Lumpur, Malaysia under the assignment of Schlumberger Technology Corporation. This patent descriptions explain that the device was designed to function by making scratches in the rock mass with powered arms and measuring

their depth into the rock mass with calipers that seem to follow the groove put into the rock by the scratchers (US Patent No. 7,921,730 B2, 2011). According to the information in the patent, the device is also capable of operating by using a video camera within the borehole that can take images of the scratches in the formation and compare them to known values of indentation for strata (US Patent No. 7,921,730 B2, 2011). It does not appear that this device has ever been used in a field setting and its functioning theory is only based on preliminary lab experiments. Considering the number of researchers who have determined accurate rock strength analysis methods as well as the growing number of inventions that use their technology, there are sure to be many more ways to successfully apply these techniques to draw conclusions about rock properties.

Chapter 3: Product Design

Design Introduction

The objectives of this design are for the device to identify changing layers of rock by interacting with the wall of a borehole. To take full advantage of all the information that may be contained in the borehole, it is important to try and extract information such as rock strength and changes in rock type that the previously explained tape measure/inspection hole test overlooks. Further, the use of outputs from this device to calculate strength values of the rock layers that it is interacting with is desired.

The design of this device must abide by several constraints in order to be useful in the location in which it is expected to work. The first element is the size constraint, the device must fit in the legally required test holes which are commonly one inch in diameter. This prevents the complication of drilling another hole in the roof and opens up many old areas to roof analysis. It additionally is constrained to be safe to operate, portable and quick to assemble. It must function in a self-contained manner, based on forces that a user generates, and with no extra power systems being run to it and it would ideally be permissible for methane air mixtures.

Given the size constraints on any device expected to fit in a test hole, a certain hierarchy was given to each possible rock analysis method so that the best process would be used. Issues of portability remained in the forefront of the design choice, but seeing as it is accomplished on account of the scale of the device's operating conditions, namely the one inch hole, and the widespread availability of transport equipment in most mining settings, maintaining mobility was easy. The acknowledgement of the size of the borehole led to the conclusion that the more of the

device that could exist outside its very limiting size constraints, the better a design choice it would be.

Immediately, issues arose when considering the use of the indentation analysis system namely because of the restrictions on size. When the experiments were conducted by Szewedzicki, the large hydraulic cylinder allowed precise displacement control normal to the rock face (1998). Furthermore, they had the potential to generate tens of kilonewtons of force and often had forces of that magnitude for Szewedzicki's test (1998). This is prohibitive in the field setting because in order to increase the force imparted on the rock surface by hydraulic pressure, the hydraulic cylinder must either increase in area, or the indentation tip must be reduced in diameter.

Noting that the hydraulic piston could never get larger than the borehole diameter of one inch (and even in the best conditions would still need to be considerably smaller than that), an enormous amount of hydraulic pressure, on the order of 20,000 psi, would need to be generated to get comparable forces (4000-8000 lbs) seen in Szewedzicki's 1998 experiment. This would also force the user to have to maintain the hydraulic fluid levels in the system, not impossible, but adding an undesired level of complexity. Additional pitfalls with indentation testing include the safety aspect of working with high pressure fluids as well as the lack of precise pressure control of the hand pumps that would have to be used to generate the necessary pressures.

The borehole size also restricts the ability to determine the amount that an indentation tip displaces into a rock surface, which is necessary to derive UCS by Szwedzicki's methodology (2002). Precise linear displacement transducers that determine such movement are very expensive and one could not be found that could conceivably be expected to fit in a borehole in such a configuration that it would be able to measure relevant displacement. Especially

considering that the indentation movement would likely have occurred perpendicular to the long axis of the borehole, which is the most confined dimension. This would require an intricate, custom designed mechanism to monitor the forces and displacements of the indentation tip in the rock mass and was thought to be too complicated for a first look at strata composition evaluation.

Scratch Head and Scratchers

The size constraints indicated that a scratching mechanism may be the most useful rock analysis method for such a small area. It provides a useful, quick, nondestructive method for determining position-specific (and therefore strata-specific) mine strata characteristics. This categorization would be useful for analyzing the competency of the anchorage layer of roof bolts and cable bolts as the anchorage depth for these devices is regulated in a mine. Moreover, by having a continuous scratch log of the wall of the borehole, any serious discontinuities may manifest in the data, which would provide useful information about the jointing network in addition to the roof formation's strength characteristics.

The acknowledgement of the merits of the scratch analysis method require one to consider the way that a scratcher would be inserted into the borehole. Firstly, the scratcher has to constantly be applying force to the rock face that lodge the scratcher tips deep enough in the rock surface to enter the ductile rock failure phase of scratching. It is in this depth of rock scratching (0.5 to 2 mm) that Schei et al. explained that scratch tests are valid and that their equations explain rock failure (2000). Insertion of this mechanism into the rock mass would ideally be done in a manner where the scratch tips would be allowed to expand into the surrounding strata after insertion. In other words, this device works by an unobstructed insertion followed by expansion of the scratch heads and then a well instrumented, controlled removal of the resistive scratch head wherein the relevant scratching parameters would be monitored. It is under this basic design principle that the Mine Roof Strata Analysis Device (MRSAD) was created (in other literature about this project, the device is referred to as the *In-Situ* Technical Compression and Hardness Evaluation System, or ITCHES).

The scratch head is the pivotal element of the system and its proper design is essential for the device to function as the theory would require. The scratch head serves as the housing for the scratching mechanism as well as the element that translates forces generated by the pull of the user to the scratcher mechanism and then ultimately to the rock surface. The scratch head is a modified one inch diameter steel rod with a hole drilled the full diameter of the rod perpendicular to its long axis and a 5/8" diameter rod welded to the top to act as a wraparound for the tension cable. The material chosen for the head is stainless steel because of its hardness and resistance to oxidation, which was expected upon use in a moist environment. The following image, Figure 3.1, was taken of the scratch head, with a number three on it, displayed next to a one inch borehole:

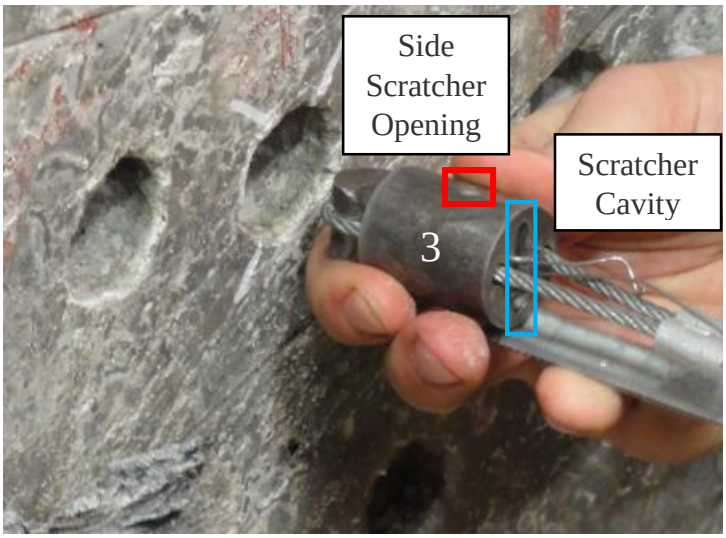

Figure 3.1: Scratch Head Immediately Prior to Insertion with Red Box around Side Scratcher Opening and Blue Box around Scratcher Cavity

The hole that the scratcher tips comes out of is viewable just to the left of the installers thumb, highlighted by the red box. This hole, called the side scratcher opening, continues through the housing to the other side of the head. There is a cavity on the bottom of the head, outlined in the blue rectangle, which provides an area to aid in the installation of the scratcher and scratch head.

This cavity exists because the design of the scratcher mechanism was contingent on having a volume into which the scratcher could deform to provide relief from the scratcher force during installation. Four additional holes (0.041” diameter) were drilled at the base of the scratcher so that stabilizing rails could be installed to keep the scratcher from shifting during operation and installation. A detailed drawing of the scratch head is visible in Figure 3.2 on the next page:

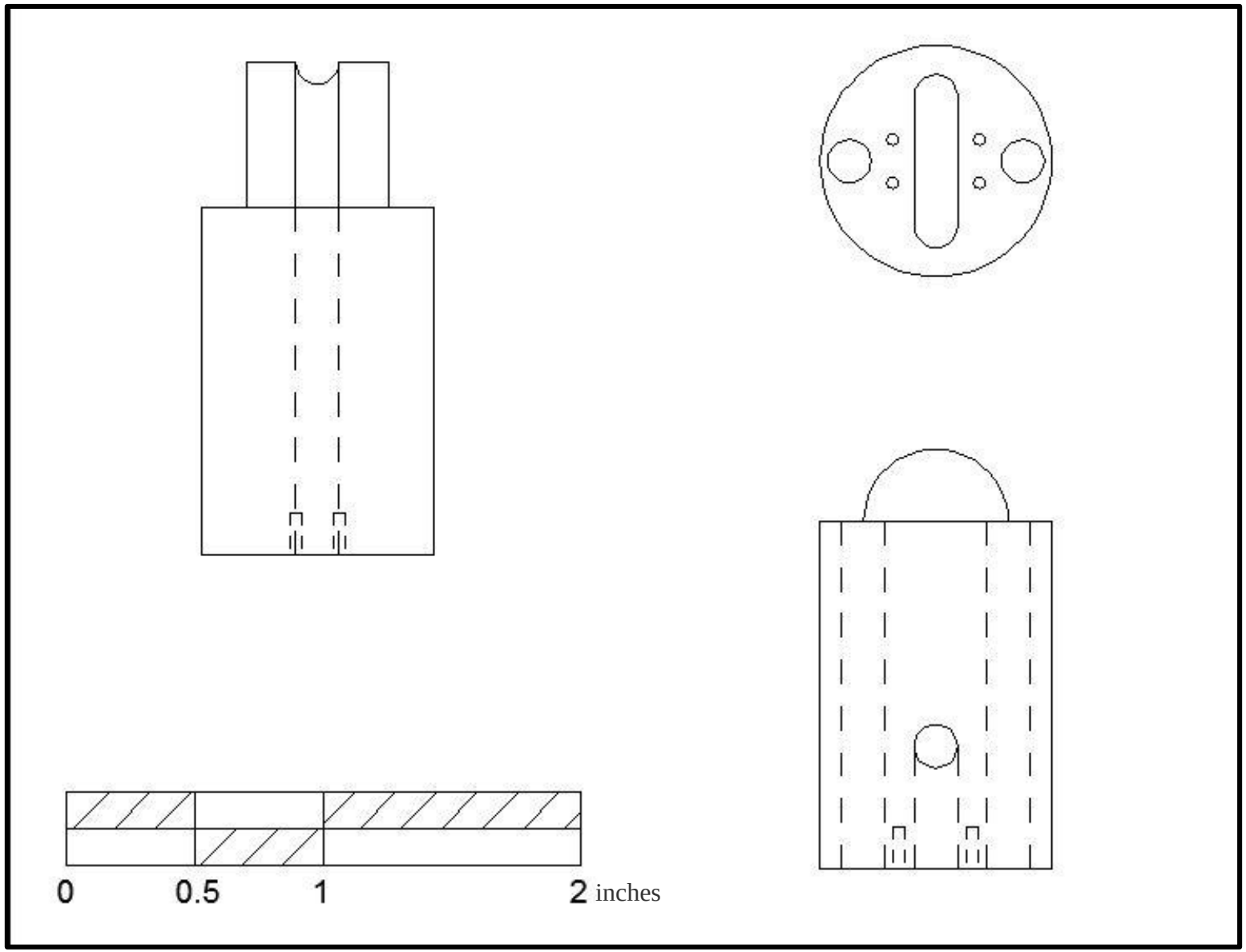

Figure 3.2: Detailed Drawing of Scratch Head - Scale in Inches

The side scratcher opening provides the holes through which scratch tips would extend into the rock face after this head was placed up the borehole. In Figure 3.3 below, a cutaway view of the scratcher housing can be seen:

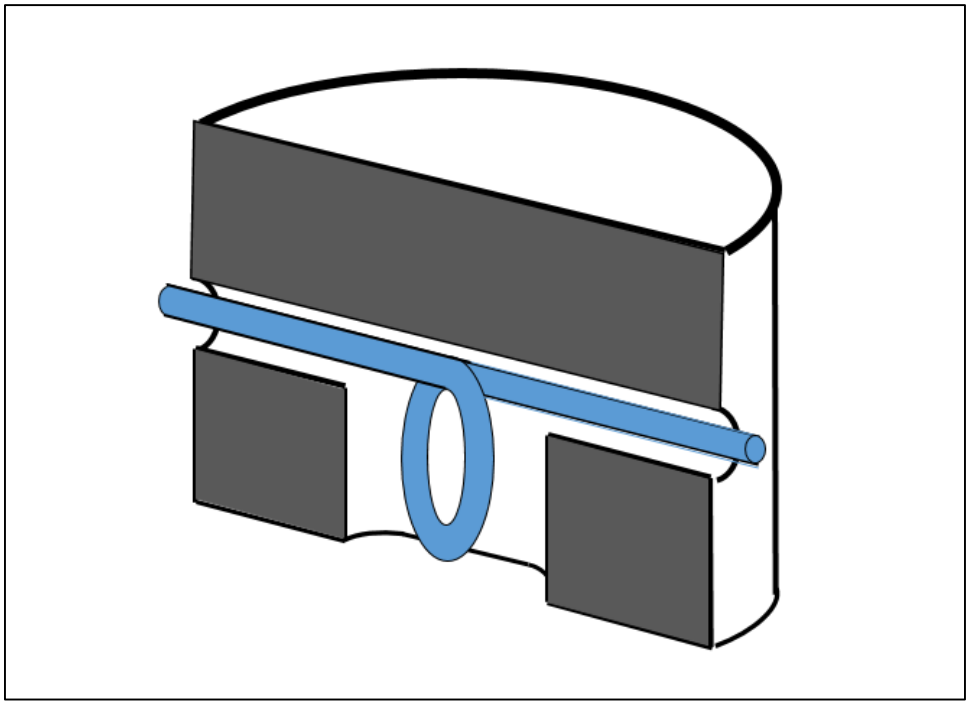

Figure 3.3: Cutaway of Scratch Head with Scratcher Shaded Blue

The scratcher is shown in blue and is in its installed state where the tips extend beyond the geometry of the head and into the surrounding strata. In order to get the head installed the arms of the scratcher are retracted by pulling the entire scratcher with a downward force into the cavity at the base of the head.

In the following image, Figure 3.4, this process is shown in a similar fashion to the one seen in previously in Figure 3.3:

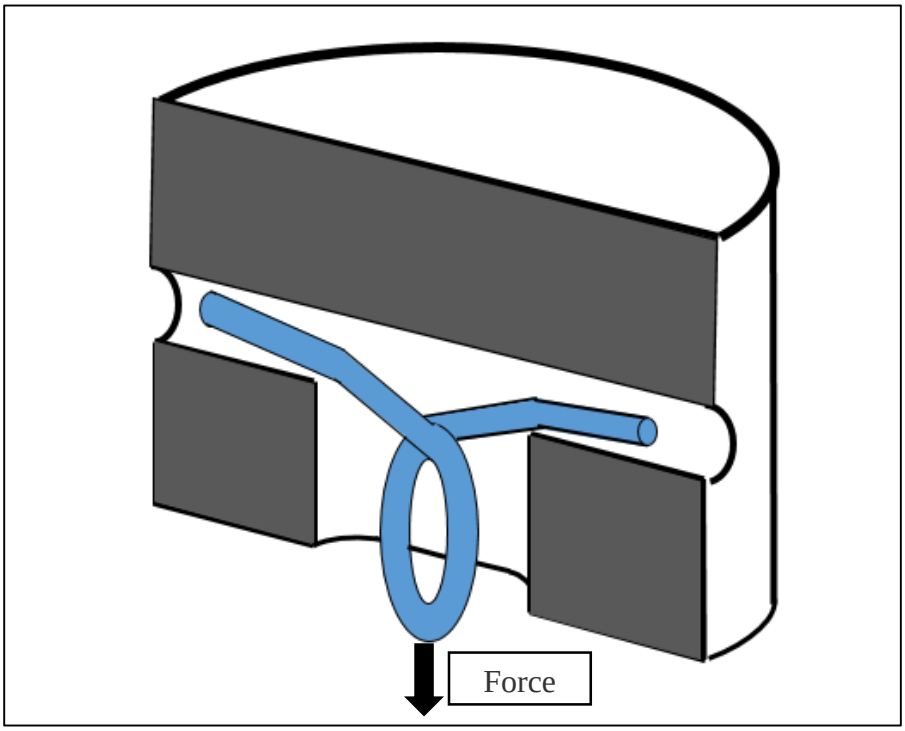

Figure 3.4: Retraction of Blue Scratcher Arms into Scratch Head Cavity from Downward Force

Take note of the fact that the loop moves downward from an induced force between Figure 3.3 and Figure 3.4, indicating that tension is being put on the loop of the scratcher causing the tips to retract into the openings of the head. The scratcher loop seen in Figures 3.3 and 3.4 would be pulled down by hand by a loop of wire that runs out the length of the borehole, this added tension pulls the tips of the scratcher into the head housing and the head can then be inserted into the borehole without the resistance of the scratch heads against the strata.

The scratchers are made from ASTM A228 stainless steel music wire of diameters 0.045”, 0.051” and 0.055”, as all were explored as possible sizes. Music wire was selected because of its hardness and resistance to fatigue, while still having the flexibility to undergo the

necessary deformation to be installed. The wire scratcher does scratch the sides of the borehole upon insertion as is visible in the following figure, Figure 3.5:

Figure 3.5: Scratch Demonstration on Sandstone Sample

This scratching demonstration was performed on a sample of sandstone in the lab. The lines coming down the side of the hole are from the scratchers housed in the head. No data was collected from this particular scratching test, it served simply to verify that there was the capacity to install the scratcher according to the method of pulling the scratcher loop into the cavity and inserting it in the borehole. The image above indicates this was done a number of times as the areas of rock removal are clearly outlined on the borehole wall. The scratcher is installed by way of a 0.029” pull wire that wraps around the loop at the base of the scratcher in the cavity, and applies tension to the scratcher, causing it to deform into the cavity at the base of the head.

A user generated force that pulls on the scratch head is the process by which the scratch head is retracted from the hole and the primary means that energy gets imparted into the rock mass. The scratch head has a loop of steel cable that runs through the body over the top of the

head, across a rounded top, and back through the body where it gets crimped to itself. This configuration can be seen in Figure 3.6 below:

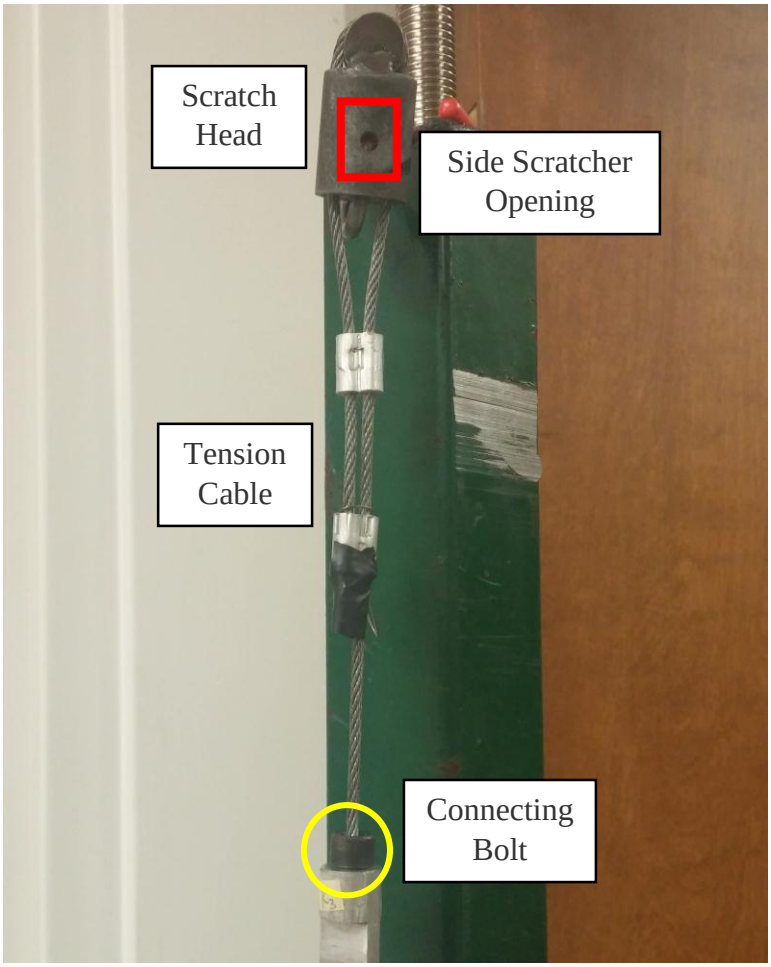

Figure 3.6: Scratch Head with Tension Cable, Scratcher Port and Connecting Bolt

The tension cable connects the head to the load cell and can be seen looping around the top of the scratch head housing. The side scratcher opening is visible in the red box within the scratch head. The top of the scratch head has a wraparound for the tension cable, this is how the scratch head is pulled, ultimately delivering the force to the scratch heads. The yellow circle in Figure 3.5 shows how the scratch head ultimately attaches to the rest of the test system by means of a

threaded bolt, called a connecting bolt, which is welded to the cable. This bolt can be unscrewed to isolate the scratching head and corresponding tension cable as one unit. When the unit is fully installed, with the scratch tips extending into the borehole wall, a coupling at the connecting bolt will provide the linkage for the rest of the tension cable to extend the remainder of the way out of the hole. It is outside the hole where tension is applied by the user to move the scratch head through the rock mass.

The interdependence of the borehole, the scratcher and the head that houses it is the principal design feature of the MRSAD testing unit. This means that the instrumentation choices were to be made after the analysis method was chosen as it was the core of the system design. When it was determined that scratch testing was going to be the method of rock analysis, the relevant parameters needed to be fully instrumented. It was known from the 2002 Suarez-Rivera et al. paper that the formula for intrinsic specific energy as a result of rock scratching had three inputs, horizontal scratching force in the numerator with scratch tip width (0.045", 0.051" and 0.055" diameter scratchers are used in the design) and scratching depth being multiplied in the denominator (Equation 2.4 in this paper). This requires the proper instrumentation of the force in the direction of scratching. Based off the use of pull forces, the movement of the scratch head would directly correspond to the movement of the cable that it attaches to and therefore any pull force in the cable is also applied to the scratch head. It is also important to note that any force imparted on the head detected by instrumentation will be divided over its two points of contact with the borehole wall.

Instrumentation

A load cell was constructed to relate the amount of force that is applied to the scratching head. This strain sensing element needs to be durable, accurate, and small enough to fit in the borehole with enough space to allow the presence of necessary signal wires and any additional installation devices. It was decided that strain gauges mounted to a specially designed element would serve well as a force transducer and would provide enough extra space to work with the size constraints.

The design of a strain element is predicated around determining the expected values of strain beforehand based on predicted load on the element and the elastic properties (Young's Modulus of Aluminum = 69 GPa) of the strained material. If the geometric dimensions of the strain element are known, then forces distributed over the area lead to calculable stresses. These stresses correspond to strain values by way of Hooke's law and elastic moduli. When strain gauges are applied to strain element, their bond to the material can be rendered ineffective if they are overstrained. It is important to ensure that applied force values should be within a range that these damaging levels of strain are not reached. Strain gauges are analog devices which only change their resistance in from deformation due to forces, meaning that the smallest useful strain value is limited by the accuracy of the data acquisition system and the environmental noise.

An I-shaped tension rod was designed to translate the tensile forces to the strain gauges. The rod is wider at the ends so that there is enough room for connecting bolts to screw into to the tension rod, the rod then thins in the middle to provide a flat surface to which the strain gauges are affixed.

A picture of the tensile member can be seen in the following image, Figure 3.7:

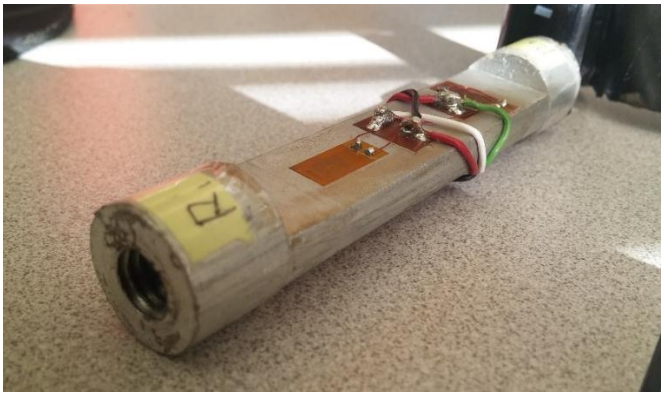

Figure 3.7: Tension Rod with Strain Gauges, Connection Terminals, and Wires

the screw opening can be seen in the bottom left of the image, it is through this chamber that the tension cable anchors to the tension rod by way of the connecting bolt.. A detailed image of the load cell can be seen on the following page in Figure 3.8:

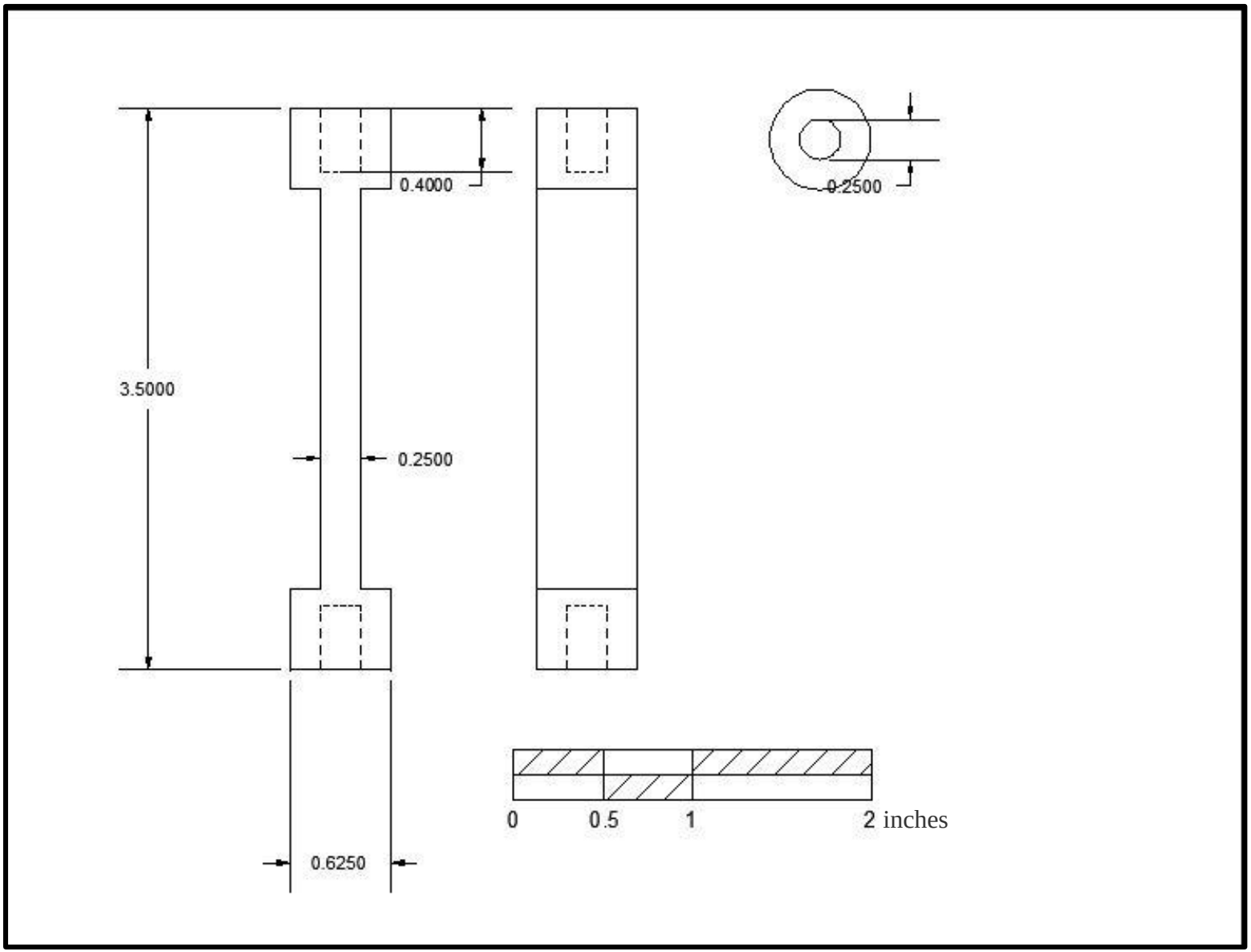

Figure 3.8: Detailed Drawings of Tension Sensing Element - Scale and Dimensions in Inches

the thickness of this tension element was designed to be wide enough to ensure easy application of the strain gauges but not so thin that it interferes with the durability of the tension member

The configuration of the strain gauges was done at the recommendation of strain gauge design guides such as “The Strain Gauge” and “Strain Gauge Configuration Types”, both sources are web documents from leading instrumentation manufacturers that indicate the merits of a full Wheatstone bridge (their source information is available in the references section). This positions two of the four strain gauges parallel to the primary deformation direction and places two that run perpendicular to this deformation, but still in the same plane as the first set of gauges. This full-bridge configuration has the added benefit of automatic temperature compensation (“Strain Gauge Configuration Types”). The strain gauges and installation kit were purchased from Micro Measurements in Raleigh, North Carolina. The strain gauges were the 250BF-EA-13 model at 350Ω resistance each. The wires were connected with 134-AWP Solid Copper Wire included in the GAK-2-AE-10 installation kit, while 22 gauge AWG wire was used on the more exposed parts. The voltage signal coming off the gauges was sent via a 25 foot 4 channel, shielded, braided and jacketed cable (Model 426-BSV) also purchased through Micro Measurements. This cable was then wired to the I/O module on the data acquisition system through the five volt excitation port, ground port and +/- inputs.

The tension force transducer had a number of features that protect it from some of the damaging circumstances that it was likely to experience in a borehole setting. Firstly, the profile of the wiring was kept as low as possible, this reduced the outer diameter of the tension member to reduce the likelihood that parts of it would snag on things in the hole or during installation. Secondly, the entire tension device was insulated with 5/8” flexible plastic tubing that was cut

and then taped to the exterior of the device. The protected strain gauge can be seen in the in Figure 3.9 below:

Figure 3.9: Force Transducer in Protective Plastic Jacket

the series of interwoven wires coming off the right of the protected load cell are the signal wires from the strain gauges. This covering protected the transducer from shock, abrasion and puncture and when that was wrapped in electrical tape, became very robust, while still being small enough to fit in the hole. The last design requirement was the use of connecting terminals between strain gauges. This provided a buffer between the different gauges that if there was any strain put on the signal wire that wasn't absorbed by other preventative features such as the taped tubing, the stress didn't manifest itself on the gauges themselves, which could damage them beyond what could be repaired in a field setting.

The method for determining the position in the borehole, as well as observing the velocity of the head through the hole is to use a string displacement transducer, otherwise known

as an extensometer. The extensometer, otherwise known as a linear position transducer, chosen for this system is the Unimeasure HX-PA-300-L3M. Extensometers function by placing a variable resistor in connection with a rotating shaft, with the shaft affixed to a string whose position is changing. A voltage change across the resistor, corresponding to a change in position, can be measured by a data acquisition system with a voltage readout. The end of the string on the extensometer was to be attached to the scratching device somewhere just below the tension sensing member, that way any force applied by the winding spool on the extensometer would automatically be accounted for in the force on the scratchers. According to the Unimeasure, inc. datasheet for this device, the tension on the spool is 2.25 lbs.

The range for the device is to be at least 20', allowing for a seven foot mining roof height as well as a 13' journey up the borehole. A steel wire extensometer made by Unimeasure was chosen that had a range of 25', allowing for a buffer to prevent overdrawing the spool which would damage the device. The potentiometer in the transducer is a one kΩ, ten-turn resistor that has a linear taper and was attached to the winding shaft by way of a precision gear. The signal wire coming of the extensometer has a ten foot length, which was suitable to attach it to our data acquisition system (an image of the signal connection between an extensometer and our DAQ can be seen in Figure A.1 in the Appendix), while keeping more fragile electronics out of the way of the operating area.

Data Acquisition and Management

The data acquisition unit used in this experiment is the National Instruments USB-6211 module. It features a USB bus port that permits configuration with National Instruments LabVIEW software to allow for easy data acquisition and management. The data acquisition system (DAQ) features an I/O module, on board five volt excitation for powering laboratory instruments, and has ports for analog as well as digital signals. There is no earth ground for this device, only a chassis ground, so all instrumentation cable shielding is grounded separately from the module via a cable that is hooked to a metal anchor. The ground circuit on the chassis simply provides a reference for the excitation voltage, without it, no current flows through the instrument. The device is not MSHA permissible, but it was assumed that the data acquisition system would function similar to one that was safe for methane air mixtures and that a future suitable data acquisition system could be substituted for this one. The USB-6211 runs off the USB device it is plugged into, making this project's entire instrumentation system (the strain gauge transducer and extensometer) fully portable when combined with a charged laptop, giving hours of portable use.

The LabVIEW software features a unique feature for assisting in making the DAQ communicate with the program. A module within the LabVIEW software, called DAQMX (or DAQ Assistant) contains all the elements to collect information and process it electronically. For this project, two channels were configured in DAQMX that allowed separate inputs both transducers while allowing them to run off the same five volt excitation source.

A screen capture of the block diagram for the LabVIEW program, with the DAQ Assistant on the left side is visible in Figure 3.10 below:

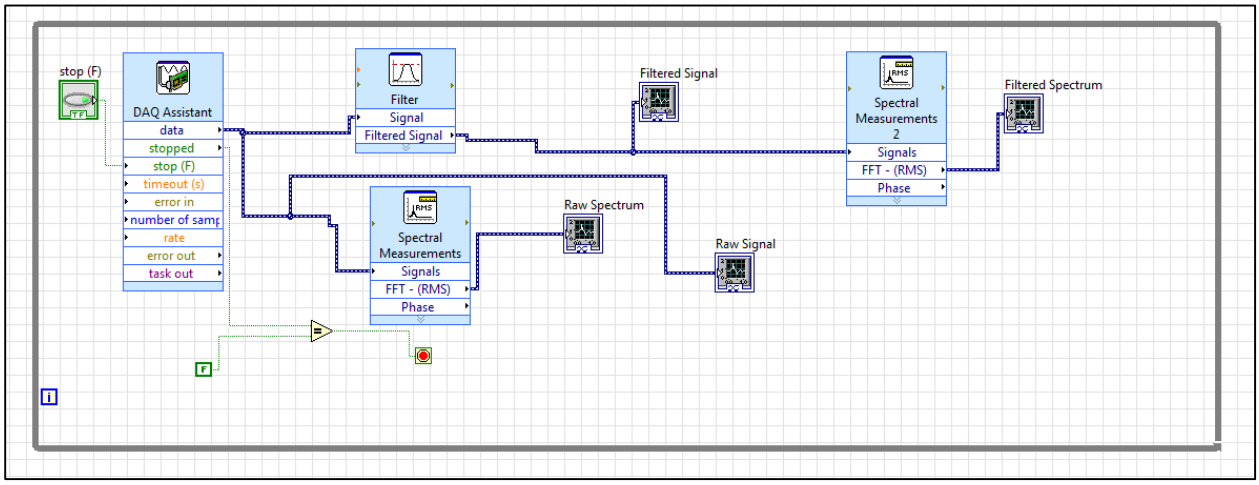

Figure 3.10: LabVIEW program with DAQ Assistant and Other Elements

the auxiliary elements visible in the image are a signal filter and two different spectrum analyzers. This allowed for easy comparison of the data readout for the filtered and unfiltered data, as well as their respective spectral components. An image of the LabVIEW Front Panel is visible in the Appendix in Figure A.6. Within the filter element, a low-pass Butterworth filter with a cutoff frequency of four hz removes the high frequency noise of the system, making the data considerably more accurate and easy to interpret.

Mounting and Installation System

A few methods of applying tensile force to the cable were explored. It was first thought that a constant-velocity electric motor would be used, but it was determined that this would be prohibitively expensive and difficult to implement/power in coal mines. Then the thought of a person simply pulling the device out of the hole by hand was considered, but the risk of injury and lack of ability to adequately control pull velocity rendered that idea unusable. This led to the adoption of using a winch, this would simultaneously handle the issues of organizing the tension cable as it came out of the borehole as well as providing a safer, more precise, tension generator that doesn't rely on electricity.

The winch selected for this device was a 1500 lb hand-cranked winch made by Torin Big Red Jacks. The spool had a selector that could do smooth, uninterrupted coiling or extending and it could do ratcheting coiling or extending so that no matter which direction was under load, hazardous and undesired slipping would not occur. A plastic drum was added to the original winding spool to increase the winding diameter to 3.45", this would make the winding process faster which is important considering how long it would take to hand wind the 30' attached to the winch. The increased wind up rate is due to the fact that each revolution had a larger circumference around which the cable wound, but this also put the steel cable under less stress to wind around the shaft which is safer, more organized and prolongs the life of the cable. It was also determined that the same 1/8" cable used for the scratch head would also be used for the rest of the tension cable.

In order to ensure a controlled insertion of the signal wires, tension cables, scratch head, scratchers and force transducer, an installation rod was designed. This rod is simply a piece of 4' long conduit pipe of around 3/4" with a slot cut the entire length. The top one foot of the device

features the majority of the pipe cut away to make a small pushing element. The idea behind this design is that all the wires will go through the slot into the center part of the pipe, protecting them from pinch points in the hole that could damage them. The part at the top that is cut away serves as a platform for the tension transducer (the largest diameter item in the borehole) and gives a tip with which the scratcher can be pushed up the hole. This device can be seen in Figures A.7 and A.8 of the Appendix. Upon full installation of the system in the borehole, the pipe could be removed without pulling any of the elements, all the while the cable would be fed through the slot cut through the side. This would leave all the cable in the hole without cutting it or damaging it while also removing the installation rod.

It was determined that for reasons of stability and consistency, that the entire MRSAD system would be affixed to a post that would brace itself against the roof and floor of the mine. This would reduce the problem of any tension (applied to the cable to remove the scratchers) manifesting itself in ways that would lead to motion of whatever was applying the tension either a person, winch or motor. Considering mines may require testing in low, and higher coal situations, this element was required to have a good deal of versatility in what variety of roof heights in which it could operate.

There are several advantages of using the stand that made it well suited for its purpose. It is simple in construction and quite robust meaning it can be assembled and dissassembled quickly and easily (on the order of one minute) and it won't get damaged from being stored in a container. The stand is comprised of a four-post base that provides stability from it tipping over, a series of fitted middle sections and a screw top for fine adjustments. The stand provides a platform to affix other elements of the MRSAD device. The winch and displacement transducer were all attached to the stand, keeping them from moving under the tension put on them, as well

as keeping the work area much more organized. The displacement transducer attached directly to the base with 3/4” bolts that ran through a piece of plastic to keep it from being too close to the floor. The displacement transducer was attached in such a way that the wire traveled as close to the stem as possible, to minimize error from not being directly under the borehole and having a horizontal component to the displacement in addition to the vertical one. The interlocking and interchangeable middle sections meant that the height that the spool was on the stem of the stand was adjustable by replacing which segments from the middle section were used in which order. This proved very useful for the eventual modifications to make the MRSAD device functional for horizontal holes as well as vertical ones.

An image showing the stand, spool and displacement transducer can be seen in Figure 3.11 below:

Figure 3.11: MRSAD Mounting Stand with Tension Winch, Roof Bearing Plate, and Displacement Transducer

in this image, the stand is lightly braced against the floor and the top of a door frame to mimic the installation conditions of being placed between a mine roof and floor. Halfway up the MRSAD tower, the brass tow winch can be seen, it is mounted to the tower by way of a series of bolts as well as a plastic riser to give it space from the stem of the unit. At the top of the stand, a

narrow silver element can be seen extending towards the roof, this is the adjustable screw component. This design feature allows for millimeter and centimeter scale adjustment to the stand height, so that it can be used in a host of different mine roof and floor dimensions. A closer image of the screw top is seen in Figure 3.12:

Figure 3.12: MRSAD Stand Screw Top and Brace Plate

the threads on the screw are clearly visible, the nuts on the screw shaft are there to aid in adjusting the stem height. There is a bearing plate between the top of the screw and the door frame. This was added to reduce the pressure on the roof surface, as well as to provide a bearing area that a roof pan, or other shim could be inserted for further reinforcement and safety.

Upon conclusion of the construction of the MRSAD, a testing facility was identified that possessed resources that would be suitable to evaluate some of the features of the device and to see if the theory behind the remote field scratch test were valid. The people at the research facility indicated that they were not able to put a rock sample in the roof mount as was planned originally and that modifications would have to be made to the MRSAD unit in order that it retain its function in the horizontal direction. This required slight modification of a few of the elements as well as relying on some useful coincidences with previous design choices. The primary concern was the need to change the winch and extensometer cable direction from vertical to horizontal. Due to the way that the winch was designed, with several crossbars across the body, the pulley and extensometer wire were simply snaked around one of these crossbars and allowed them to function sideways. In order to compensate for friction on the cables as well as any damage that may be induced from wrapping cables around small diameter cylinders, a larger pipe was fitted to one of the crossbar elements and seemed to serve very suitably for stress relief.

Additionally, the MRSAD tower has the ability to brace against a rock sample horizontally. For this change in orientation, a series of three inch by three inch by two inch pieces of wood were arranged to brace against the base and keep it from sliding toward the direction of the tensile force. In a prior iteration of the design cycle of the MRSAD brace, a 1/4" threaded bolt was put through the frame, an additional piece of wood was drilled with a hole the diameter of that bolt and this served as a mount for this element.

An image showing the MRSAD in the testing phase as adapted to test on a horizontally oriented borehole can be seen in Figure 3.13 below:

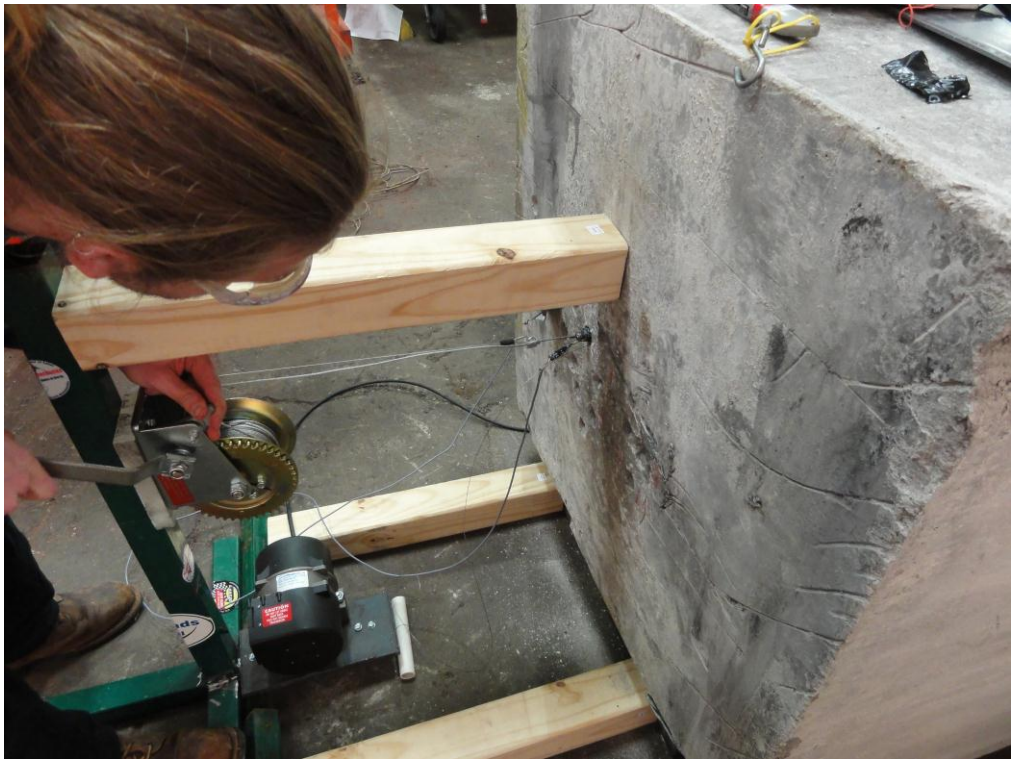

Figure 3.13: MRSAD Device with Wooden Braces for Horizontal Borehole Scratching

the important elements to note from this picture are the wooden braces for stabilizing the MRSAD unit as well as the fact that all the tension-dependent cables are oriented horizontally, visible near the user's left hand. The signal wire from the strain transducer is seen at the collar of the hole and drops towards the ground where it then routs to the DAQ. With these three pieces of wood and the winch cable modification installed, the device was able to function horizontally.

Calibration

Expected values for tension to remove the scratch unit from its installation were on the order of 20 to 100 lbs. The tension values were estimated by considering the amount of force that a person could generate with their own strength, as the device was constrained to not be externally powered. The first calibration was done with 0, 20.325, 40.325, and 47.110 lbs, which were the order of magnitude of the forces that a person could generate to pull on the device. Calibration of the force device was predicated on taking 1,000,000 samples from the strain transducer as weights of increasing mass were applied to induce tension on the load cell. This sampling was done for four different weights (including zero) three times each. The gauge output can be seen in Figure 3.14 below:

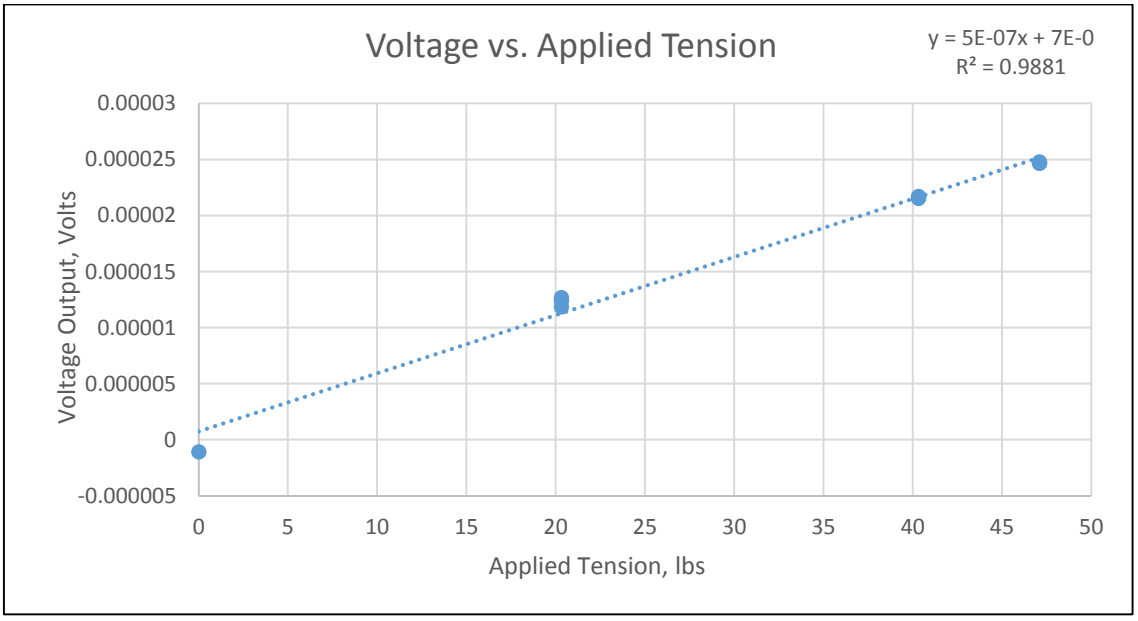

Figure 3.14: Voltage vs. Applied Tension with Trend Line, Equation and Coefficient of Determination

The trend line and coefficient of determination are also visible and indicate a linear voltage change with changing force. There was an error with the data reader that was not recognized

until after calibration that cause there to be only one data collection test instead of three for the zero force point. This means the variance for this force value is not as well-known as it is for the other force values.

The results for the first calibration, while indicative of the linear deformation of the strain element, did little to indicate the variability of force readings at smaller force changes. This led to further calibration efforts that focused on smaller scale forces (0, 0.506, 1.016, 3.016, and 5.25 lbs). When the device output was analyzed under the smaller scale loads later seen in the tests, the following output was obtained, visible in Figure 3.15:

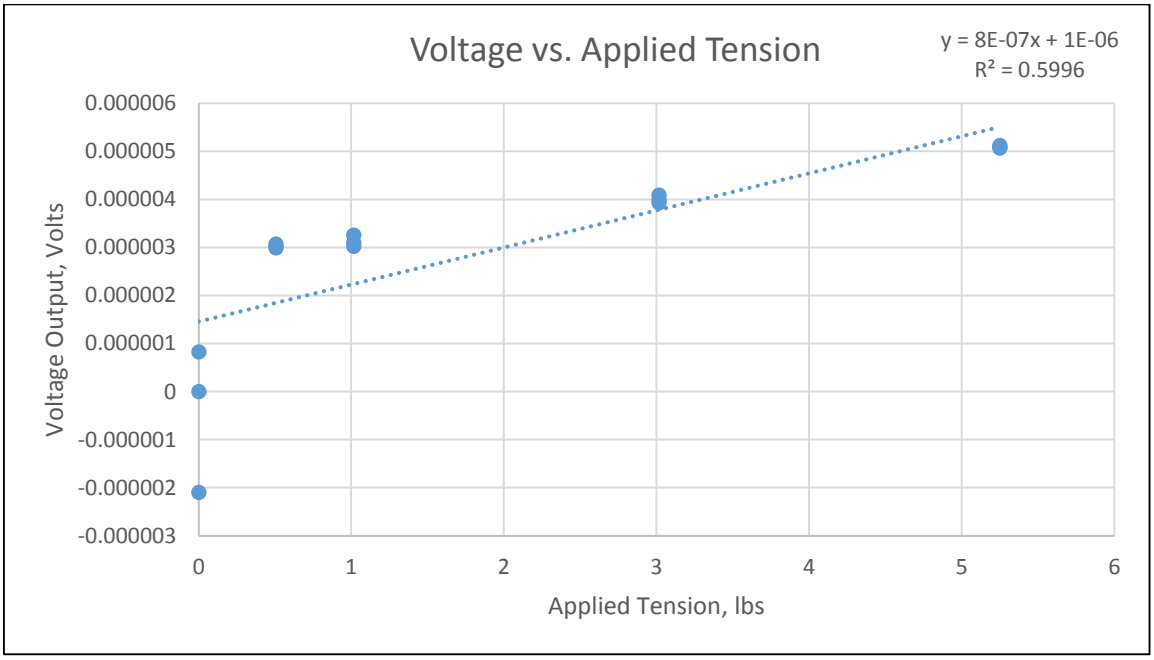

Figure 3.15: Voltage vs. Applied Tension with Trend Line, Equation and Coefficient of Determination

Note the trend line and coefficient of determination, these values are not the same as in the original calibration. Additionally, the variation of the voltage at the zero force level has a dramatically different variance than the rest of the values. If this zero-force voltage output is neglected and the graph properties recalculated, the coefficient of determination returns to its

previous level of precision. This omission of the zero-force could be justified on the grounds that the tension sensing member would never actually be measuring forces at the zero-load level because at the very least, it will have the tension of the extensometer applied to it. Additionally, when the full device comes out of the hole, the scratch head will still be attached to the tension transducer and will continue to apply tension as it dangles from the MRSAD unit. The modified graph can be seen in the next image, Figure 3.16:

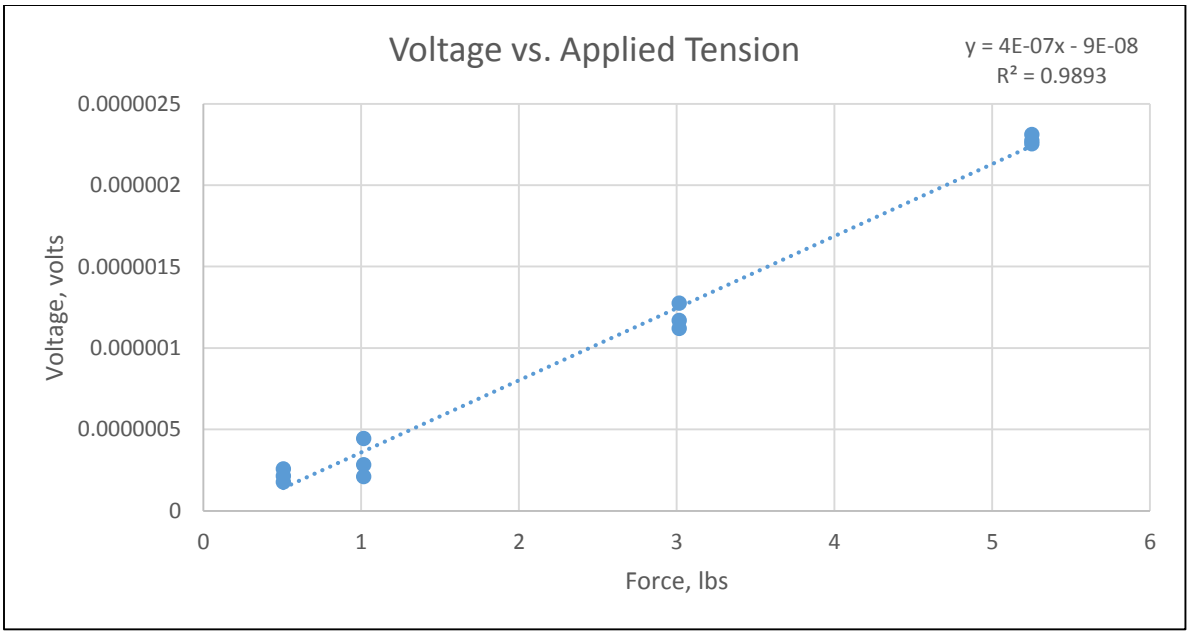

Figure 3.16: Voltage vs. Applied Tension - Omitting Zero-Force Values - with Trend Line, Equation and Coefficient of Determination

Take note of the graph returning to an almost 99% linear fit among the data. There are differences between the first graph, which calibrates weight between zero and about 45 lbs and the last one which does zero to five lbs. The intercepts can be ignored because they serve only to shift the outputs up and down. If the zero force value for the graph is set based off a low point on the graph, then the intercept is not important because the force values change linearly. Since the plots from the data acquisition system reference the zero force values computed from the graphs themselves, the intercepts are ignored. The equation from Figure 3.14 is the most justifiable for

determining the force exerted on the tension member and is rearranged to relate force applied to the load cell in the following equation, Equation 3.1:

$$Tension\ Force\ (lbs) = Voltage * 2{,}500{,}000 \qquad \text{Equation (3.1)}$$

note that the voltage input is the voltage from the graph. Equation 3.1 converts the force voltage values from the data to force values. The data were recorded with a scaling factor included, so if further processing of the results from the original experiments is desired, the above value of 2,500,000 should be reduced to 50,000.

The same calibration principles were applied to the displacement transducer. The string on the extensometer was drawn out to predetermined lengths and held for 1,000,000 samples, done three times for each length. These samples were averaged and then all three tests plotted on a graph which can be seen in Figure 3.17:

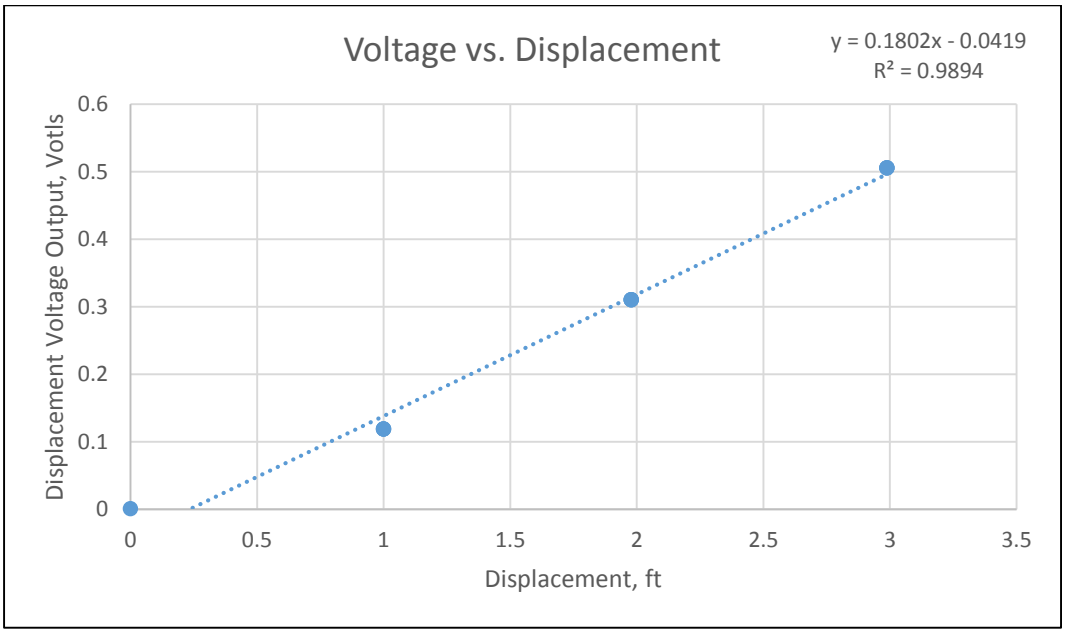

Figure 3.17: Voltage vs. Displacement with Trend Line, Equation and Coefficient of Determination

The displacements used were 0', 1.000', 1.979', and 2.989' with three points at each position except zero feet. The same error described for Figure 3.12 (where the point at zero on the X-axis had one test instead of three) was observed. The equation from the graph is outlined in the following formula, Equation 3.2:

$$Position\ (ft) = Voltage * 5.55 \qquad \text{Equation (3.2)}$$

This equation is used to convert the extensometer voltage output to actual displacement values in feet. The same intercept principle described earlier for determining the zero point of displacement can be ignored in this case because again, the zero position location is referenced from the output graphs themselves. The lengths used were taken from a steel ruler and markings were made on a surface that the transducer was drawn out to and the voltage output at these known locations was used for calibration.

Information Processing

To look at the data closely, it is imported into MATLAB to process the large output matrices. The force, displacement and time values then run through a series of programs that were written that help with the organization of the data. The first program, called “rename”, takes the output from LabVIEW and determines the zero values for displacement and force and converts the names given to the data matrices by LabVIEW to ones that are easier to read and type. It is in this program that the voltage outputs are converted to force or displacement, whichever the data correspond to.

An additional program, “trim”, cuts the first n-number of cells off the beginning of the dataset, where n is a number set in the program, usually 2000 or 5000. This task is performed because the voltage values spike immediately after initializing the program and skews the minimum and maximum data values. After this initial surge (which lasts a few thousand data points) is removed, the data is much easier to plot and interpret. A third program, “itchesplot”, takes the data and plots the displacement and force on the same graph versus time so that they are easier to compare to each other and so that relationships between force and displacement become immediately apparent. The source code for “itchesplot”, “rename”, and can be found in Appendix B and C, respectively. The “itchesplot” program produces another graph of force vs. displacement, but that type of graph will be covered later in the results section.

Design Summary

The components for the device consist of a stand, a hand cranked pulling winch, a position transducer, a load cell, a scratch head, an installation rod and scratchers. These parts, and the parts that they are made from are categorized in the bill of materials. The bill of materials for the device is included in the following table, Table 3-I:

Table 3-I: Bill of Materials for Formation Evaluation Tool

Tier				Component	Unit	Number	Make/Buy
1				Mine Roof Strata Analysis Device (MRSAD or ITCHES)	Tool	1	Make
	2			Mount	Stand	1	Make
		3		Interchangable Metal Assembly	Stand	1	Buy
		3		Adjustable Roof Threaded Bolt	Bolt	1	Buy
			4	Brace Plate	Plate	1	Make
			4	Bolt Nuts	Nut	3	Buy
		3		1" thick Plastic Mount for Extensometer and Winch	Sheet	2	Buy
			4	Bolt	Bolt	2	Buy
			4	Nut	Nut	2	Buy
	2			Hand Winch	Winch	1	Buy
		3		Mounting Bolts	Bolt	3	Buy
		3		Spool	Spool	1	Make
			4	3" Plastic Cylinder	Plastic	1	Buy
		3		3/16" Steel Cable	Feet	35	Buy
			4	Connecting Bolts	Bolt	4	Buy
			4	Crimps	Device	3	
	2			Unimeasure HX-PA-300-L3M Position Transducer	Device	1	Buy
		3		Signal Wire	Feet	10	Buy
	2			Load Cell	Device	1	Make

		3		350 Ohm 250BF-EA-13 Strain Gauge	Gauge	4	Buy
		3		134-AWP Signal Wire	Feet	10	Buy
		3		426-BSV Braided Shielded Signal Wire	Feet	30	Buy
		3		5/8" Diameter Aluminum Rod	Feet	1	Buy
		3		GAK-2-AE-10 Strain Gauge Installation Kit	Kit	1	Buy
		3		Plastic Tube for Protection	Feet	1	Buy
	2			Installation Rod	Device	1	Make
		3		3/4" Conduit Pipe 5' long	Pipe	1	
	2			Scratch Head	Device	1	Make
		3		Stainless Steel Rod 1"	Feet	1	Make
		3		Stainless Steel Rod 5/8"	Feet	1	Make
	2			Scratchers			Make
		3		0.045" Music Wire	Spool	1	Buy
		3		0.051" Music Wire	Spool	1	Buy
		3		0.055" Music Wire	Spool	1	Buy
	2			USB 6211 Data Acquisition System	Unit	2	Buy

The table works on a tier system, the most encompassing aspect of the project is labeled tier one and in this case is the Mine Roof Strata Analysis Device. Components in tier two assemble to form tier one items and similarly, tier three assembles into tier two and finally tier four assembles into tier three. This allows for easy categorization about what is needed for the device and how the parts come together. The unit section dictates how the product is sold with number

indicating in what quantity it is needed. The make/buy column indicates how the manufacturer obtains these products. Most of the items that aren't instrumentation or data acquisition specific can be purchased at local hardware stores. The full weight of the system including the wooden braces is 39 lbs. With the device fully assembled and the means to process the data determined, it was ready to be tested in lab and field settings.

Chapter 4: Experiment

Concrete Block Scratch Test

The testing of the device took place at a facility that researches the design of mine roof drilling equipment. This was selected because of its close proximity to Virginia Tech as well as the availability of pre-drilled 10,000 psi concrete blocks with river gravel that had one inch blind holes that are drilled four feet into the rock. A picture of the full scale concrete block can be seen in Figure A.2 in the Appendix. These blocks came pre-installed with two different rock types that were an artifact of prior research. The presence of these differing rocks in the block matrix was desired because it means that the MRSAD can look for differing rock types in the block material in a manner that is similar to analyzing the varying strata in a coal mine roof.

This goal of this concrete block test was to control the velocity of the scratch head in the borehole and try to see if the force varied with any regularity as a result of scratching and motion. It was thought that an increase in force over sections of the block would indicate a stronger or more resistive rock type and that the presence of decreases in force could indicate weaker rock types. Controlling the velocity of the scratch head for each test with steady winding of the winch allows the results of one hole's similar velocities to be compared. In essence, if the velocity of each scratcher pull test is held constant, the forces seen in each individual attempt can be compared to other forces in the same attempt because it moved at a constant velocity through the hole.

The blocks were taken into the research warehouse and the pre-drilled holes were then analyzed to see if they would be able to serve as good hosts for the scratch head by inserting the scratch head into each of the holes on the face. Immediately, the geometry of the holes became problematic because it was difficult to insert the device more than a few inches into the block.

There were aspects of the initial drilling of the holes that made them have an undulating profile along their length which was difficult for the scratch head to move past. However, observed holes where at least a foot of depth could be reached were considered promising, and were marked to be used for testing of the MRSAD.

The following image, Figure 4.1, shows the scratch head being installed with the horizontal installation rod pushing the scratcher into the borehole:

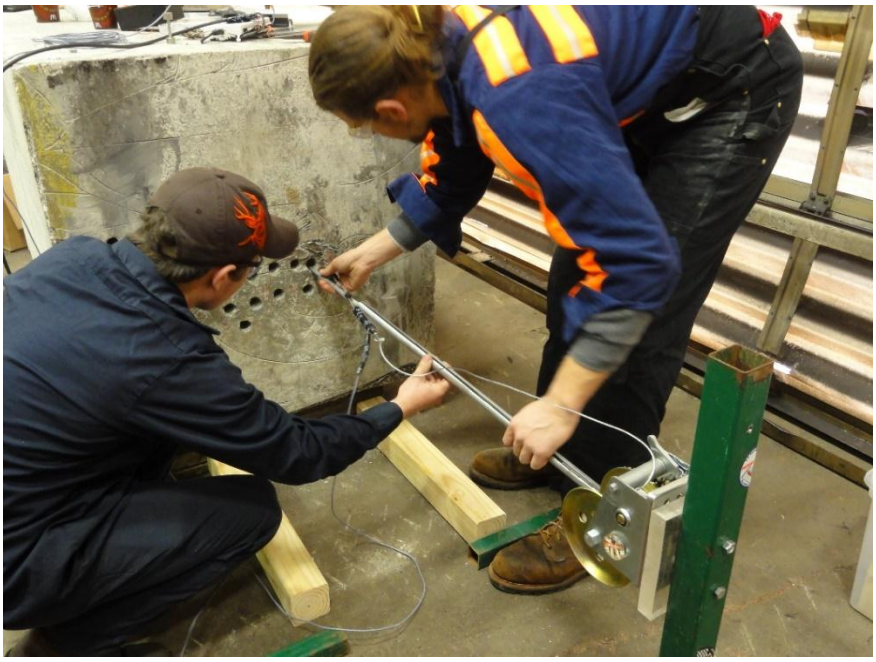

Figure 4.1: Installation of the Scratcher into the Borehole

The MRSAD unit is in the bottom right of the image, it is moved away for the installation to allow more room to work, and then placed back up against the block for the test. The test holes and their markings can be seen in Figure A.3 and Figure A.5 in the Appendix.

During the first two attempts at installation, the device did not install correctly and it was decided that modifications to the scratch head would help with the process. The facility assistant

ground the circumference of the scratch head to try and give it more room as it moved up the hole. After this modification, a successful installation took place, but a weld broke on the unit and needed repair. The first successful test was performed with the newly repaired testing element. The test consisted of a 2.3' installation and consistent motion that occurred over the full length. The test starts at the zero feet of displacement on the left side of the blue line and increases in displacement as the device was removed from the hole. The results for that test can be seen in the following image, Figure 4.2 with a green line that corresponds to the zero line of the force values and a blue line that corresponds to the collar of the hole:

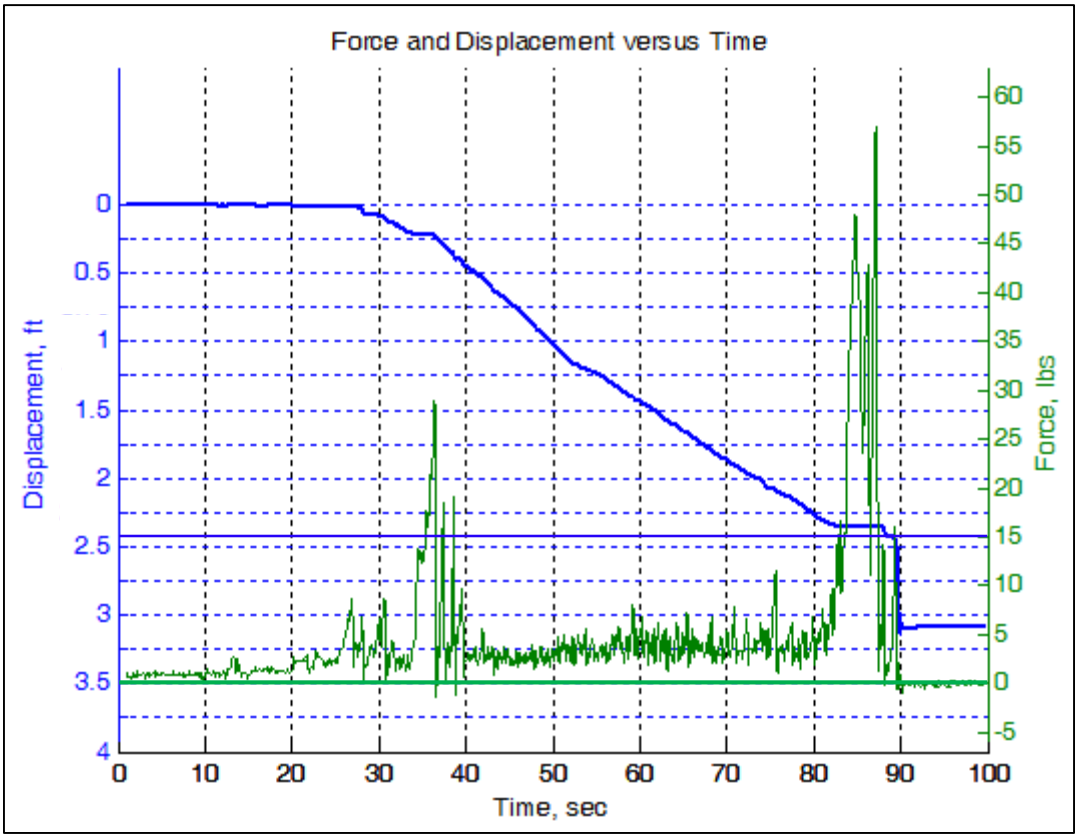

Figure 4.2: Force and Displacement vs. Time for First Test in Concrete Block

This graph has a distinct increase in force during the motion phase which is indicative of resistance from the rock. The velocity for the first motion region between 28 and 51 seconds is 0.045 ft/sec (0.54 in./sec) with an R^2 of 0.98 for that velocity for that interval. The velocity of the second motion phase, between 51 and 82 seconds is 0.041 ft./sec. (0.49 in./sec.) with an R^2 of 0.999 for the velocity over that time window. The region between 40 and 80 seconds shows an applied force value that although spiking, hovers around the same value while the displacement changes constantly over the course of the hole. This motion corresponds to two velocity regions the first one between about 40 seconds and 50 seconds and then the second, slower one between 50 and 80 seconds. The velocity of the scratch head is dictated by the user carefully cranking the winch handle and when it is under operation, keeping a consistent, steady pace is needed to look for changes in the rock type along constant velocity sections.

There were no further technical difficulties with the scratcher at this point, the second test was performed promptly in the same hole, hole one. The force and displacement results can be seen in Figure 4.3 below, with the thin blue horizontal collar line and the green zero force line:

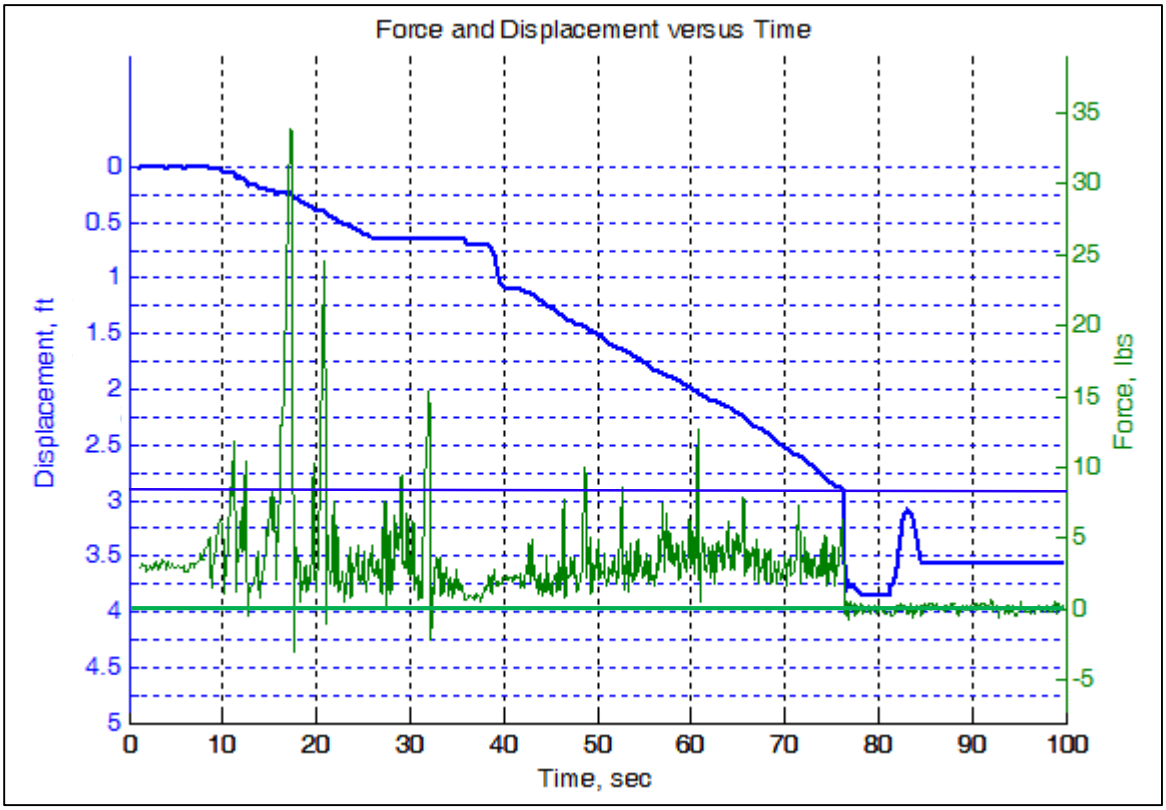

Figure 4.3: Force and Displacement vs. Time for Second Test in Concrete Block

A constant velocity of 0.036 ft./sec. (0.43 in./sec.) in Figure 4.3 occurs between 10 and 25 seconds with an R^2 of 0.987 for the velocity value over that time. There is another constant motion region in this graph between 40 and 75 seconds with a velocity value of 0.05 ft./sec. (0.6 in./sec.) and a the closely mirrors the velocity slope of the first velocity region that occurs between 40 and 75 seconds.

It was decided at this point to resume testing in a different hole, hole two, adjacent to hole one. The data readout for this test can be seen in the subsequent image, Figure 4.4:

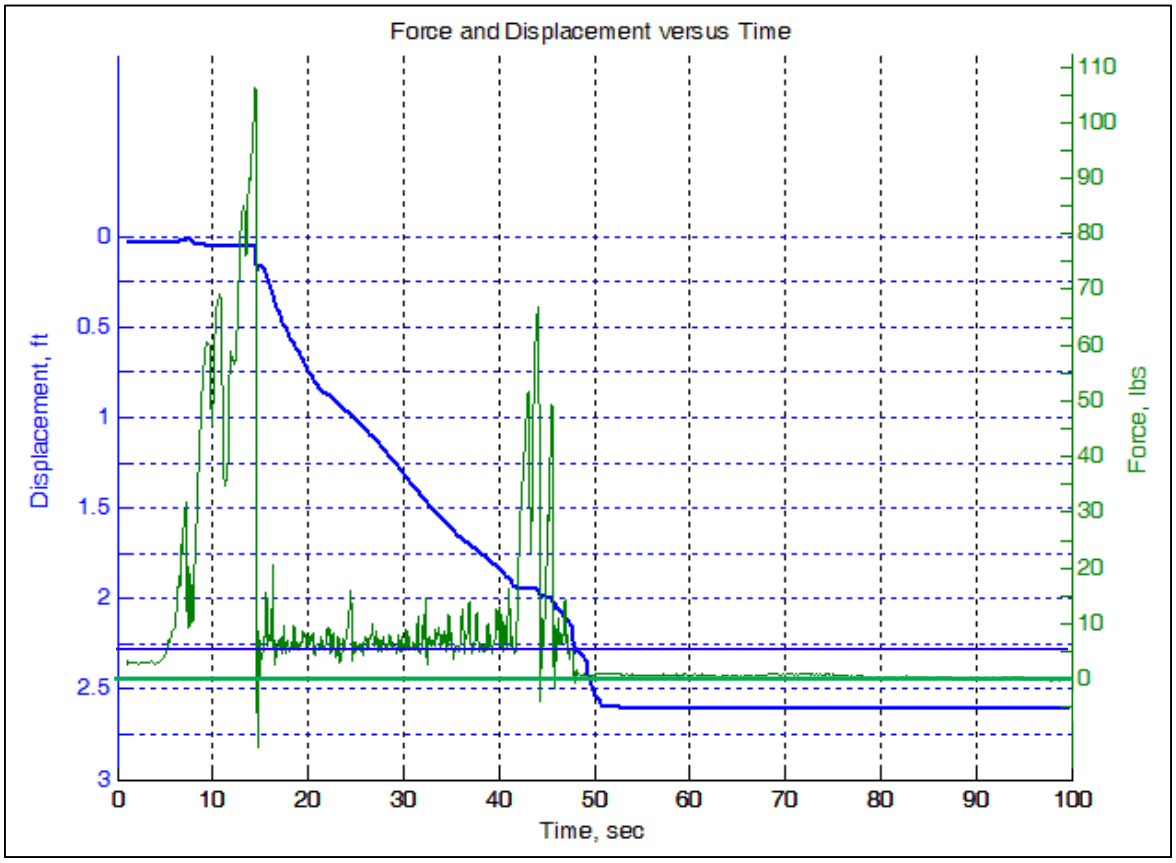

Figure 4.4: Force and Displacement vs. Time for Third Test in Concrete Block

This test begins with a very distinct spike in force at 15 seconds, this is showing the amount of force it took to initiate motion of the scratch head in the borehole because at that point, the displacement profile is flat, indicating no motion is occurring. The velocity of the first phase of motion between 15 and 20 seconds is 0.11 ft./sec. (1.36 in./sec.) with and R^2 of 0.989 for that velocity over that interval. The velocity seen in the second part of the motion phase between 21 and 41 seconds is 0.055 ft./sec. (0.66 in./sec.) with an R^2 of 0.996 over that interval for that average velocity value. It is often the case that the head will lodge itself in the rock with the

scratchers providing resistance and sufficient force must be applied to the head to overcome the frictional resistance. In some other cases, the device will become stuck as a result of its malfunction and large forces will be generated before motion will follow, because it may not be friction that needs overcoming, but something stronger like a wobbly profile, or a discontinuity.

The last test, the fourth test, was performed on a control hole which was at the far edge of the block, assumed to be outside the realm of the embedded rock samples and therefore pure concrete. The hope was that any difference in behavior of this hole when compared to the previous tests would be indicative of changes in strata. This proved to be the final test for the work at the research facility as serious technical difficulties were encountered and it was decided to abandon the stuck device.

The results for this final test are available in Figure 4.5 below:

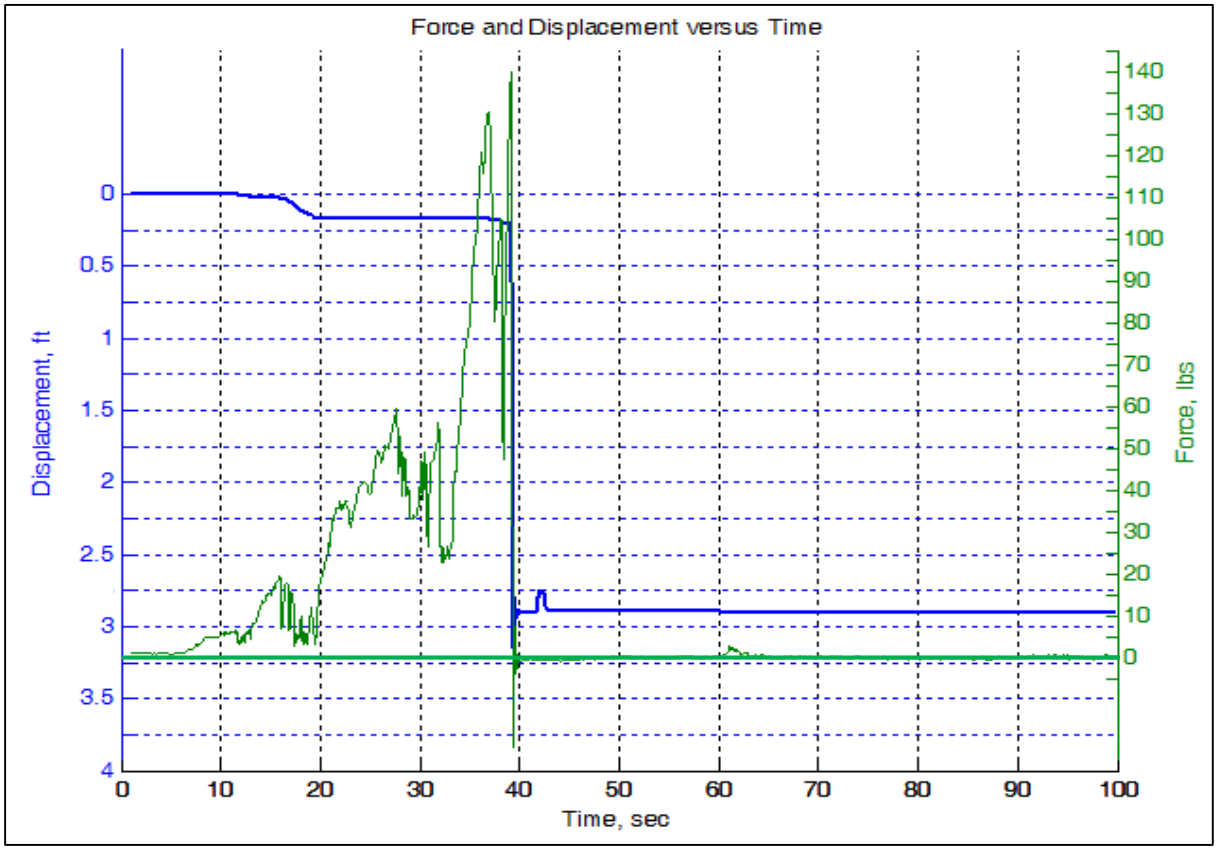

Figure 4.5: Force and Displacement vs. Time for Fourth Test in Concrete Block

There is a clear trend from the image that the force built up to a sudden energy release after 0.25 feet of motion, where no further information was available. This test the head got very stuck possibly as a result of installation error where one of the scratch tips got pulled around the scratch head and got wedged between the head and rock. As the force built up, the same weld that had broken earlier had a third complete breakage and rendered the device irretrievable until the machinist devised a way to hook it out.

The pull forces for the successful tests (tests one through three) were averaged over the motion phases and arranged in the following table, Table 4-I:

Table 4-I: Concrete Block Test Pull Force Averages and Statistics

Scratcher Diameter (Inches)	Concrete Block							
	Pull Force Averages (lbs)			Test Statistics			Overall Statistics	
	Test 1	Test 2	Test 3	Test 1 Stdev	Test 2 Stdev	Test 3 StDev	Average	Std. Dev.
0.045	4.4795	3.85	10.23	3.49	3.87	10.818	6.19	2.87

The averages were taken in areas where displacement was occurring by highlighting the dataset with the data selection tool in the MATLAB plot function, making it a variable, and finding its average and standard deviation. The test statistics in the middle are the amount that the pull forces varied as it traveled the length of the hole for each test. The overall statistics on the right are the averages and standard deviations for the three test's pull force averages.

The results of this test were indicative of the successful application of resistive forces to the scratch head and borehole as well as a demonstration of the instrumentation and installation tools. However, there was a variability in the test circumstances especially in controlling variables such as rock composition, scratcher dimensions and anchorage characteristics which meant a lack of definitive conclusions. The failure of the mechanism and installation was important because it illuminated weak points in the design. The data readouts from the failed tests can be seen in Figure A.25 and Figure A.26 in the Appendix. The decision was made to reapply the MRSAD device to better regulated circumstances in the lab which entailed testing it a one inch inner diameter PVC pipe and a small sandstone block to serve as more homogenous controls.

PVC Pipe Scratch Test

The PVC Test serves as a platform for comparing differing wire scratcher diameters in a more controlled material, in this case PVC plastic. Two wire scratcher diameters, 0.045 inches and 0.051 inches were used in this experiment. The test paired MRSAD unit with a five foot long PVC pipe. The pipe was clamped down to a table and then the stand for MRSAD was placed next to the table with horizontal braces installed. The pipe setup can be seen in Figure 4.6 below:

Figure 4.6: Clamped PVC Pipe with Scratch Head Visible Emerging from Pipe

This image was taken after the scratcher had been set and shows the direction that the head moves in the pipe as it is drawn toward the far hole. The plastic pipe was longer than the installation rod used for the concrete block test and this meant that that installation method would no longer be feasible. Instead, the scratch head was dropped down the pipe with the other

cables attached to it having gravity pull it down. The scratcher was installed when the head emerged from the other side as seen in the following image, Figure 4.7:

Figure 4.7: Scratch Head Embedded in PVC Pipe Walls Prior to Extraction

There is a small gap between the head and the PVC pipe, it is thought that this gap is one of the most critical elements of the test. If this annulus is too small, the head is more likely to get stuck in the hole. If it is too wide, the thin scratchers will get bent into the gap and not engage in the type of scratching behavior desired. Being able to see the scratcher from the other side of the hole removed a lot of the uncertainty about anchorage behavior because it allowed for a close look from the other open end of the PVC pipe where it could be easily determined that the scratch tips had contact with the plastic.

The results for the first part of the first test can be seen below in Figure 4.8:

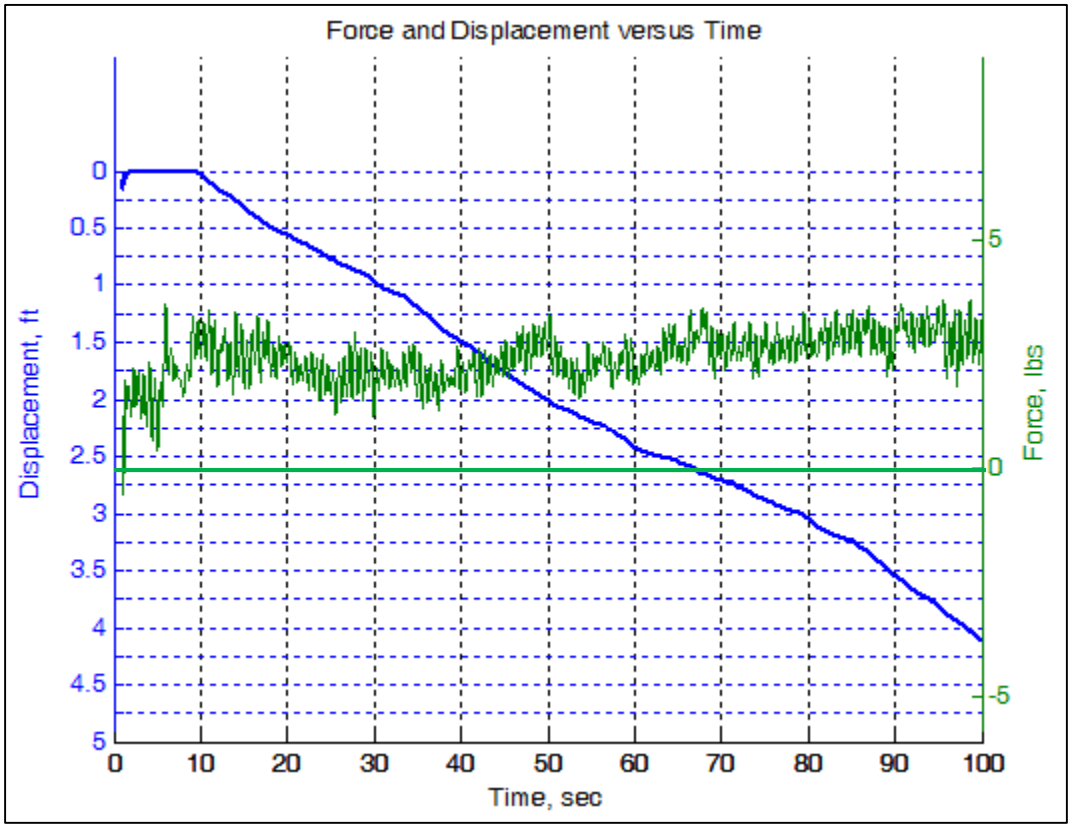

Figure 4.8: Force and Displacement vs. Time for First Part of First PVC Test with 0.045" Scratcher

The pulling force remains around the same value (2.48 lbs) for the entirety of this part of the test where the displacement occurred with a consistent velocity of 0.042 ft./sec. (0.504 in./sec.) and an R^2 of 0.995 over the region. The final recorded position for this test is approximately 4.15'. Any difference in this final position value in Figure 4.8 and the first displacement value in the second part of the test (Figure 4.9) is how far the head was drawn out the hole before it was noticed that the recording session had expired and a new one was needed.

Upon discovery of the termination of the data collection. The LabVIEW program was reinitiated and the results are visible in Figure 4.9:

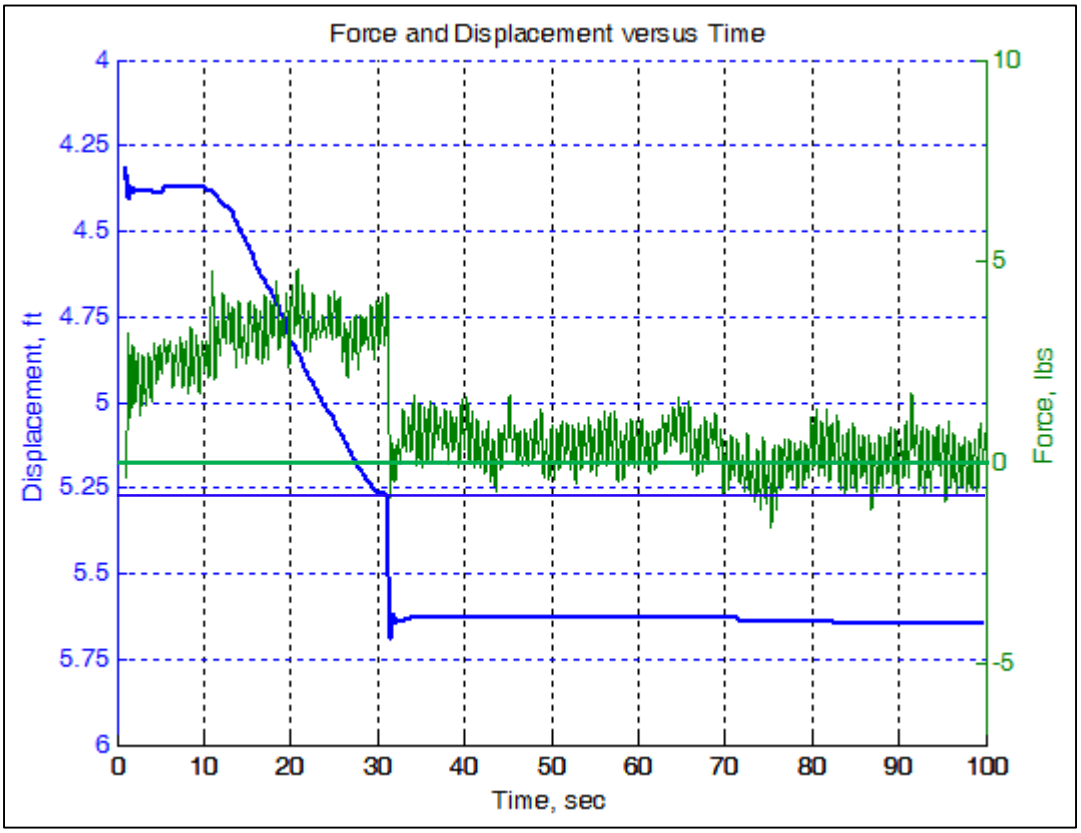

Figure 4.9: Force and Displacement vs. Time for Second Part of First PVC Test with 0.045" Scratcher

Note the drop in force that occurs as the scratcher leaves the pipe at 32 seconds. The velocity over the motion between 10 and 30 seconds is 0.0496 ft./sec. (0.60 in./sec.) with a velocity R^2 of 0.997 over that interval.

A second 0.045" wire diameter test commenced when it was determined that the installed anchorage was suitable. Suitable anchorage implies that contact with both scratcher tips and the borehole wall is visually guaranteed by inspection of the device. This ensures that for the pulling, the designed action of contact of both scratcher tips on the wall of the hole will take place.

The results from the second test with the 0.045” scratchers can be seen in the following graph, Figure 4.10, with the horizontal blue line demarking the collar position:

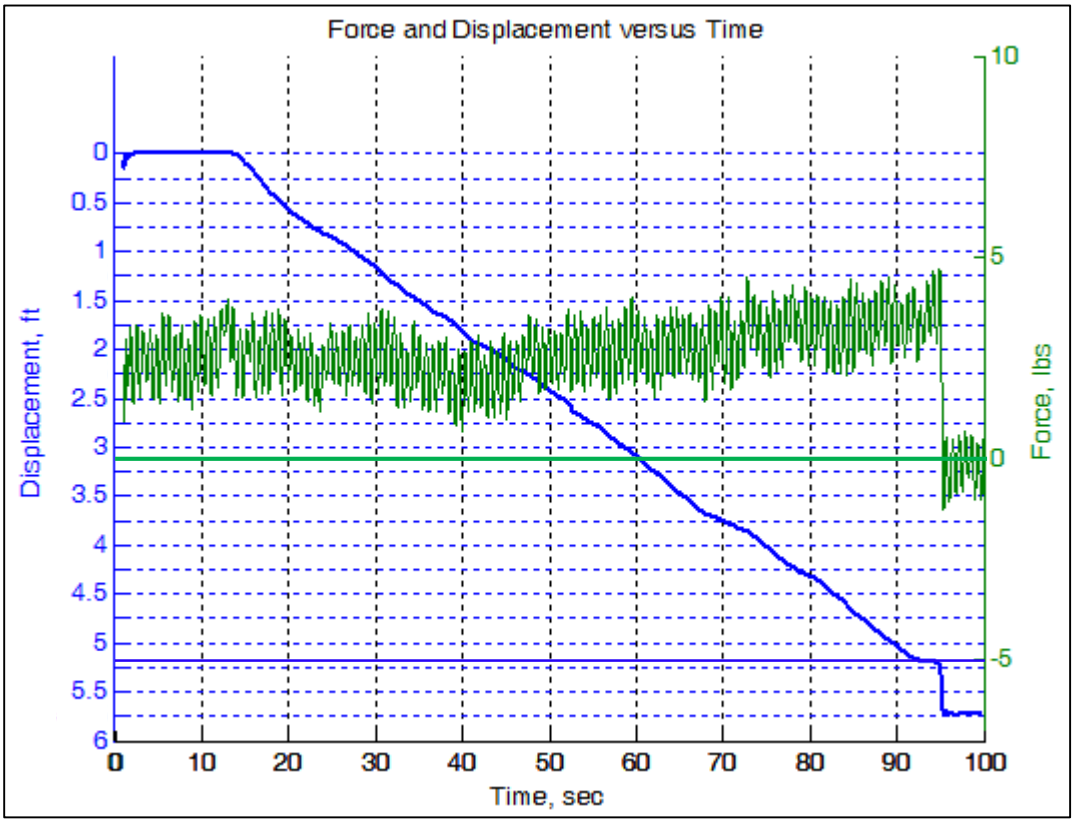

Figure 4.10: Force and Displacement vs. Time for Second PVC Test with 0.045” Scratcher

Note the drop in force as the scratcher exits the PVC pipe at the right side of the graph at around 95 seconds. The velocity over this interval is 0.064 ft./sec. (0.768 in./sec.) with a velocity R^2 over this interval of 0.99. This force data is considerably noisier than in prior tests in spite of the fact that no changes were made to the digital filter.

Figure 4.10 shows that for the initial period (0-13 seconds), there was a force magnitude comparable to the magnitude during the motion phase (13-90 seconds). This is because when the device was installed, it sometimes had tension put on it as the spool was wound to help organize

the hanging wire. This ensured that the cranking could commence as soon as the data acquisition program was initiated, instead of cutting in to the data logging time as the spool was wound and reorganized. When the initial force is the same as the traveling force, it is a byproduct of this testing procedure.

It was decided that for the third test, the scratch tips would be changed from the 0.045 inch diameter tips to the 0.051 inch diameter tips. With the homogenous nature of the plastic pipe, more control could be expected for the behavior of the surrounding matrix and the consequences of changing the diameter of the scratcher wire could be evaluated. A picture showing prepared scratch tips laying on a 0.196 inch x 0.196 inch grid is visible in Figure 4.11:

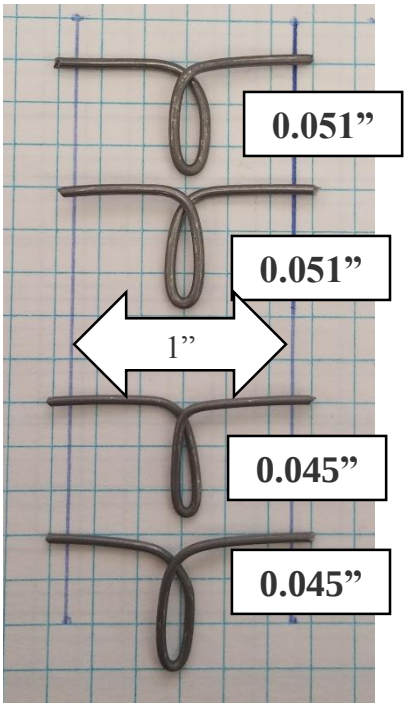

Figure 4.11: Prepared 0.051” and 0.045” Scratchers with One Inch Parallel Lines Simulating Borehole Dimensions

All the scratchers are the same width and all extend 1.1811 inches from tip to tip, which is 0.091 inches wider on each side than a one inch borehole. The tips of the wire scratchers were filed

after being cut to attempt to control the profile of the scratcher surface. The fact that they are the same dimensions was important to consider for control as having them at the same cut width, 1.1811 inches, kept ruled out the width of scratchers as a variable.

Once installed, the pull test was performed on the PVC pipe with the new 0.051" scratchers. Scratching commenced and immediately more resistance was observed, which at this point felt like gouging of the plastic. The clamps were losing their hold and the pipe had to be held by two people as the head was drawn out. Again, the time was cut short, with the output for the first part of this test seen in Figure 4.12 below:

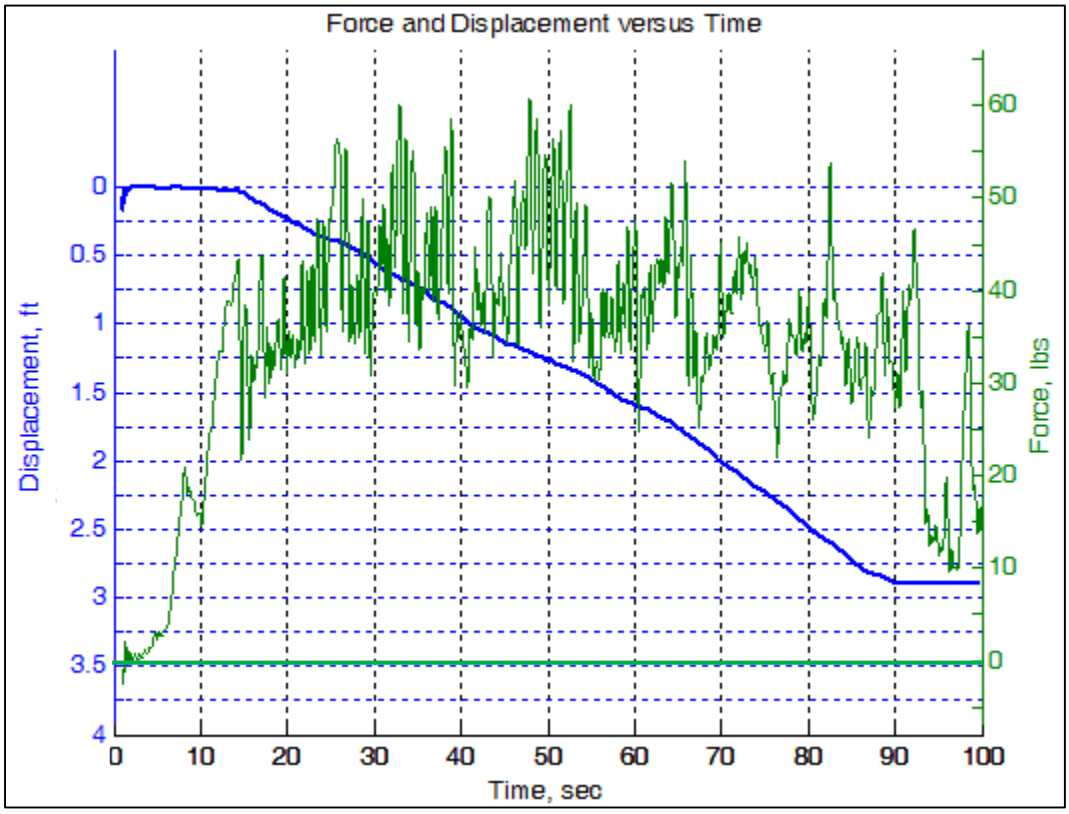

Figure 4.12: Force and Displacement vs. Time for First Part of First PVC Test with 0.051" Scratcher

Although the force applied to it is highly erratic, the velocity of the scratcher stays largely the same (R^2 for velocity of 0.99) throughout the first part of this test at 0.037 ft./sec. (0.44 in./sec.).

The forces measured in this iteration of the test are considerably larger than in the previous tries with the thinner scratchers (36.46 lb average versus 2.81 lb average).

The test was ceased at 90 seconds when the program was about to expire its data acquisition because it functioned on a 100 second timer. The test was then restarted and the same strong resistance that was seen in the first part of the test was observed in the second. At this point, it became evident that plastic shavings were accumulating in the hole and starting to come out, indicating a gouging of the plastic. The second part of this third test is visible in the following figure, Figure 4.13:

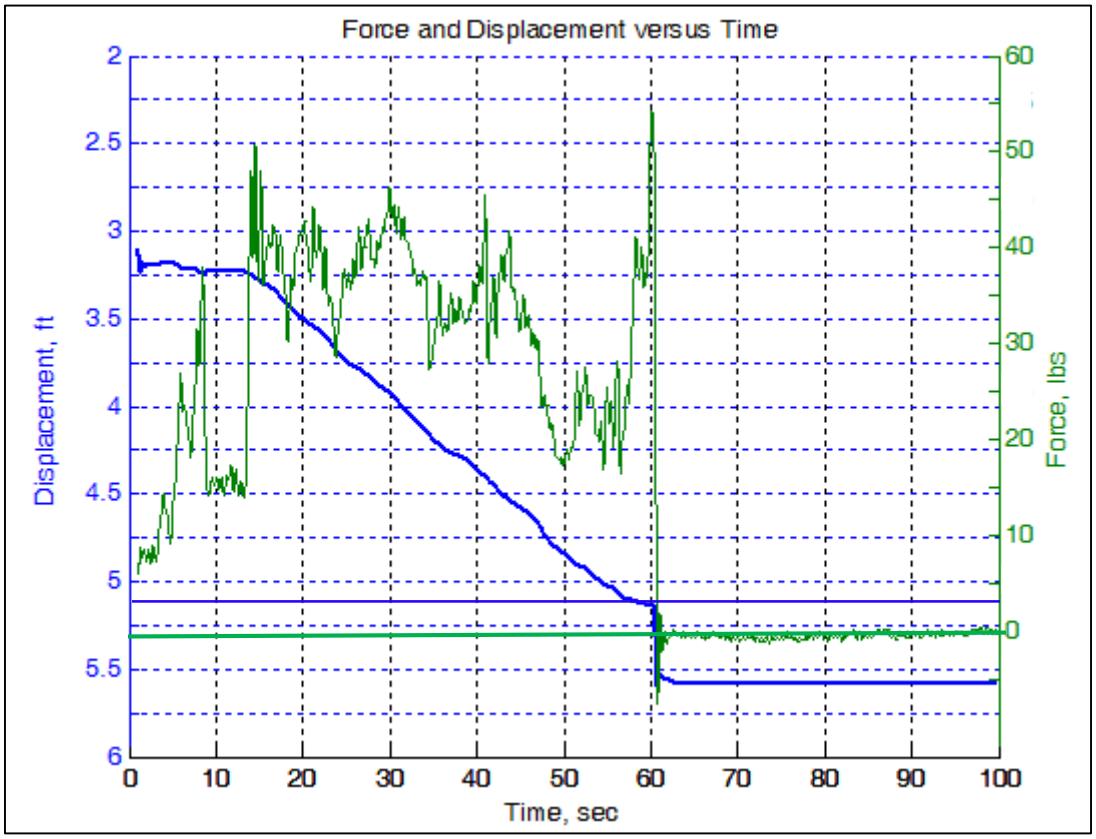

Figure 4.13: Force and Displacement vs. Time for Second Part of First PVC Test with 0.051" Scratcher

Take note that the large magnitude tensile forces correspond strongly with the motion through the PVC between 10 and 60 seconds. The velocity of the motion over the interval between 12 and 60 seconds is 0.043 ft./sec. (0.516 in./sec.) with an R^2 of 0.998.

Table 4-II is shows the averages of the forces for the differing scratch tip diameters in the PVC tests and can be seen below:

Table 4-II: PVC Test Pull Force Averages and Statistics for Differing Scratcher Sizes

Scratcher Diameter (Inches)	PVC Pipe						
	Pull Force Averages (lbs)			Test Statistics		Overall Statistics	
	Test 1.1	Test 1.2	Test 2	Test 1.1 Std. Dev.	Test 1.2 Std. Dev.	Average	St. Dev.
0.045	2.48	3.23	2.71	0.48	0.69	2.81	0.38
0.051	39.27	33.65	n/a	7.35	7.69	36.46	3.97

This table highlights the difference in force between the PVC tests. The test showed a large change in magnitude of pull force from an increase in scratch tip diameter, 2.81 lbs as opposed to a 36.46 lbs average. The test statistics section in the middle refers to how much the forces were varying during the testing phase for test one for each scratcher type. The test with the 0.051" scratch diameter had more force variability over its motion (7.35 & 7.69 lbs) than the 0.045" scratch diameter (0.4771 & 0.69 lbs). The overall statistics to the right are the averages and standard deviations of the pull force averages in the left section of the table.

When the scratch head was removed from the hole, it left interesting marks on the inside of the pipe. A pairing of deep cuts corresponding to the diametrically opposed scratch tips traversed the entire length of the pipe's inner surface. The marks from the first two tests (0.045" scratcher diameter) were almost indistinguishable compared to the profile of the pipe, but the third (0.051" scratcher diameter) left cuts on the pipe.

Figure 4.14 shows the deep, spiraled grooves left on the inside of the pipe by the 0.051” diameter scratch tips as well as some of the shavings produced from the test:

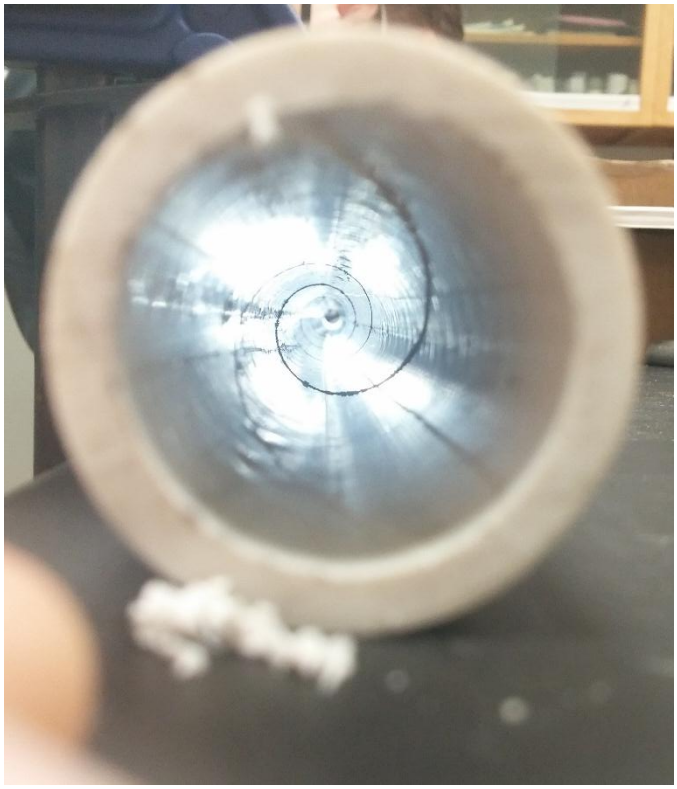

Figure 4.14: Spiraled Grooves and PVC Shavings from Third Scratch Test

In this image, a lab assistant held a light at the end of the pipe to help outline the grooves in the plastic. It is not immediately clear what causes the scratcher to rotate instead of simply moving straight although factors such as torsional stiffness in the tension cable and the shape of the cutting tips have been considered as possible reasons. It was at this point that the testing of the PVC pipe was concluded as concerns about the scratch tips connecting with and following the deep grooves would yield inaccurate results.

Sandstone Scratch Test

0.045”, 0.051”, and 0.055” wire scratchers were then used on a new test, one looking at their interaction with a small sandstone sample. This was to mimic the control of the PVC test but while still testing the device on rock. The holes after being tested can be seen in the following image, Figure 4.15:

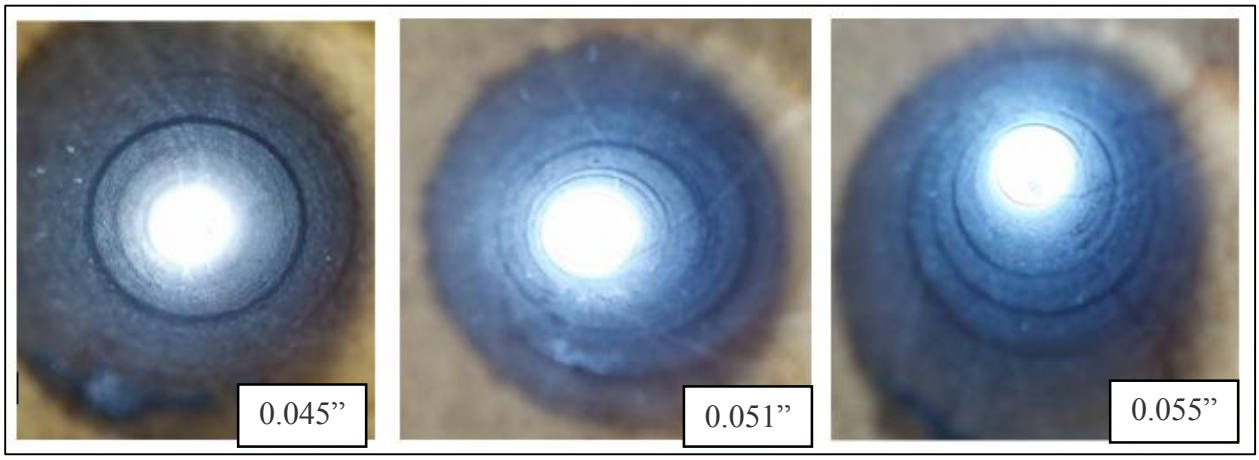

Figure 4.15: Sandstone Holes after Testing the 0.045”, 0.051” and 0.055” Wire Scratchers

Markings are visible on the rock surface resulting from contact with the scratchers. The sample was held to the table by a series of clamps and was carefully monitored to ensure that it was not undergoing slippage during the duration of the test. This rock was a suitable length to obtain a velocity profile and to measure the associated pull force as can be seen in the next several images. The plots of time, displacement and force were recorded and graphed for each run of the tests. The results for the first test from every scratch diameter are displayed below with the remainder of the graphs being available in the Appendix in Figures A.9 through A.24.

The output from the first test is visible here in Figure 4.16:

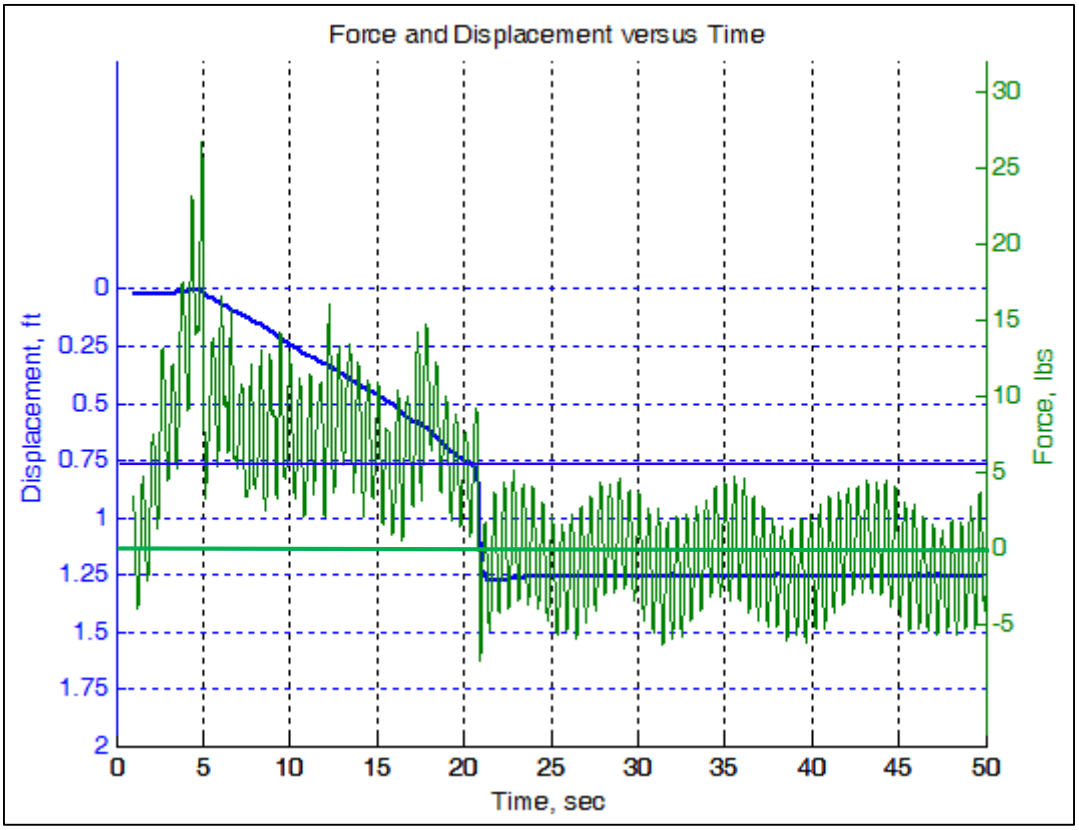

Figure 4.16: Force and Displacement vs. Time for First 0.045 Inch Sandstone Test

The profile for the force distribution is evident in this graph, with the force peaking rising to initiate motion followed by a constant velocity (0.6 in/sec) region with a sustained maximum force.

Another scratch test was conducted on the same sandstone sample, but in a different hole. Again the wire scratcher tip diameter was increased to 0.051" as was done with the PVC. It appeared that the clamps were doing a suitable job at holding the sample in place so no changes to that arrangement were instituted.

The results for the first attempt at this test can be seen below in Figure 4.17 again cataloguing the values for position, tension force and time:

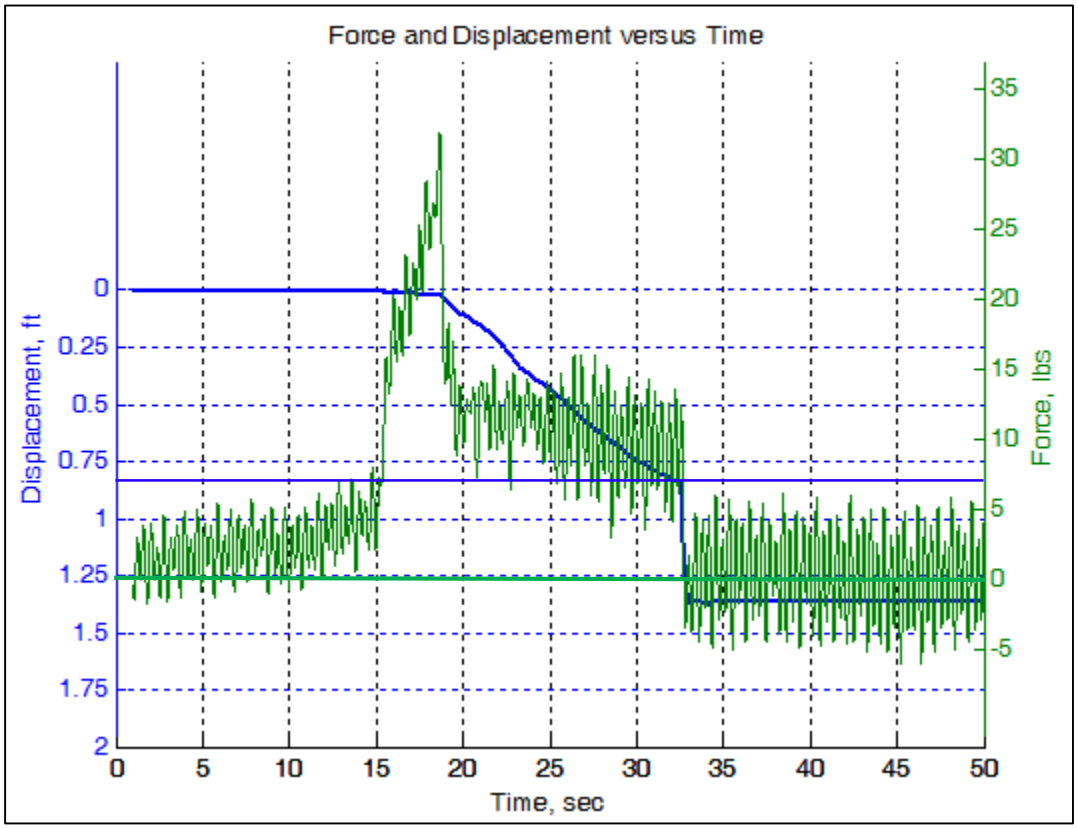

Figure 4.17: Force and Displacement vs. Time for First 0.051 Inch Sandstone Test

This test featured a dramatic increase in force, around 30 lbs, which corresponds to the initiation of motion of the head. The force values seen in this graph increase in magnitude by around 10 lbs between the initial tension at 10 seconds and the tension during motion.

The test was repeated with the 0.055 inch diameter scratcher in the same sandstone block with the results in Figure 4.18:

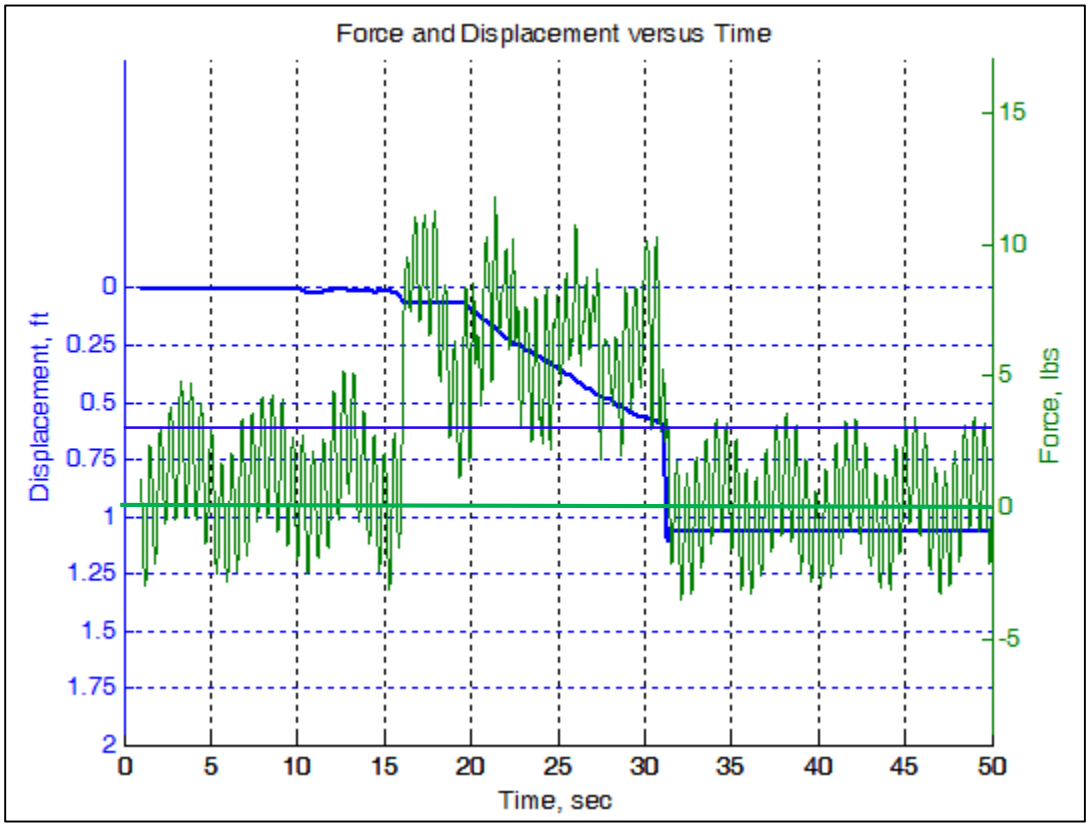

Figure 4.18: Force and Displacement vs. Time for First 0.055 Inch Sandstone Test

There are three distinct areas where force was applied to the scratching head, although very low frequency noise made the forces from this test iteration difficult to distinguish.

The results from these tests call into question the selected calibration details for the strain gauge transducer. The transducer was operating over a range of different tension values and the use of a more sensitive load cell may provide further information about the scratching. The graphs were all generated by taking the average of the last 50,000 samples in the test, which was always its unloaded state, and setting that value as the zero. In light of the corrections applied to

the graphs, it is believed that the force values still carry the linear relationship seen in every one of the calibration curves.

It is clear that the scratchers were able to apply resistive forces to the borehole walls either by friction or scratching, and most importantly that the force and position transducers were able to convey their respective changes in force and position values. Additionally, the stand mechanism performed well at stabilizing all the constituent parts and maintaining a constant velocity throughout much of the motion of the scratchers so that each test run can have its areas of similar velocities compared. What is yet to be investigated is if there are any conclusions about rock properties that still remain in the data. It is also hopeful that the difference between friction sliding and scratching will become clear once certain graphs get looked at more closely.

Chapter 5: Discussion of Results

Force and Displacement versus Time Analysis

The three differing experiments did reinforce some of the behaviors expected from the scratch head and its movement through the hole such as increased forces during the motion phase. To outline some of the observations from the test, the first part of the discussion section will focus on test one from the concrete block. The original force and position vs. time graph is found in Figure 4.2, but is included below in Figure 5.1., as well:

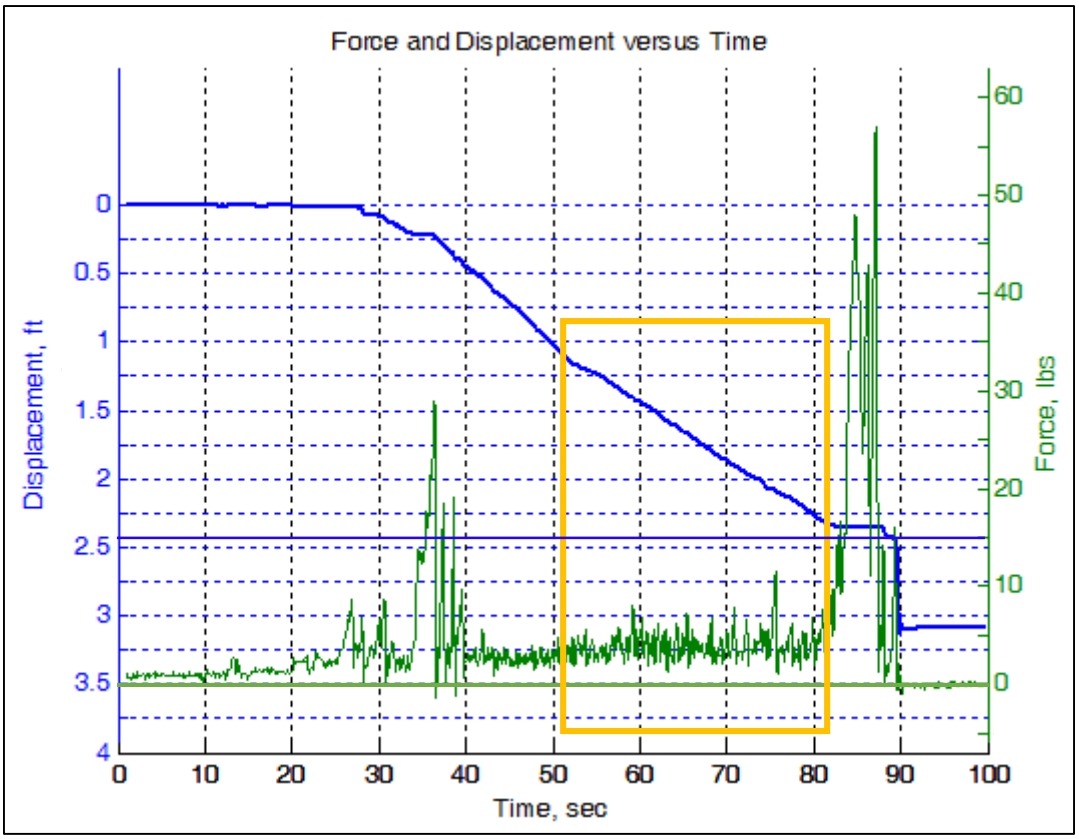

Figure 5.1: Force and Displacement vs. Time for Test One on Concrete Block with Highlighted Constant Velocity Area

The area highlighted in orange in Figure 5.1 between 51 seconds and 83 seconds is chosen as an area of study. The velocity profile in this area is consistent and means that it can be analyzed to look for changes in force. First the scratcher motion characteristics are analyzed in the following image, where Figure 5.2 shows a regression curve of displacement from test one on the concrete block, between 55 and 80 seconds:

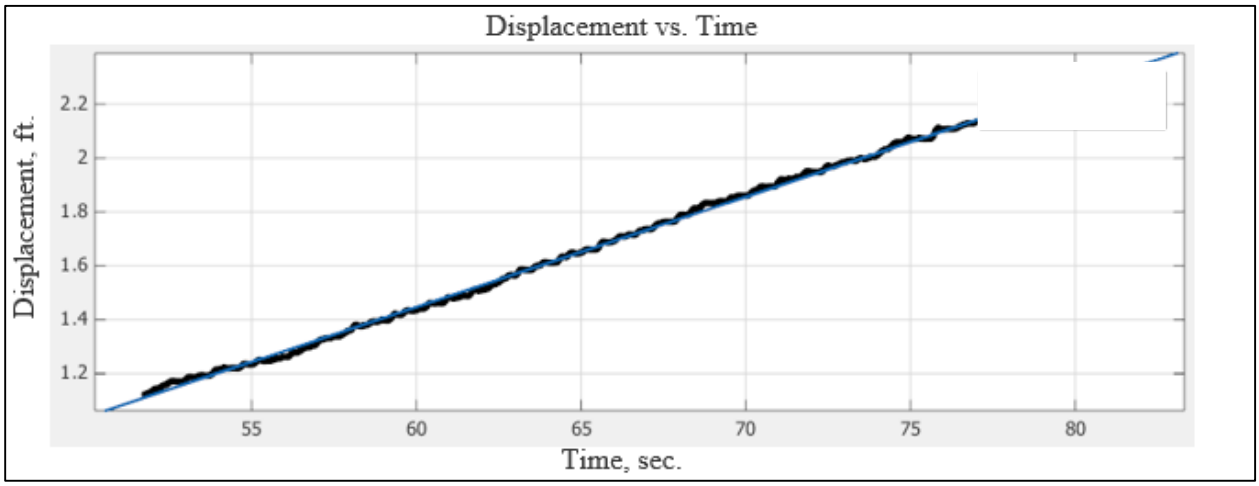

Figure 5.2: Position vs. Time for Constant Velocity Region of First Concrete Block Test with Line of Best Fit

The data set was run through the curve fitting tool in MATLAB to determine the slope of the line, which is the velocity. The average velocity over this region is 0.041 ft./sec., or 0.49 in./sec. (moving out the hole) and the R^2 value for this region is 0.999, indicating a consistent velocity profile.

A plot that instead outlines changes in force over the same timeframe is seen below in Figure 5.3:

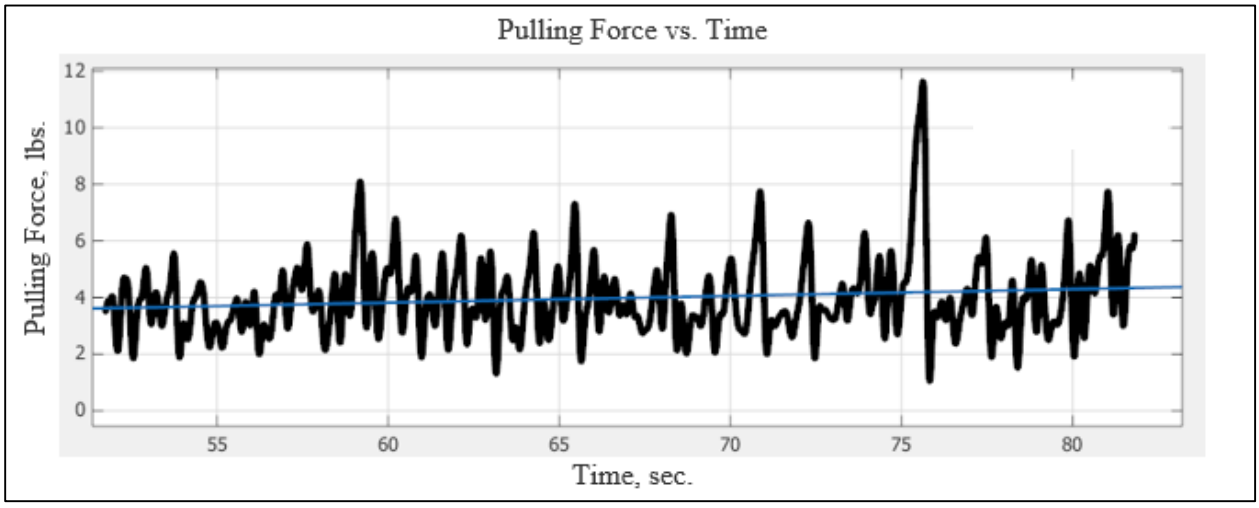

Figure 5.3: Force vs. Time for Constant Velocity Region of First Concrete Block Test with Line of Best Fit

In this case, the best fit line for the force is significantly less representative of the force compared to that of the velocity values in Figure 5.2. This data shows forces that range around four lbs being applied to the scratch head. The regression data for this region in Figure 5.3 have an R^2 of 0.023 and show no discernible change in force magnitudes over the course of the scratch head motion that would indicate the change of rock types over this area.

The velocities for all the PVC pipe tests and concrete block tests were organized and compared to identify if an overall consistent scratch velocity was maintained throughout the tests that occurred with more than a foot in insertion. Most graphs seen in the experiments section that did not suffer a massive dislodging of the scratch head, or a breakage of the tension wire will show a region of constant velocity motion. The output of these velocities is available in Table 5-I below:

Table 5-I: Average Velocity Values for PVC and Concrete Scratch Tests

Test Name	Scratcher Diameter (in.)	Average Concrete Block Velocity (in./sec.)	Average PVC Velocity (in./sec.)	Average Velocity (in./sec.)
1 Zone 1	0.045	0.54		0.54
1 Zone 2	0.045	0.49		0.49
2 Zone 1	0.045	0.43		0.43
2 Zone 2	0.045	0.6		0.6
3 Zone 1	0.045	1.36		1.36
3 Zone 2	0.045	0.66		0.66
1.1	0.045		0.5	0.5
1.2	0.045		0.6	0.6
2	0.045		0.768	0.768
3.1	0.051		0.44	0.44
3.2	0.051		0.52	0.52
	Average	0.68	0.57	0.63
	Standard Deviation	0.31	0.11	0.25

The data indicate an average velocity of the movement of the scratcher head for the combined PVC pipe and concrete block tests to be 0.63 in./sec. with a standard deviation for these values of 0.25 in./sec.. The movement in the concrete block had a higher average velocity (0.68 in./sec.) than the average velocity in the PVC pipe (0.57 in./sec). Additionally the PVC pipe had a smaller standard deviation of scratcher velocity, which means it had better velocity consistency than the concrete block tests.

Force versus Displacement Analysis

Another useful type of plot can be developed for the collected information that portrays how the force values change relative to the scratcher's position in the hole. This makes the buildup and release of stored energy from friction slippage on the rock become more evident. This plot is generated in the "itchesplot" program and simply pairs the force and position values for a given time value. A view of this plot for test two is seen in Figure 5.4 below, with a region outlined in orange to be assessed further, the scratch direction, and a vertical red line denoting the collar of the drilled hole:

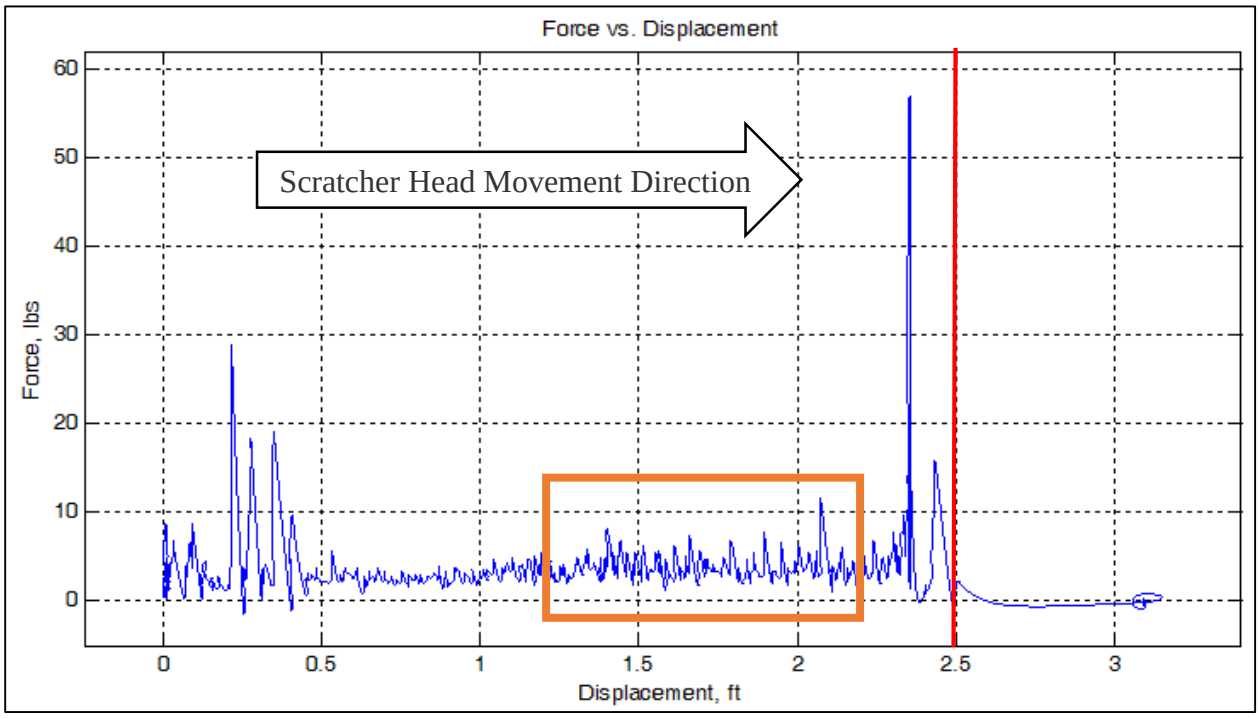

Figure 5.4: Force vs. Displacement graph for Test One on Concrete Block with Orange Outline of Study Area, Red Collar Line and Movement Direction Arrow

The outlined region corresponds to the constant velocity region from Figure 5.2. When visualized up close, certain behaviors become evident. The highlighted region was selected for an in-depth analysis because it is known that this area corresponds to constant velocity motion.

Upon close inspection, the snag-and-slip pattern becomes obvious, the force increases in magnitude with no corresponding increase in displacement. That elastic potential energy manifests itself in the scratchers, rock mass, transducer and the tension cable, and when the force gets to a level where it overpowers the frictional force between the rock and scratchers, it slips and the force returns to a stable level. The zoomed in view of this behavior is seen below in Figure 5.5:

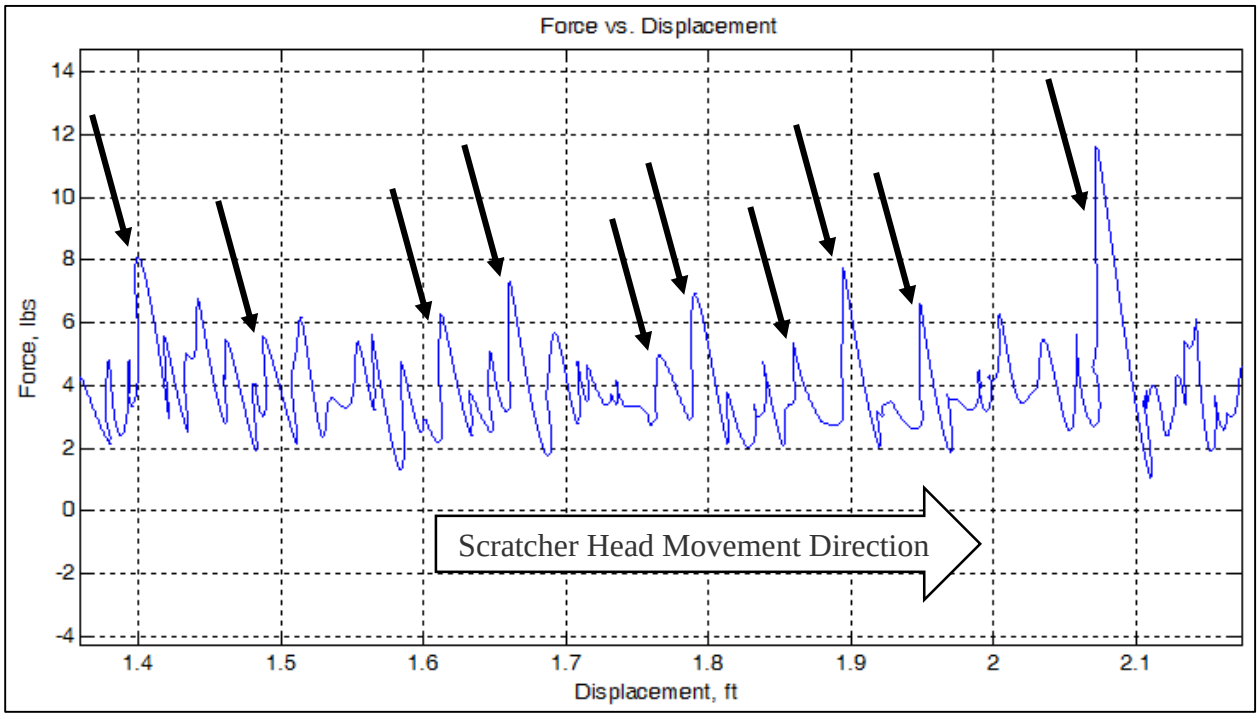

Figure 5.5: Magnified Force vs. Displacement Graph for Constant Velocity Range with Marked Areas of Force Buildup and Slippage Behavior

Note the black arrows corresponding to areas of increase of force without a significant increase in displacement. This means that the scratchers became stuck and the force increased until the resistance was overcame and the device could move again.

To get a more generalized view of the force and displacement values seen in these graphs, a program was written titled “movav”, short for moving average. The source code for the program is found in Appendix D. The “movav” program functions by breaking the force vs displacement data into user defined intervals and showing the average for each of these intervals. The smaller the intervals, the more representative of the true graph the data comes. The “movav” program’s output can be seen for test two on the concrete block in Figure 5.6:

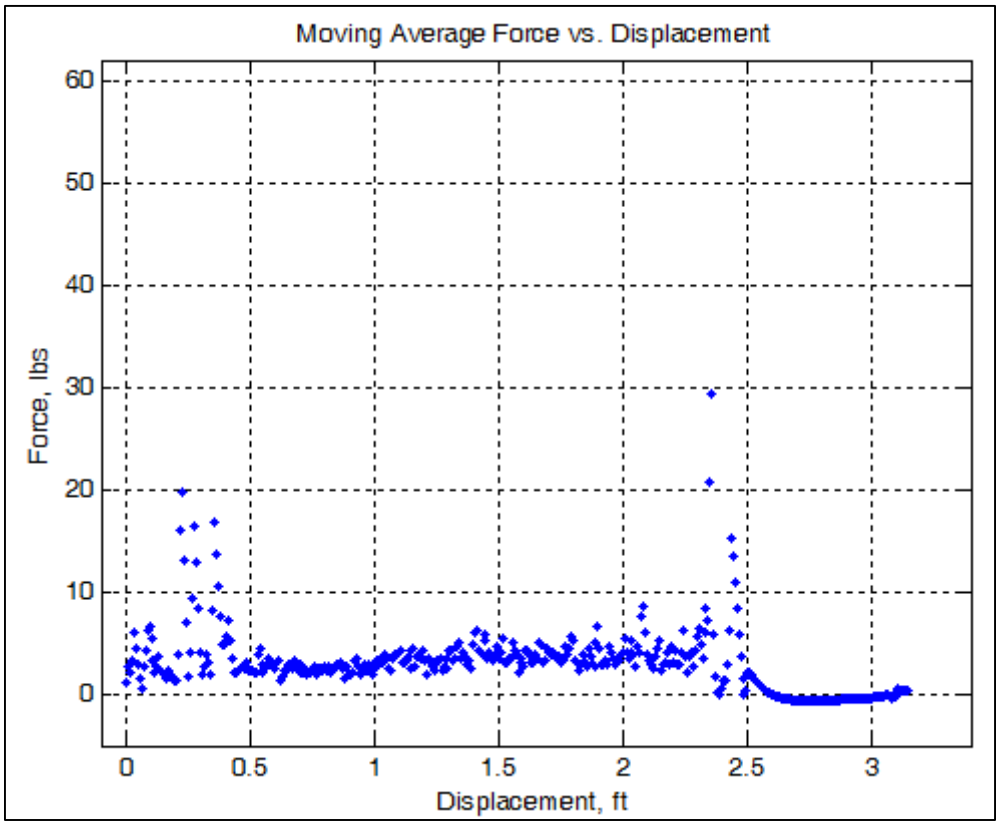

Figure 5.6: Output of “movav” Program for Test One with 412 Data Points

The similarities between this graph and the one seen in Figure 5.4 are easy to see, as they are representing the same data, but with varying resolutions. The true advantage of this program comes when the data is simplified even further to reflect the averages of larger intervals. The

number of data points from a further reduction is small enough that a matrix can be generated denoting the averages over easy-to-follow intervals. This would be extremely useful for determining the strength characteristics for that interval if one were to know the average scratch depth over the same interval by applying to the scratch test formula that requires applied force, cutter width and cut depth as inputs.

Figure 5.7 shows the results from "movav" program with 10.2% as many data points as were seen in the last image:

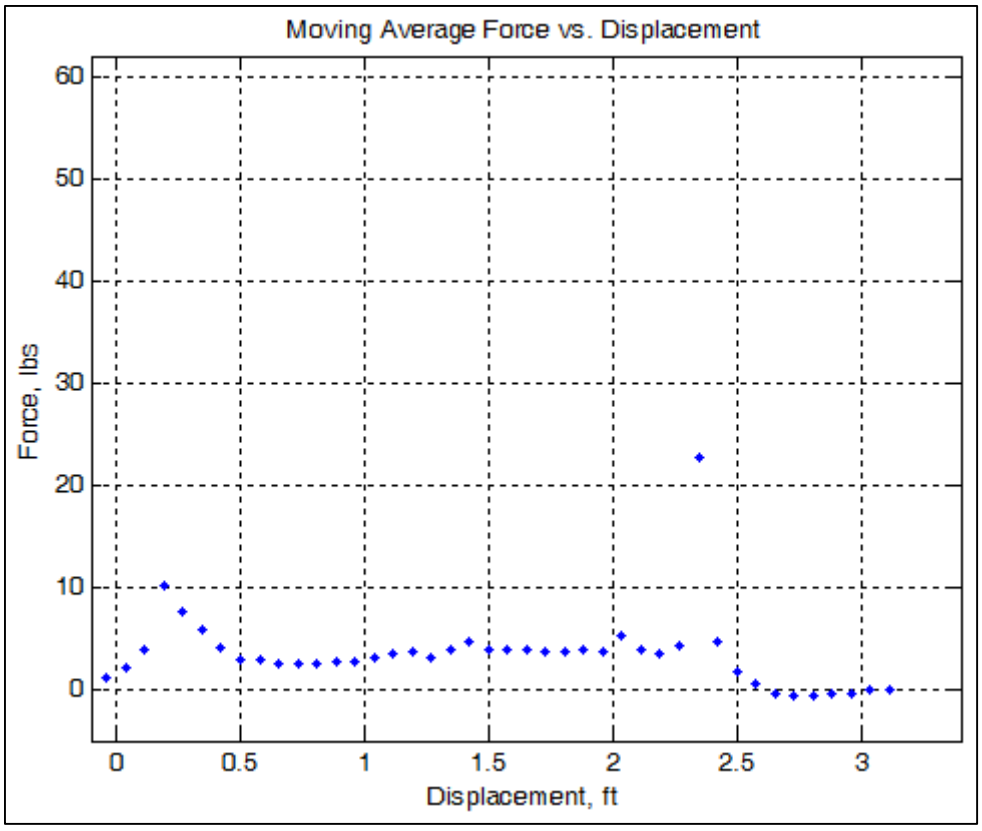

Figure 5.7: Output of "movav" Program for Test One with 42 Data Points

The same general shape is kept for this image compared to Figures 5.4 and 5.6, but it gets much easier to see the magnitude of force applied to certain sections such as between 1.3' and 2.3',

where the constant velocity was observed. This is not to lead the reader to conclude that these data are any more accurate than their noisy source material from Figure 5.4, as it is a strong reduction in force profile that may even be omitting other useful, more detailed, information. The program simply helps visualize the concept that if large changes in force were seen in different parts of the borehole during the scratching procedure from changes in host rock strength, they would likely be easier to see from a graph such as this one.

Sandstone Scratch Analysis

One final type of analysis was conducted on the data from the sandstone sample scratch tests. Considering the only chosen change between the tests was the diameter of the scratchers, it was deemed useful to consider the way that the forces may change between these tests. Some of the original graphs for the sandstone tests can be seen in Figure 4.16, Figure 4.17, and Figure 4.18 where force and displacement are plotted against time, with the rest available in the Appendix in Figures A.9 through A.20. An analysis of these images shows an increase in force for the parts of the test where motion occurred followed by a flatline after the scratcher exited the hole and hung until the test ceased. The mean force in the motion phase and was calculated and organized in Table 5-1:

Table 5-II: Comparison of Force Averages for Different Scratch Diameters for Sandstone Sample

Scratcher Diameter (Inches)	Sandstone								
	Pull Force Averages (lbs)							Overall Statistics	
	Test 1	Test 2	Test 3	Test 4	Test 5	Test 6	Test 7	Average	St. Dev.
0.045	8.28	6.19	5.34	4.48	n/a	6.59	6.55	6.24	1.29
0.051	12.75	7.76	10.39	4.509	5.44	11.63	4.87	8.65	3.49
0.055	6.49	15.19	12.22	9.17	6.71	n/a	n/a	9.96	3.73

The magnitude of the force averages are visible in the blue column on the right. These results indicate that increasing the scratch tip diameter will increase the force necessary to move it along the rock surface. This is a result of the friction forces of the scratcher tips as they drag along the rock surface and are subject to larger normal forces with increasing scratcher stiffness. As well as the fact that if scratching occurred, the force would be applied over a wider area, which would provide more resistance.

Chapter 6: Conclusions

After conducting an analysis about the ability to quantify mine strata conditions, a scratching device was developed to extract useful strength characteristics from legally mandated one inch diameter test holes in mine roofs. The applied rock analysis technique is based off of pre-existing methods of scratching core logs and determining their strength properties from measured forces and cutting dimensions. A thorough review of mine strata conditions was conducted in the literature review to identify what types of hazards exist in mine roofs as well as how their geologic formation lead to some of the features that would be important for a strata analysis device to target and identify.

Titled MRSAD, short for Mine Roof Strata Analysis Device, this rock analysis unit consists of a mounting system and a series of instruments to gather properties from the rock. The scratcher, pulled through the hole by a tension cable, has scratch tips contained within it that interact with the rock to generate cutting forces. A winch attached to a stand winds this tension cable and the generated forces are relayed by a custom-made tension transducer affixed in-line with this cable. A position transducer, attached to the scratching head, travels the length of the hole and relays position values to correspond to the force values. An installation protocol was developed, as well as the modified pipe and special scratch tip retraction mechanism necessary for installation.

The signal from the transducers connected into a data acquisition system that is paired with a laptop computer. On the computer, a specially written LabVIEW program converts the voltage signal into a spreadsheet. This spreadsheet can be imported into MATLAB where a series of routines were written to aid in their processing. The results, when viewed as functions of time and functions of position conveyed information about the motion of the scratch head in

the borehole. This device was first tested in a lab setting at a roof drill manufacturer facility where a concrete block with various embedded strata was scratched to see if any changes in rock could be observed. The data were too erratic to determine any changes in rock type along the borehole. A second and third test were performed in a campus laboratory by conducting the same scratch test in a PVC pipe and a sandstone block. This guaranteed proper anchorage and allowed additional variables to be constrained such as scratcher diameter which were not controlled during the tests at the roof drill facility.

Force measurements from the tension transducer relayed pulling forces in the sandstone averaging 6.24 lbs, 8.65 lbs, and 9.96 lbs for the 0.045", 0.051" and 0.055" diameter wire scratchers, respectively. Additionally, tests performed on the PVC pipe show a similar increase in applied force with increased scratcher diameter from 0.045" to 0.051" with a respective force increase from 2.81 lbs. to 36.46 lbs. This indicates that increasing the scratcher wire diameter increases the pull force and therefore, the force applied to the rock. Increasing the diameter of the wire increases the stiffness of the scratcher and therefore increases the normal force exerted into the surrounding media. Increasing wire diameter also reduced the deflection the scratchers may undergo from scratch forces. The displacement transducer performed as expected and indicated that the winch was able to control the velocity of the scratch head with an average of 0.63 in./sec. velocity with a standard deviation of 0.25 in./sec.. The output from the graphs indicates a pattern of sticking and slipping between the scratchers and the surrounding material as the head would build up force and then travel a small amount. Although the numerical results didn't provide an ability to find rock strength values, it did indicate the promise of certain aspects of the device to be used in later iterations of similar technology.

Chapter 7: Future Work

In spite of the promise of several of the designed components, there were identified aspects of this project where reevaluation could significantly simplify the system and increase accuracy. The most glaring improvement would be to rework the force-sensing element to be better suited for the forces that were encountered in this trial (many tests had valuable information contained between 0-10 lbs but the load cell was designed for higher forces). Additional efforts to improve filtering of the data as well as signal stability would also increase precision and accuracy. A better configuration would be if the force sensor could be mounted to the tension winch so that the forces would manifest themselves in the winch and the forces applied could be derived from there and there bypass putting a force sensor in the hole.

Another improvement would be to integrate the position sensing properties of the extensometer with the winch. Since the winch already has the cable in the hole, all the cable that it pulls from the hole is moving at the same rate at the scratch head. With this knowledge, it should be possible to configure a gear system to the pulley so that every N turns of the winch will manifest themselves as a smaller number of turns on a potentiometer and therefore give a position specific voltage output. This would bypass the expensive, delicate and cumbersome extensometer with its accompanying cable and reduce the amount of things that need insertion into, and could be damaged by, the borehole.

The scratch head also has areas of improvement. It is suggested here that the ideal means of implementing the scratchers would be to have a head shaped much like the one from this project, but have it sit within a sheath. This sheath would restrain the installed scratchers from pushing into the rock mass and when placed in the correct position, the sheath could be slid off the scratch head, with the scratcher arms springing into the surrounding strata. This would serve

several functions, as it would remove the amount of skill that the installer would have to have for installing the device as well as increasing the stiffness of the scratchers that could be used. There was no means for determining or controlling the contact force of the scratchers on the rock, a method of doing that would provide other areas of improving scratcher design.

The use of thicker scratchers would increase the likelihood of gouging of the rock as the PVC and sandstone experiment suggested that small changes in scratcher tip thickness can yield higher pulling forces. A closer examination of the relationship between tolerance of the scratch head and tolerance of the hole diameter would also likely provide more information about circumstances that result in scratching versus simple friction sliding in the hole. Modifications to the shapes of the scratching tips to better control their effect on the test should also be considered. Lastly, a more portable (hopefully permissible), autonomous data acquisition system that could bypass the cumbersome LabVIEW to Excel to MATLAB file transfer that had to occur for this project would prove very convenient, especially if it could bypass a computer altogether.

Several factors were identified that should be investigated further as sources of error in the testing. The buildup of dust of certain amounts and compositions on the hole wall may impact the effectiveness of the cutting system and its effect on this research is unknown. Also, the presence of water in the rock may affect how the rock reacts to scratching. Controlled dimensions of borehole diameter during scratching would be helpful for determining how out-of-gauge hole profile affects scratcher behavior. Recommended safety practices include: keeping only the most necessary people around the testing unit at any given time so that if an unlikely failure occurs, there would be no risk to them, and only winding the spool from behind the device so that nobody is in the way of the unit in the event of failure.

References

Bahrampour, S., Rostami, J., Naeimipour, A. (2013). "Instrumentation of a Roof Bolter Machine for Void Detection and Rock Characterization." In: *Proceedings of the 26th International Conference on Ground Control in Mining.* Morgantown, WV: West Virgina University, pp. 113-118

Iannacchione AT, Zelanko JC [1994]. Pillar mechanics of coal mine bursts: a control strategy. In: Proceedings of the 16th World Mining Congress, The Mining Industry on the Threshold of XXI Century (Sofia, Bulgaria). Vol. 5, pp. 15-23.

Mark C, McWilliams LJ, Pappas DM, Rusnak JA [2004]. Spatial trends in rock strength: can they be determined from coreholes? In: Peng SS, Mark C, Finfinger GL, Tadolini SC, Heasley KA, Khair AW, eds. Proceedings of the 23rd International Conference on Ground Control in Mining. Morgantown, WV: West Virginia University, pp. 177B182.

Mark, C., Molinda, G.M., Burke, L.M., Preventing falls of ground in coal mines with exceptionally low-strength roof: two case studies, in: Proc. 23rd Int. Conf. Ground Control Min., Morgantown, WV, 2004, pp. 327–333.

"Mining Topic: Ground Control Overview." Centers for Disease Control and Prevention. Centers for Disease Control and Prevention, 27 Sept. 2012. Web. 25 Jan. 2015. <http://www.cdc.gov/niosh/mining/topics/GroundControlOverview.html>.

Molinda, Gregory M. *Geologic Hazards and Roof Stability in Coal Mines*. Pittsburgh: NIOSH, 2003. Print.

Molinda, Greg, and Chris Mark. "Ground failures in coal mines with weak roof. "*Electronic Journal of Geotechnical Engineering* 15 (2010): 547-588.

Molinda GM, Mark C, Pappas DM, Klemetti TM [2008]. Overview of coal mine ground control issues in the Illinois basin. SME preprint 08B017. Littleton, CO: Society for Mining, Metallurgy, and Exploration, Inc.

"MSHA - Interactive Training - JTA Spiders - Roof Bolter Operator." *MSHA - Interactive Training - JTA Spiders - Roof Bolter Operator*. Web. 11 Feb. 2015. <http://www.msha.gov/interactivetraining/Spiders/RoofBolter/>.

Peltier, Bertrand P.ierre Marie, Emmanuel Detournay, and Anthony Kevin Booer. Formation Evaluation Tool. Services Petroliers Schlumberger, Schlumberger Technology B.V., Schlumberger Holdings Limited, assignee. Patent US 5,323,648 A. 31 July 1996. Print.

Reddish. D.J. & Yasar. E. 1996. A New Portable Rock Strength Index Test Based on Specific Energy of Drilling. International Journal of Rock Mechanics and Mineral Sciences. 33 (5): 543-548.

Schei, G., Fjær, E., Detournay, E., Kenter, C. J., Fuh, G. F., Zausa, F. (2000, January 1). The Scratch Test: An Attractive Technique for Determining Strength and Elastic Properties of Sedimentary Rocks. Society of Petroleum Engineers. doi:10.2118/63255-MS

Suarez-Rivera, Roberto, Sidney J. Green, Joel Wesley Martin, and Robert Michael Griffin. Apparatus for Continuous Measurement of Heterogeneity of Geomaterials. Terratek Inc., assignee. Patent US 8,234,912. 7 Aug. 2012. Print.

Suarez-Rivera, R., Stenebråten, J., Dagrain, F. (2002, January 1). Continuous Scratch Testing on Core Allows Effective Calibration of Log-Derived Mechanical Properties for Use in Sanding Prediction Evaluation. Society of Petroleum Engineers. doi:10.2118/78157-MS

"Roof Bolting." Title 30 Code of Federal Regulations §75.204 (f) (2). 2011 Edition.

Stewart, C., G. Hunt and C. Mark, "Geology, Ground Control, and Mine Planning at Bowie Resources, Paonia, CO", Proceedings of the 25th International Conference on Ground Control in Mining, Morgantown, WV, August 1-3, 2006, (in press).

"Strain Gauge Configuration Types." *National Instruments*. Web. 11 Feb. 2015. <http://www.ni.com/white-paper/4172/en/>.

Szwedzicki T. Technical note on indentation hardness testing on rock. Int. J. Rock Mech. Min. Sci. 1998;35:825–9.

Tan, Chee Phuat. Downhole Rock Scratcher and Method for Identifying Strength of Subsurface Intervals. Schlumberger Technology Corporation, assignee. Patent US 7,921,730 B2. 12 Apr. 2011. Print.

Teale, R., "The Concept of Specific Energy in Rock Drilling," Int. J. Rock Mech. Mining Sci. Vol. 2, Pergamon Press 1965, pp. 57–73.

"The Strain Gage." *The Strain Gage*. Omega Engineering. Web. 11 Feb. 2015. <http://www.omega.com/literature/transactions/volume3/strain2.html>.

Appendix A: Supplementary Pictures

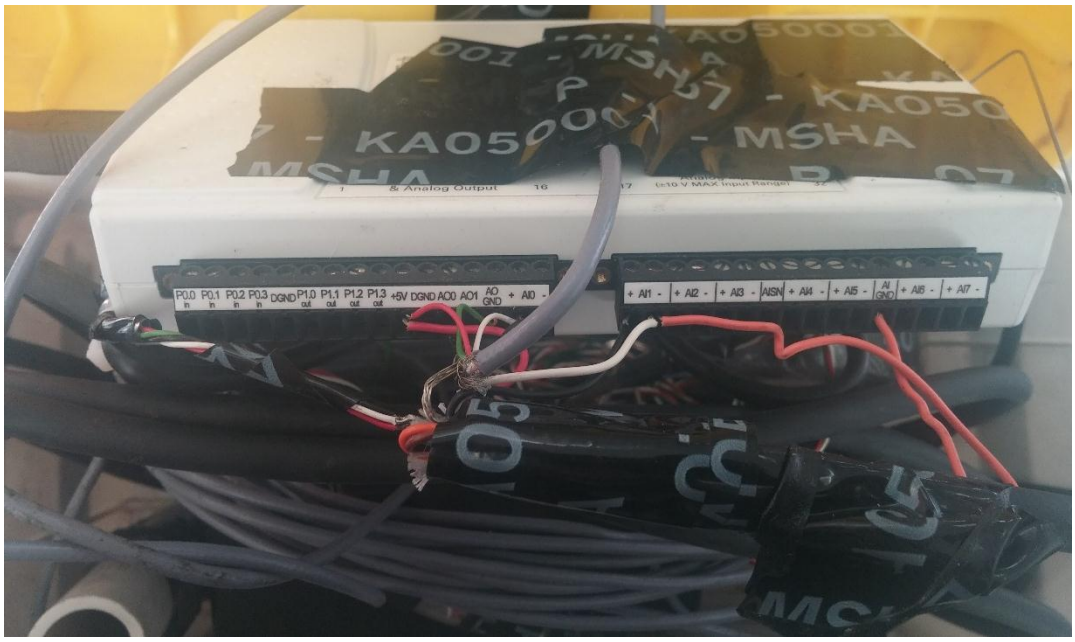

Figure A.1: I/O Configuration for Extensometer and Strain Transducer for NI USB-6211

Figure A.2: Concrete Block at the Testing Facility

Figure A.3: Drilled Holes in the Bottom Face of the Block

Figure A.4: Force Transducer Pulling from Concrete Block, Displacement Transducer Visible at Base of Green Stand

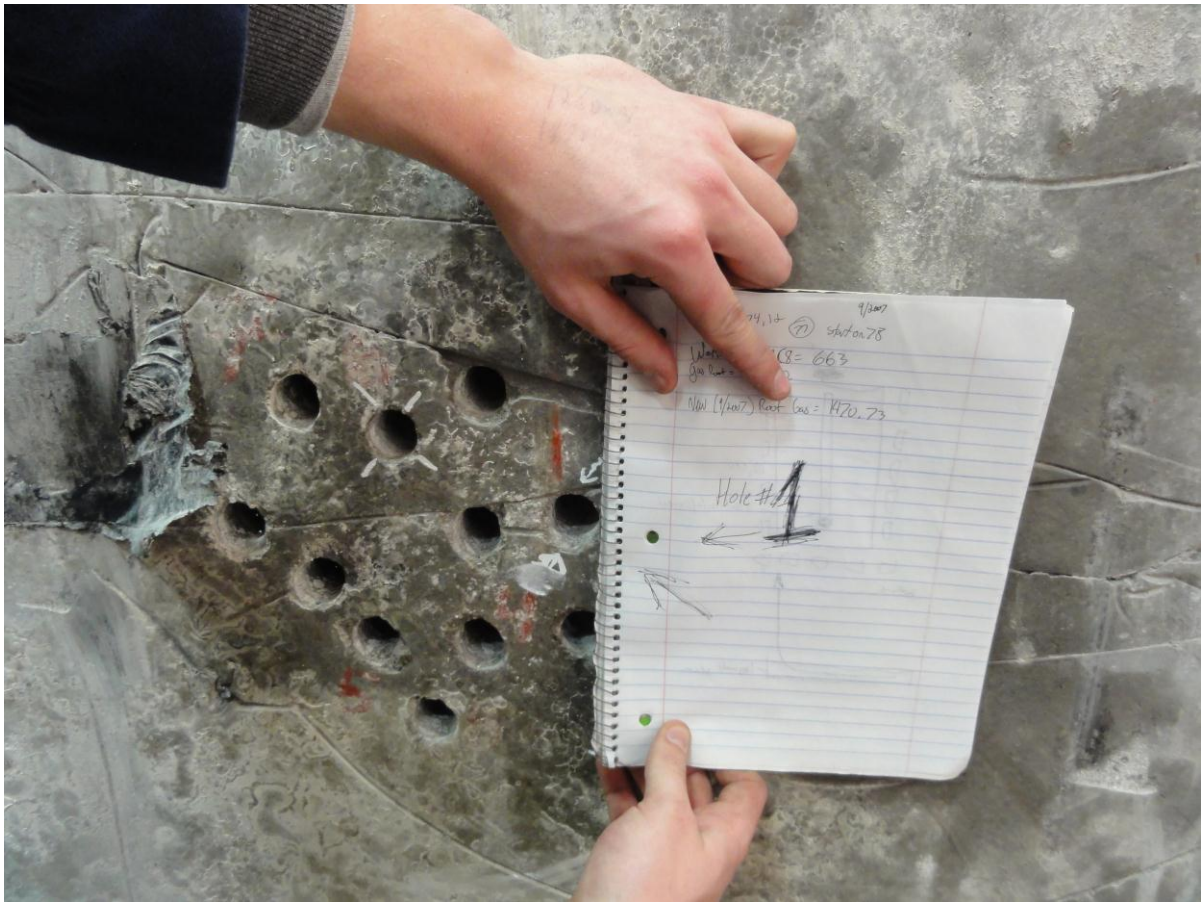

Figure A.5: Location of Hole one on Concrete Block, Hole Zero Visible with four Diagonal Lines

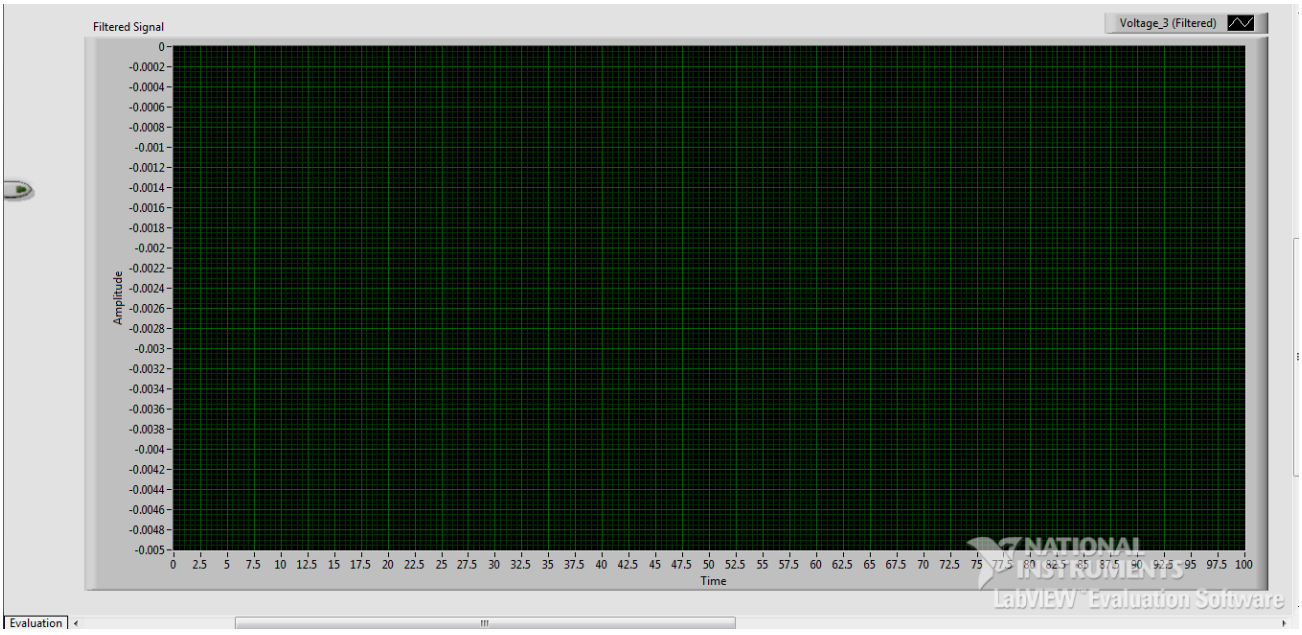

Figure A.6: LabVIEW Front Panel, www.NI.com/labview/, Used under Fair Use, 2015

Figure A.7: Installation Rod with 8” Ruler for Scale

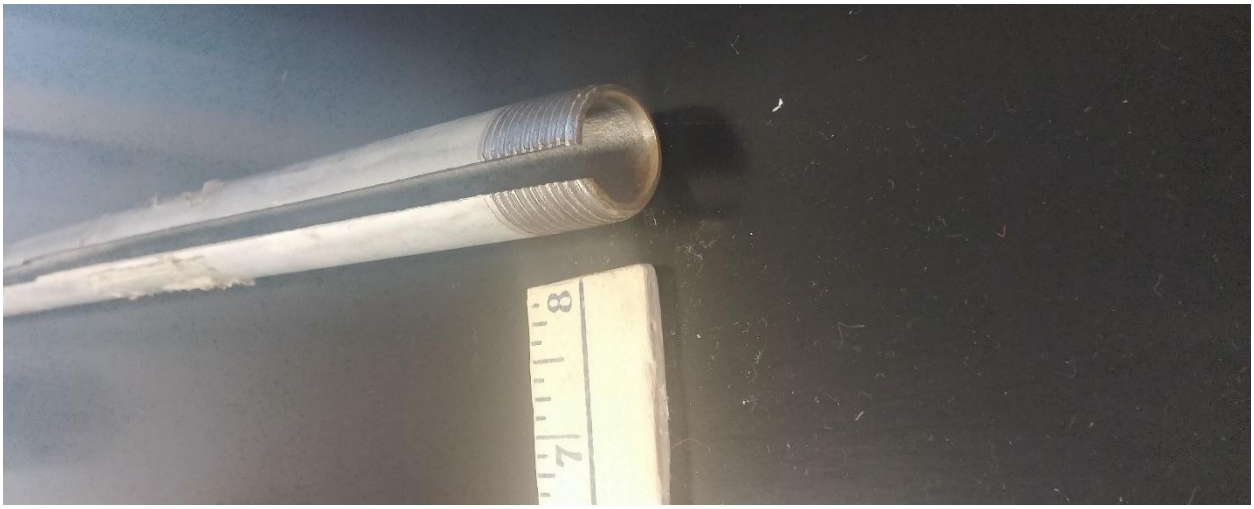

Figure A.8: Close View of Installation Rod Showing Cutaway Along Length for Removal Around Wiring

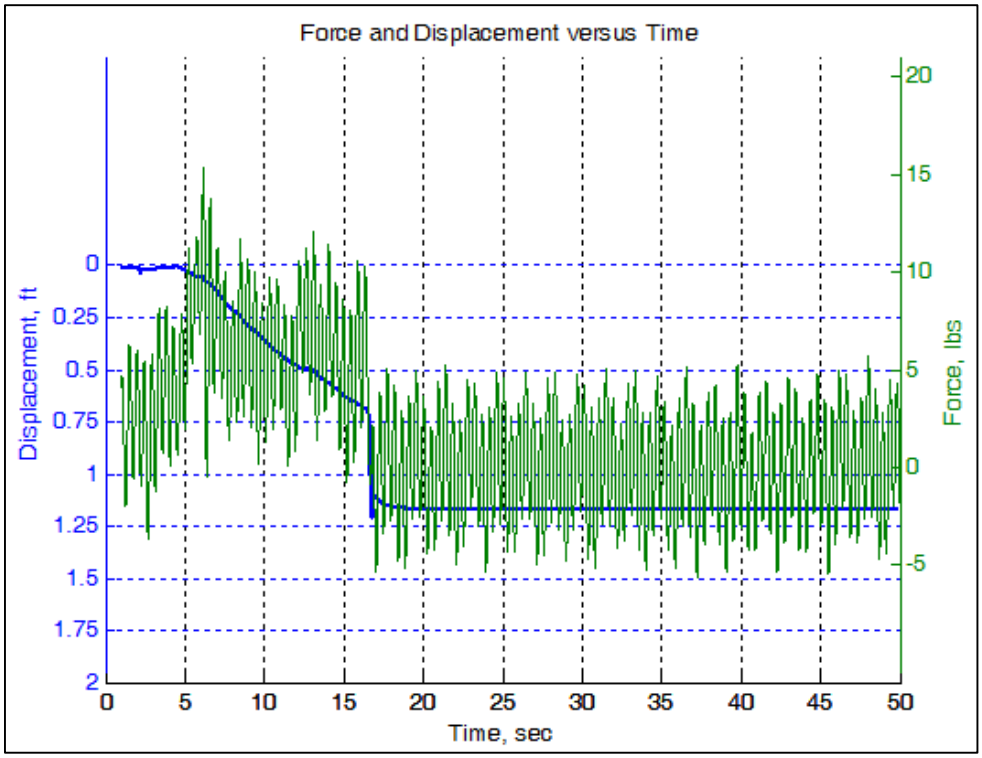

Figure A.9: Force and Displacement versus Time for Second 0.045" Sandstone Test

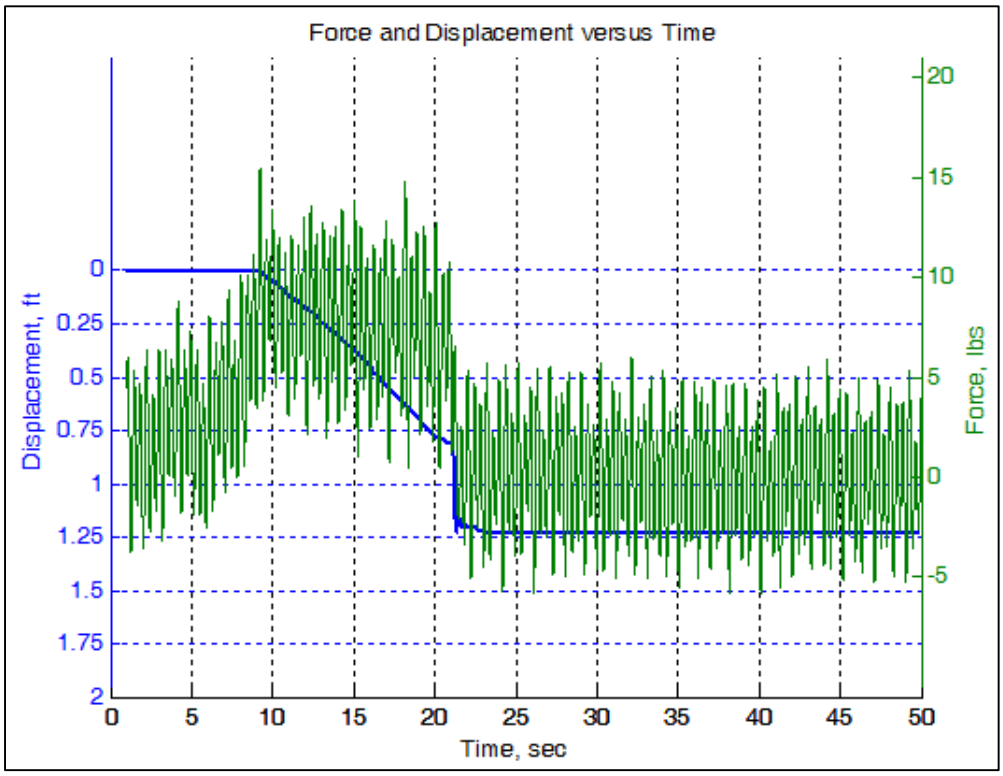

Figure A.10: Force and Displacement versus Time for Second 0.051" Sandstone Test

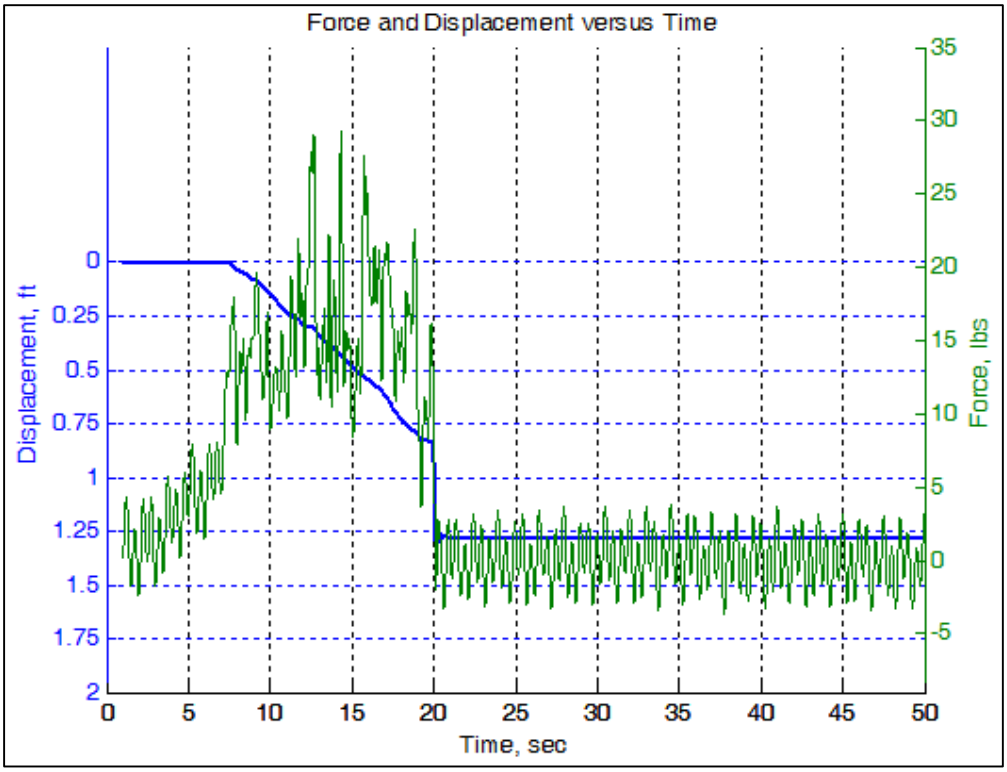

Figure A.11: Force and Displacement versus Time for Second 0.055" Sandstone Test

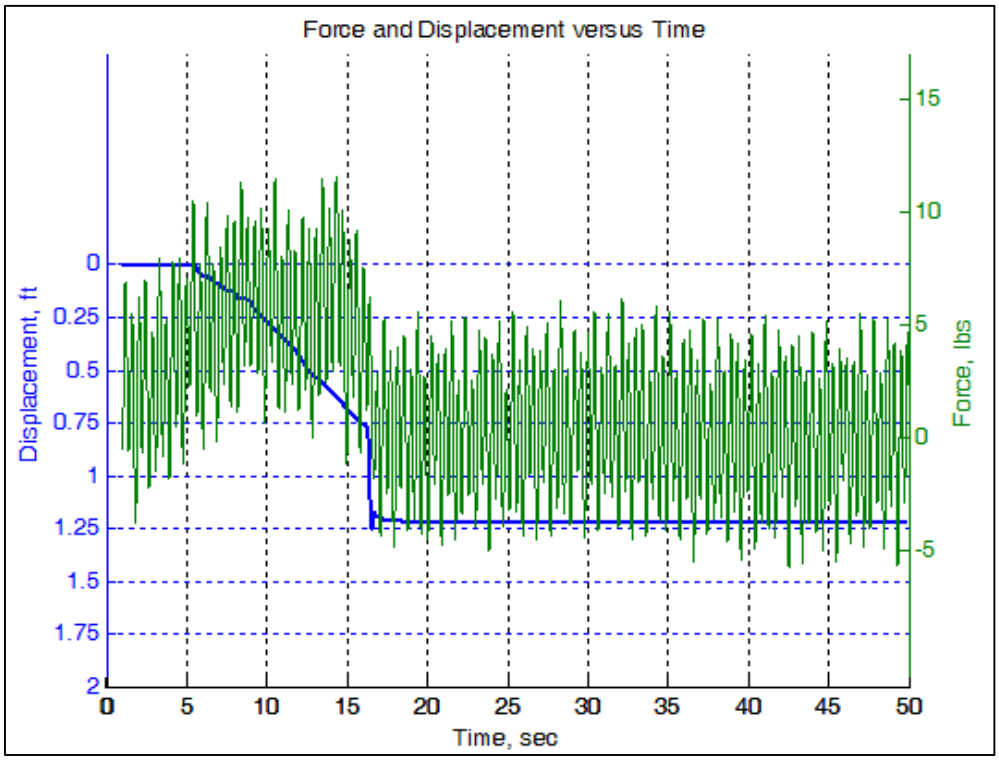

Figure A.12: Force and Displacement versus Time for Third 0.045" Sandstone Test

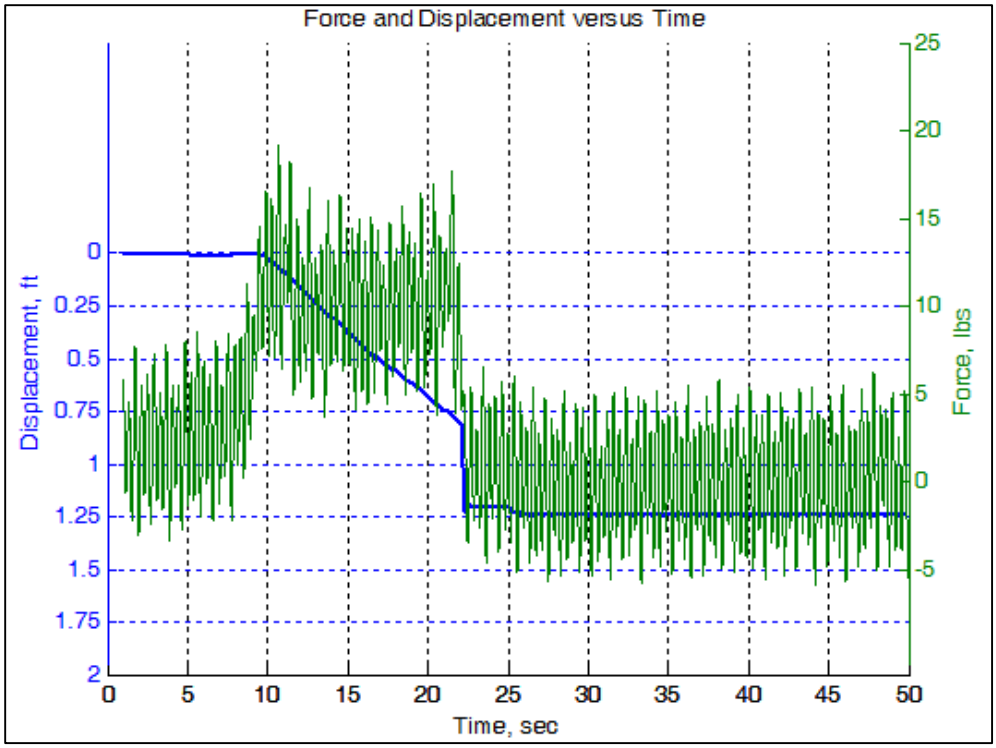

Figure A.13: Force and Displacement versus Time for Third 0.051" Sandstone Test

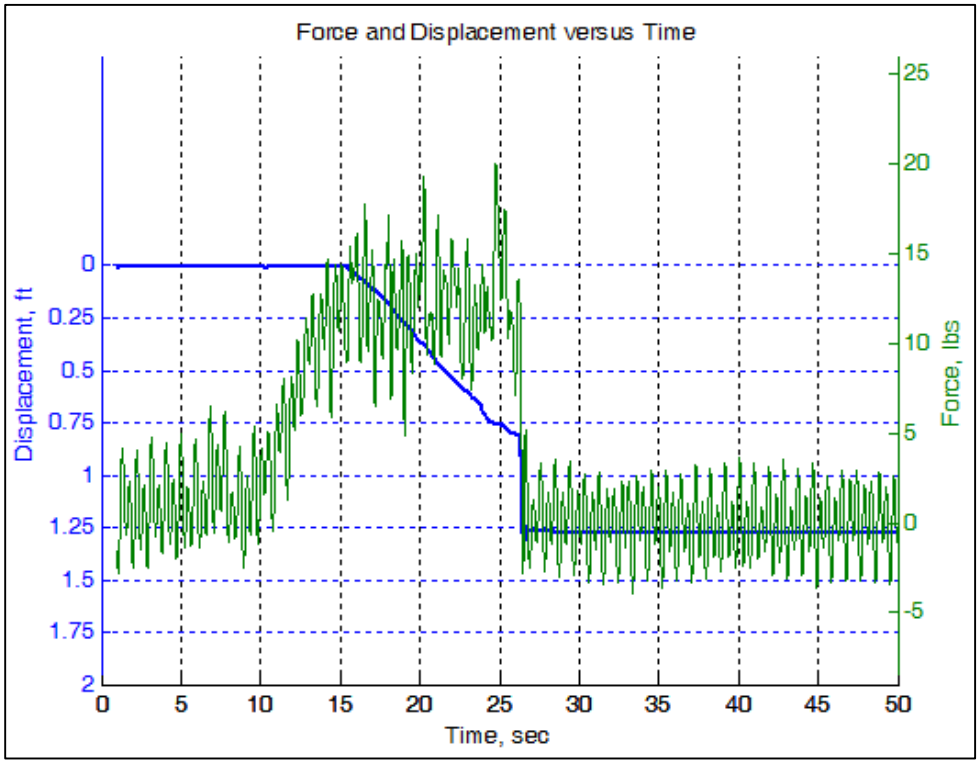

Figure A.14: Force and Displacement versus Time for Third 0.055" Sandstone Test

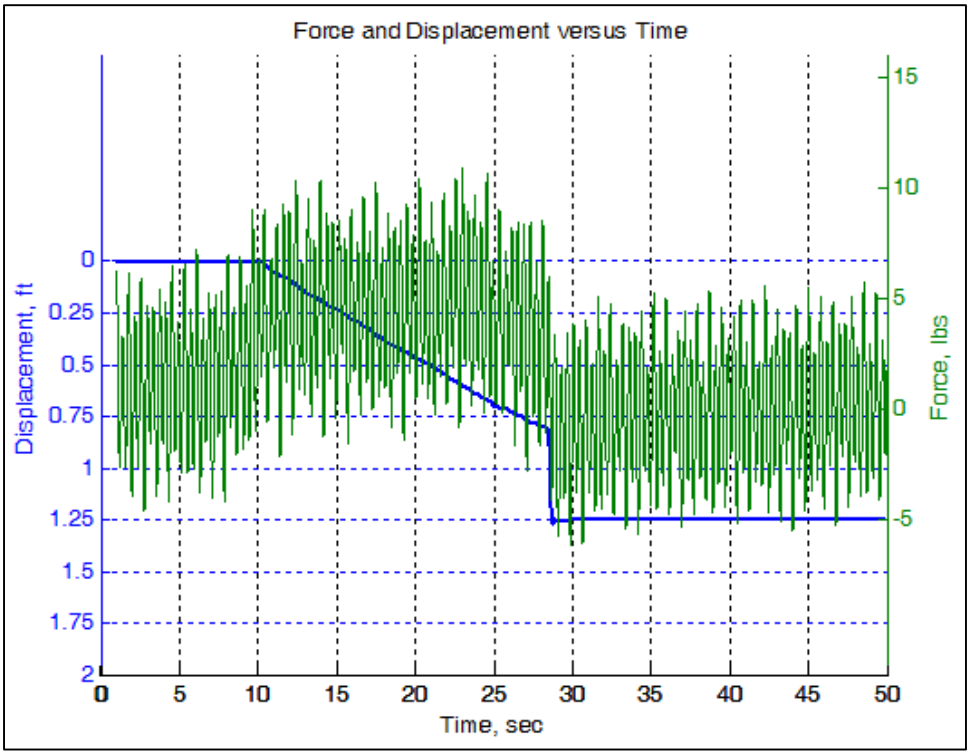

Figure A.15: Force and Displacement versus Time for Fourth 0.045" Sandstone Test

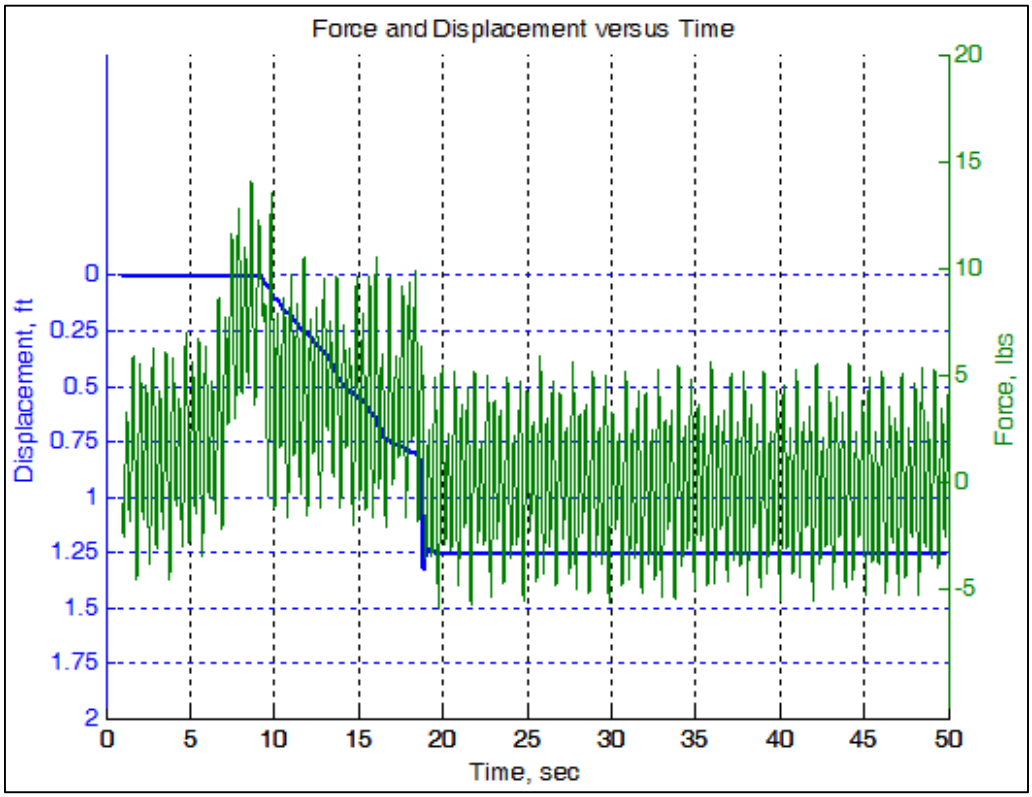

Figure A.16: Force and Displacement versus Time for Fourth 0.051" Sandstone Test

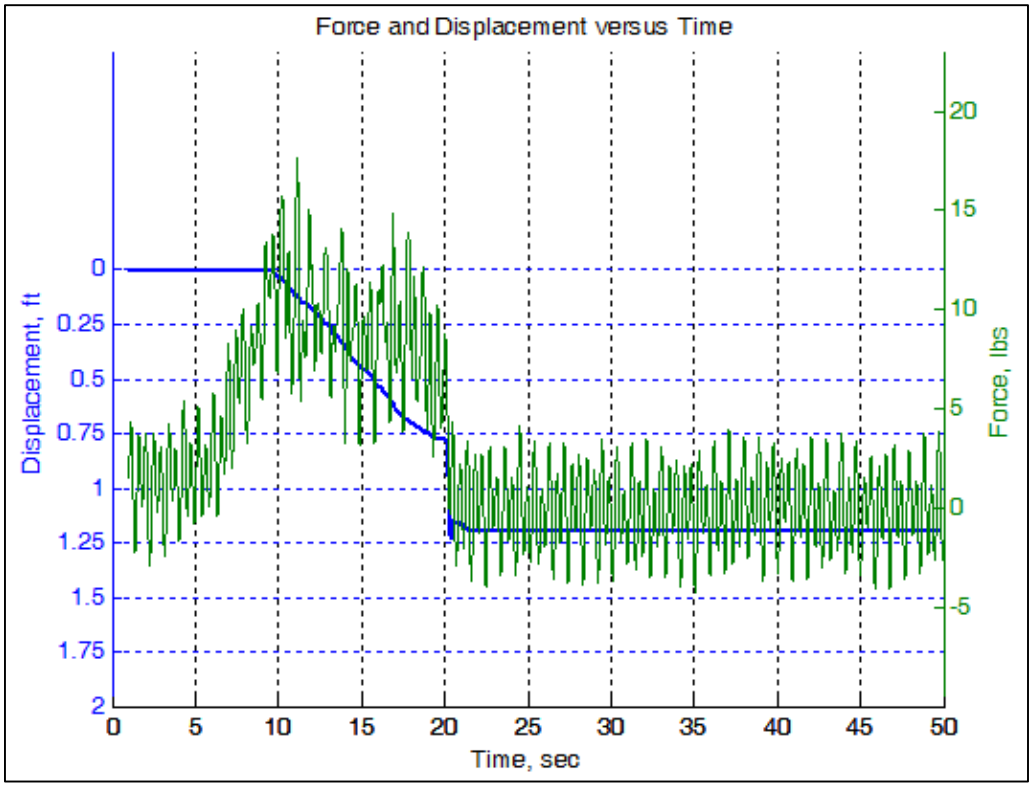

Figure A.17: Force and Displacement versus Time for Fourth 0.055" Sandstone Test

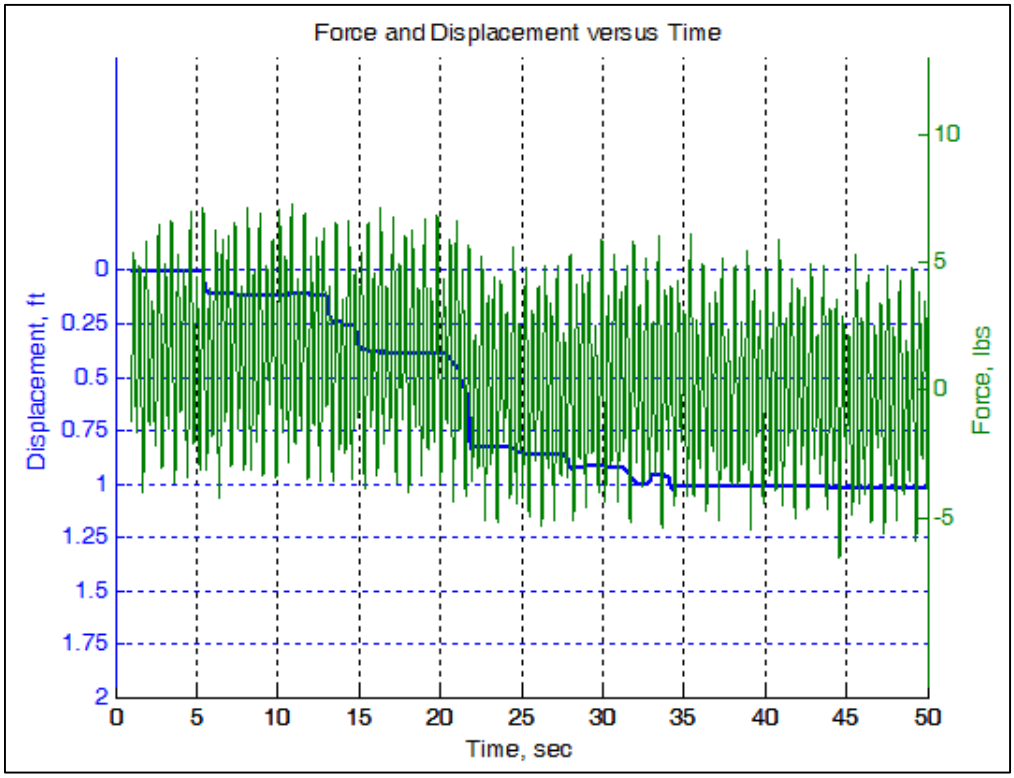

Figure A.18: Force and Displacement versus Time for Fifth 0.045" Sandstone Test

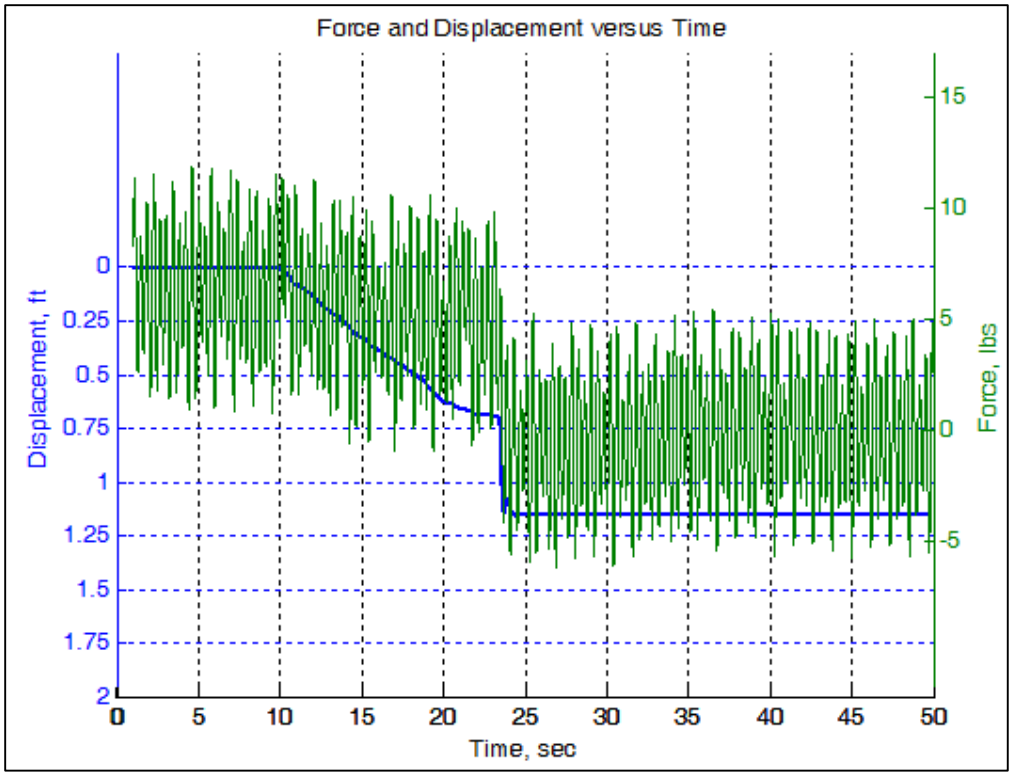

Figure A.19: Force and Displacement versus Time for Fifth 0.051" Sandstone Test

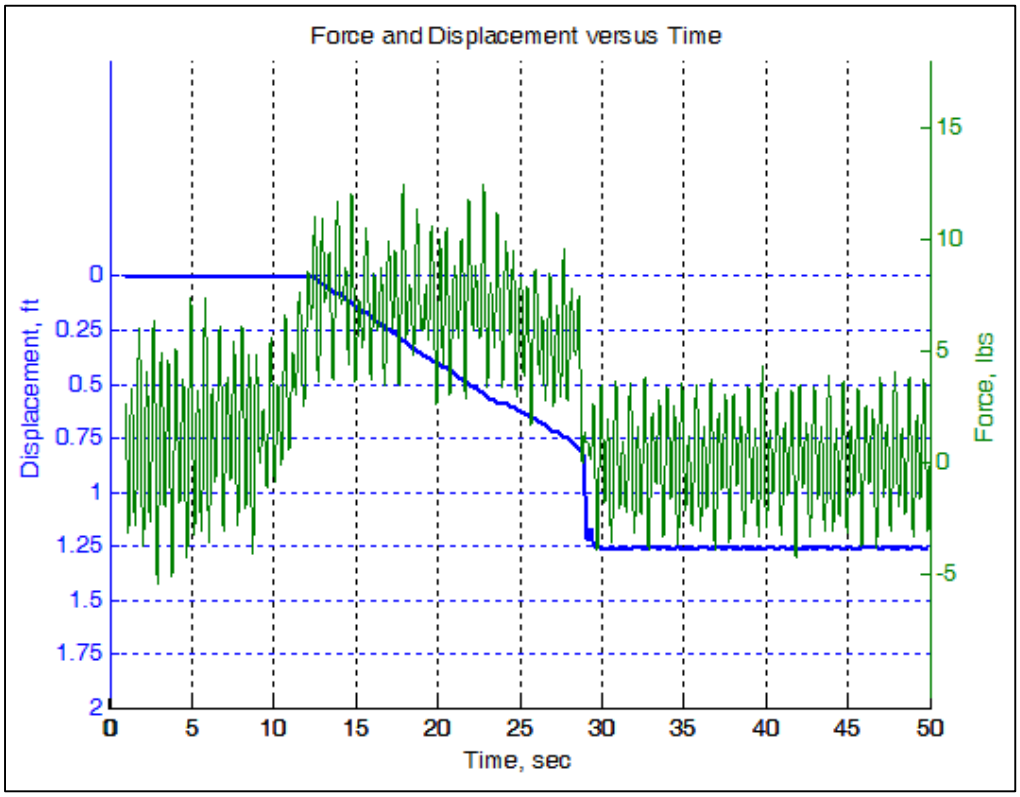

Figure A.20: Force and Displacement versus Time for Fifth 0.055" Sandstone Test

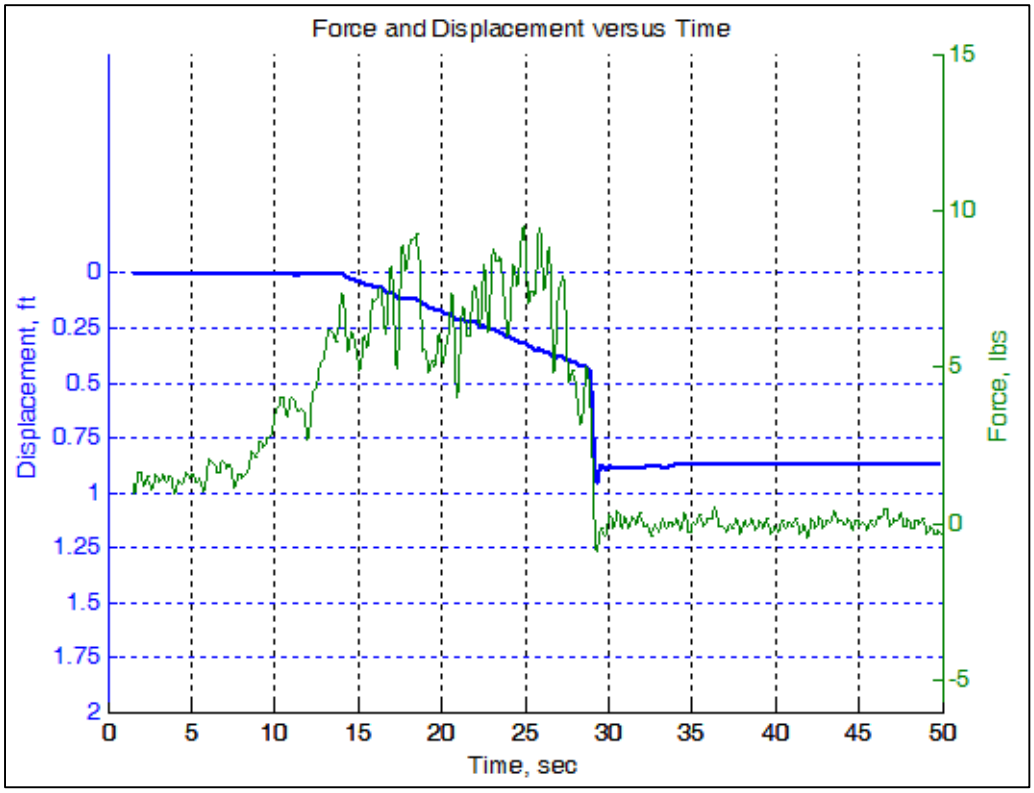

Figure A.21: Force and Displacement versus Time for Sixth 0.045" Sandstone Test

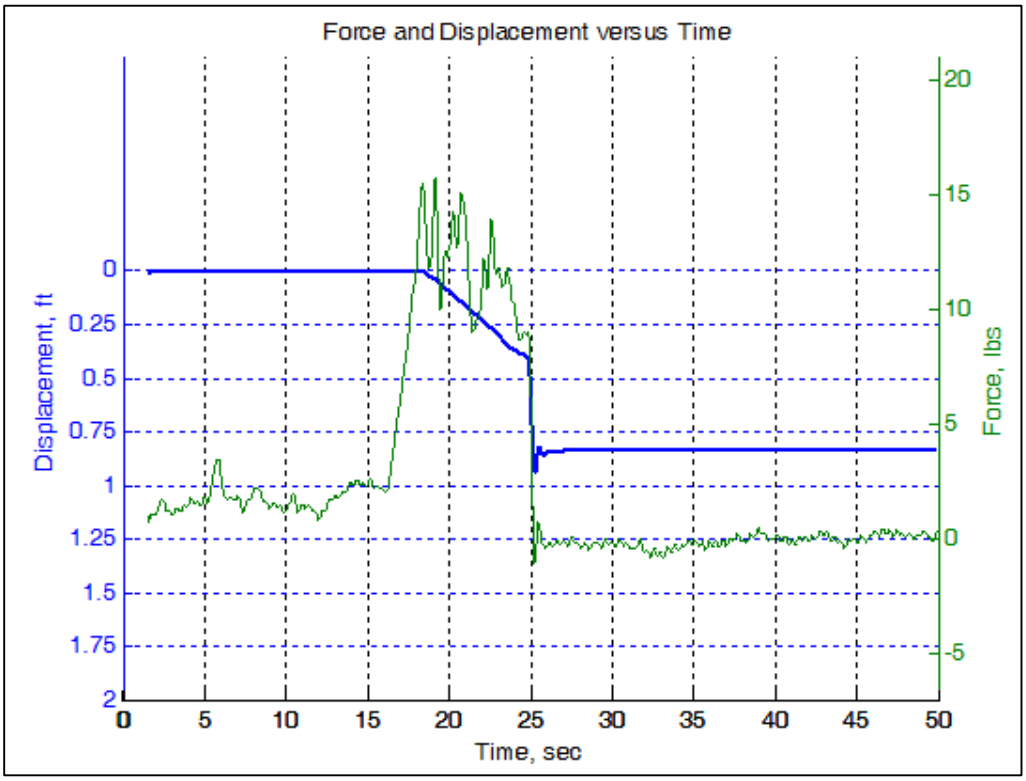

Figure A.22: Force and Displacement versus Time for Sixth 0.051" Sandstone Test

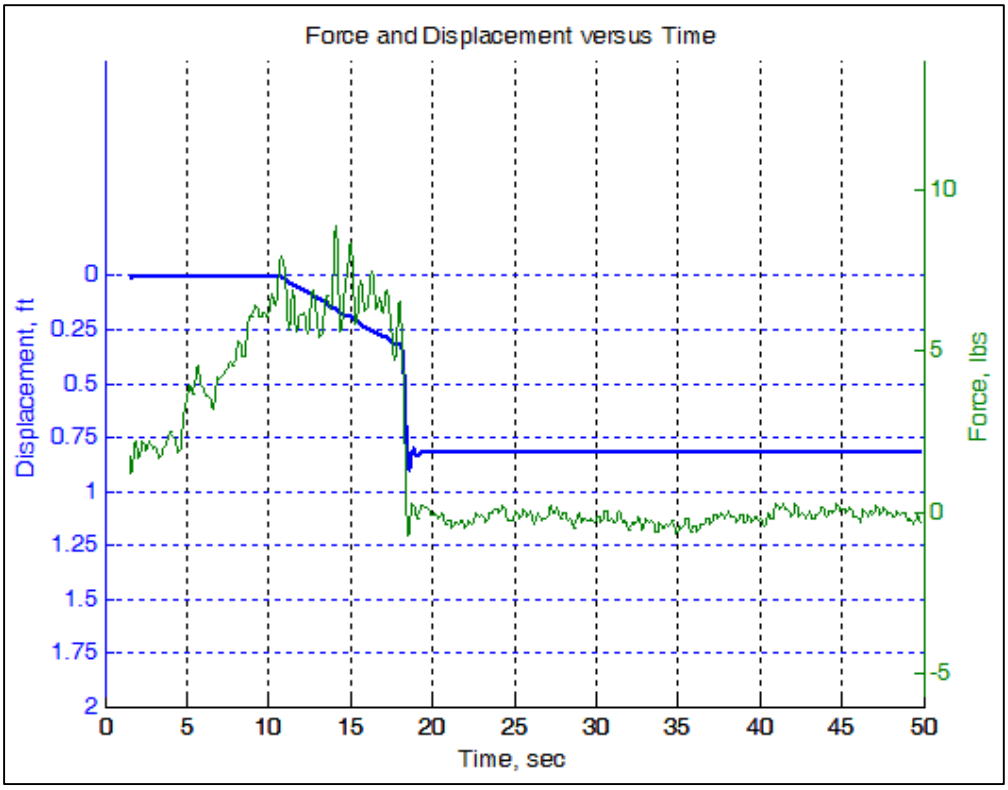

Figure A.23: Force and Displacement versus Time for Seventh 0.045" Sandstone Test

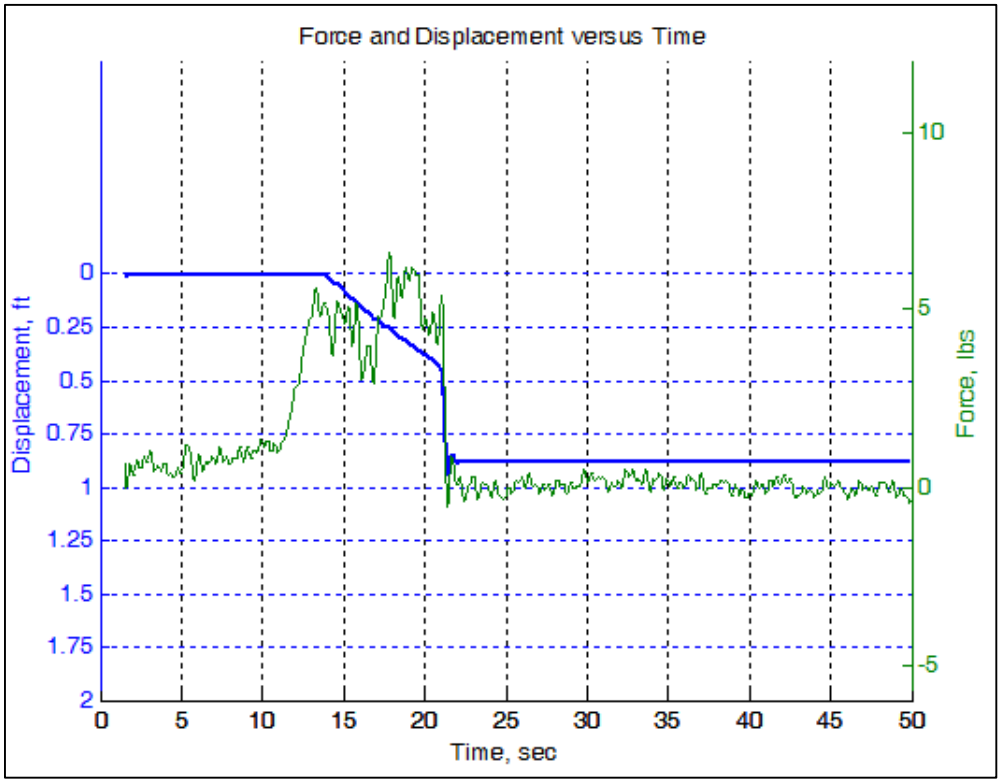

Figure A.24: Force and Displacement versus Time for Seventh 0.051" Sandstone Test

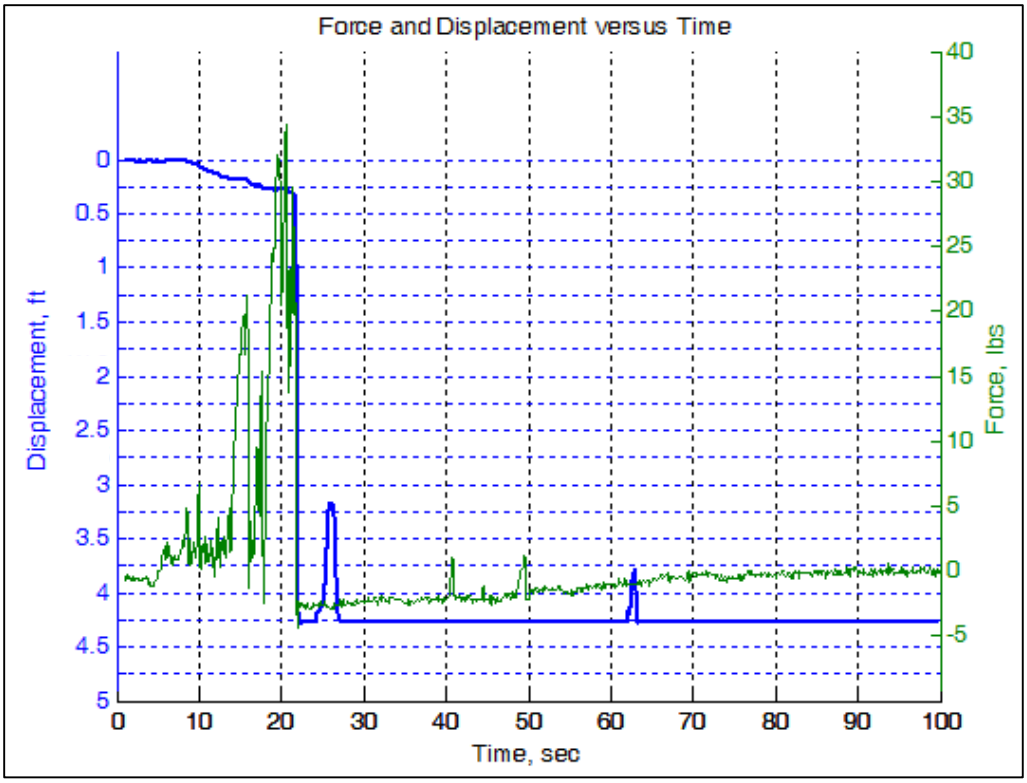

Figure A.25: Force and Displacement versus Time for First Failed Concrete Block Test

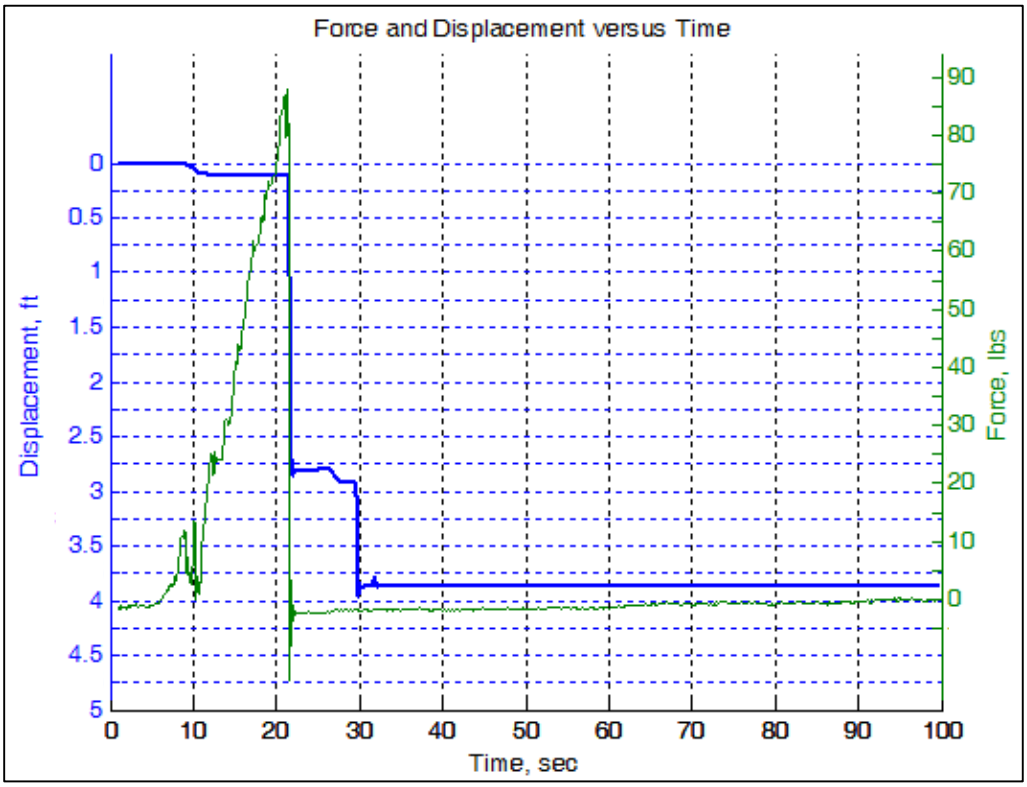

Figure A.26: Force and Displacement versus Time for First Failed Concrete Block Test

Appendix B: MATLAB Code for "itchesplot" Program

```
p1=disp;
p2=force;


h1=figure;

[ax, p1, p2]=plotyy(time, disp, time, force);
set(p1,'linewidth',2);

hold on

alpha=(ceil((max(disp)+0.25))-floor((min(disp)-0.25)))/10;
beta=(ceil((max(force)+5))-floor((min(force)-5)))/10;

title('Force and Displacement versus Time')
ylabel(ax(1),'Displacement, ft')
ylabel(ax(2),'Force, lbs')
xlabel('Time, sec')
%grid(ax(2),'on')
grid(ax(1),'on')
set(ax(1),'YLim',[floor((min(disp)-0.25)) ceil((max(disp)+0.25))])
set(ax(1),'YTick',[0:.25:ceil((max(disp)+.25))])
set(ax(1),'Ydir', 'reverse')
set(ax(2),'Ylim',[floor((min(force)-5)) ceil((max(force)+5))])
%set(ax(2),'YTick',[5])
%set(ax(2),'YTick',[(round(floor((min(force)), 1))-
5):5:(round(ceil((max(force)), 1))+5)])
set(ax(2),'YTick',[-5:5:ceil(max(force))+5])
set(ax(1), 'Box', 'off')
%(ceil(abs((max(disp)+0.25)))-floor((abs((min(disp)-0.25))))/10)
%(ceil((abs((max(force)))))-floor((abs((min(force))))))/10
set(gcf,'color','w');

h2=figure;
he=axes;
ax=gca;
plot(disp, force)
ylabel('Force, lbs')
title('Force vs. Displacement')
xlabel('Displacement, ft')
axis([(min(disp)-0.25) (max(disp)+0.25) (-5) (max(force)+5)])
set(ax,'Xdir','reverse')
ax.YTick=[-5:5:ceil(max(force))+5];
set(gcf,'color','w');
grid on



hold off
```

Appendix C: MATLAB Code for "rename" Program

```
force=(AmplitudeStrainFiltered)/(2*(10^(-5)));
disp=(AmplitudeVoltage_3Filtere)/(0.1828);
time=TimeStrainFiltered;


avie=mean(force(950000:990000));
%avie=mean(force(450000:490000));
%avie=-7.15;
%avie=-8.122;
force=force+abs(avie);
%avia=7.0256;
%avia=6.928;
avia=mean(disp(40000:100000));
disp=abs(disp-abs(avia));

trim
trim

clear('TimeVoltage_3Filtered');
```

Appendix D: MATLAB Code for "movav" Program

```
maxdisp=max(disp);
z=0.1;
%z is the increment value averaged if z=0.25 then every .25 of 1 foot will
%be analyzed, or every 3 inches. Reducing this number increases the
%resolution of the figure but becomes less and less useful for wide
%averages.
dispran=maxdisp-z;
%lowlim=input('What is the lower limit of displacement analysis?');
lowlim=0;

arrayspan=(maxdisp-lowlim)/z;
arrayspan=floor(arrayspan);
avarray=zeros(1, arrayspan);
maxar=zeros(1, arrayspan);
minar=zeros(1, arrayspan);

i=1;
while dispran>lowlim

maxar(i)=maxdisp;


dispran=maxdisp-z;
minar(i)=dispran;
avg=mean(force(disp<(maxdisp)& disp>dispran));
maxdisp=dispran;
avarray(i)=avg;
i=i+1;

end

avarray=avarray';
maxar=maxar';
minar=minar';
avx=((maxar+minar)/2);
%transpose arrays to vectors, create new vector of average x values
h3=figure;
hd=axes;
plot(avx, avarray, '.');
title('Moving Average Force vs. Displacement')
xlabel('Displacement, ft')
ylabel('Force, lbs')
set(hd,'XDir','reverse')
grid on
%plot image
tempe=size(avarray);
CountMovav=tempe(1)
%code provides a count number of the number of data points
commat = horzcat(avarray, maxar, minar, avx);
```